Abstract

Electrophysiological and Psychophysical Assessment of Visual Contrast Sensitivity in Humans

The contrast sensitivity function (CSF) is an informative measure of visual function and offers a more comprehensive evaluation of the visual system than acuity alone. Standard psychophysical and electrophysiological measures of visual function and contrast sensitivity (CS) can be time-consuming, tedious, imprecise, and many require the functional and cognitive capacity to generate volitional responses. These drawbacks can make it challenging to assess CS in healthy populations and severely limit CS assessment in clinical settings and in clinically impaired populations. The visual evoked potential (VEP) is a longstanding, valid, and reliable measure of visual function and contrast sensitivity. The VEP measures electrophysiological cortical responses to visual stimuli to objectively evaluate CS and does not require verbal or behavioral responses as in many traditional psychophysical measures. Despite its utility, the procedures of VEP recording can make it impractical for regular use in some clinical settings and in populations with certain patterns of impairment who are intolerant to the methods.

The Curveball (CB) and Gradiate (GR) procedures are novel psychophysical tools designed to increase accessibility to visual evaluation and contrast sensitivity assessment in clinical settings and impaired populations through smooth pursuit eye tracking. Steady-state contrast and spatial frequency sweep VEPs (C-swp VEP and SF-swp VEP, respectively) were employed in the current study to explore relationships between VEP, Curveball, and Gradiate CSFs and grating acuity measures. The neural mechanisms involved in the

Curveball and Gradiate tasks were explored through comparison to VEP responses elicited from stimuli known to selectively target the magnocellular (M) and parvocellular (P) visual pathways.

CSFs generated by C-swp VEP stimuli varied significantly from those generated by the CB and GR tasks. VEP CS estimates were lower than CB and GR for lower SFs and higher for higher SFs. The CSFs elicited from the CB and GR tasks showed a steep drop-off at ~ 6 cycles per degree, whereas the VEP CSFs showed a more gradual reduction in CS and generated higher CS estimates than CB and GR at SFs above ~ 6cpd. This pattern of responses suggests that the CB and GR tasks may target the M pathway, particularly at low SFs. Acuity estimates derived from SF-swp VEP and the GR task showed poor agreement. VEP grating acuity estimates were higher than those derived from GR across all participants, suggesting that at high SF, the P pathway may not be implicated in the GR tasks as it is in the SF-swp VEP. Taken together, these results suggest that the CB and GR tasks may preferentially target M pathway processing.

Electrophysiological and Psychophysical Assessment of Visual Contrast Sensitivity in Humans

by

Renée M. Root, M.A.

Submitted in partial fulfillment of the requirements

for the degree of

Doctor of Philosophy in Clinical Psychology

in the Ferkauf Graduate School of Psychology

Yeshiva University

September 2021

The committee for this doctoral dissertation consists of:

Vance Zemon, Ph.D., Chairperson, Ferkauf Graduate School of Psychology, Yeshiva University

Glen Prusky, Ph.D., Burke Neurological Institute, Weill Cornell Medicine

Charles Swencionis, Ph.D., Ferkauf Graduate School of Psychology, Yeshiva University

Acknowledgements

I would like to thank Vance for his support, direction, patience, advocacy, and time. Without his willingness to share his wealth of knowledge, expertise and experience and our countless hours in his kitchen and on zoom there would be no dissertation. I am truly grateful for everything you have done for me and helped me to accomplish. And thank you to Jane for putting up with everything and letting me take up so much of Vance's time and energy. I would like to thank Glen for welcoming me into his lab, sharing his knowledge, perspective, and passion and making this project possible. I have learned so much and I am grateful to you for letting me stick around even though I'm afraid to sing karaoke. I want to express my heartfelt gratitude to Nazia for her infinite reserve of patience, stamina, and self-less kindness. You are a true superhero and friend and none of this would have been possible without you. Thank you to Scott for creating these programs and for your patience in helping me understand it all. I would like to thank Leul and Jeremy for their technical expertise and for always being available to help. I would also like to Dr. Swencionis for his flexibility, patience, and willingness to step up on short notice. Thank you as well, to the Ferkauf faculty for being such an amazing group of mentors and educators, and for all their support throughout this process. I need to thank my awesome and amazing family for supporting me in every way possible, helping me get through this, and for being just the right amount of distracting. Thank you Adam for always believing in me and for your unconditional support and encouragement. And last, but certainty not least, I need to thank my friends for keeping me sane and always being ready for a party when we need one.

Dedication

This dissertation is dedicated to my grandmother, Antonina Migliaccio: the woman with the sharpest wit, sharpest tongue, and sharpest style. You taught me to think critically, to stay curious, and always speak my mind.

Table of Contents

List of Figures

List of Tables

List of Abbreviations

4AFC	–	Four-Alternative-Forced-Choice
AD	–	Appearance Disappearance
AUC	–	Area Under the Curve
BNI	–	Burke Neurological Institute
C	–	Contrast
CB	–	Curveball
CoR	–	Coefficient of Repeatability
cpd	–	Cycles per Degree
CR	–	Contrast Reversing
CS	–	Contrast Sensitivity
CSF	–	Contrast Sensitivity Function
C-swp	–	Contrast Sweep
CT	–	Contrast Threshold
CVI	–	Cerebral Visual Impairment
DFT	–	Discrete Fourier Transform
GR	–	Gradiate
GR-1	–	Gradiate – Single Presentation (1 Ball)
GR-F	–	Gradiate – Full Presentation (5 Ball)
K	–	Koniocellular
LCA	–	Low Contrast Acuity
LGN	–	Lateral Geniculate Nucleus
M	–	Magnocellular
MAR	–	Minimum Angle of Resolution
MC	–	Michelson Contrast
MSC	–	Magnitude-Squared Coherence
P	–	Parvocellular
RMS	–	Root Mean Squared
SF	–	Spatial Frequency
SF-swp	–	Spatial Frequency Sweep
SNR	–	Signal to Noise Ratio
ssVEP	–	Steady-State Visual Evoked Potential
swpVEP	–	Sweep Visual Evoked Potential
tVEP	–	Transient Visual Evoked Potential
VA	–	Visual Acuity
VEP	–	Visual Evoked Potential

Chapter 1: Introduction

More of the human brain is involved in processing vision than any of our other senses. Direct and indirect processing of visual information occurs in over 30 distinct areas of the brain (Felleman & Van Essen, 1991; Van Essen et al., 1990), and recent estimates assert that more than 50% of the human cortex is involved in processing the complexity of visual information (Felleman & Van Essen, 1991). Neurally, vision is far more complex than the functioning of optics and optical receptors. The breadth of cortical and subcortical neurons implicated in vision demonstrates that while the anatomy of the eye allows light signals to enter our nervous system, it is our brains that turn those signals into interpretable and actionable visual information. As a result, visual health and function are inextricably linked to brain health and function.

For most humans, vision is the primary tool for navigating, understanding and learning from the environment. Visual impairment, either due to ocular or neurological impairment or disease, can be debilitating and drastically impact an individual's ability to interact with their environment safely and effectively. Visual deficits can impede optimal functioning in multiple areas of human experience, including cognitive, interpersonal, and emotional. Accurate measures of visual function are vital in assessing multiple levels of functioning in healthy as well as neurologically impaired individuals and those with cerebral visual impairments. Accurate assessment of the bounds of visual function can aid in diagnostic clarification of ocular and neurological deficits and disease as well as inform the

establishment of appropriate and effective interventions (Arden, 1978; Cockerham et al., 2009; Guzzetta et al., 2001).

The human visual system and the visual information that it processes are incredibly complex. It is important to understand the features of visual information that are being processed to understand methods of assessing visual function. There are numerous characteristics of visual information that impact the visual experience, including color, luminance, depth, orientation, and form, among many others. Two of the most fundamental elements of vision, and the two that we will focus on here are spatial frequency and contrast. Spatial frequency (SF) describes the periodic distribution of light and dark in an image. SF is often represented in assessment and research by repeating patterns of alternating dark and light bars and is typically quantified as the number of cycles of bright and dark bars that occur within 1 degree of visual angle on the retina or cycles per degree (cpd) of visual angle (Campbell & Maffei, 1974).

Contrast (C) refers to the difference in luminance between the brightest and darkest features of an image which will be discussed in detail later. Examples of square-wave gratings of varying SF and C and a representative luminance profile are shown in Figures 1a and 1b. SF and contrast information are processed differentially in the visual system (Bex & Makous, 2002; Maffei & Fiorentini, 1973; Tootell & Nasr, 2017; Zemon et al., 1986). Assessment of the visual system's ability to process spatial and contrast information provides insight into the functioning of specific retinal and neural mechanisms associated with processing each feature (Campbell & Maffei, 1970; Pokorny & Smith, 1997; Tootell et al., 1988; Zemon & Gordon, 2006; Zemon et al., 1997). There are several methods available to measure spatial resolution and contrast thresholds in humans.

Figure 1a.

Examples of Square-Wave Gratings at Low, Mid and High Spatial Frequency and Contrast

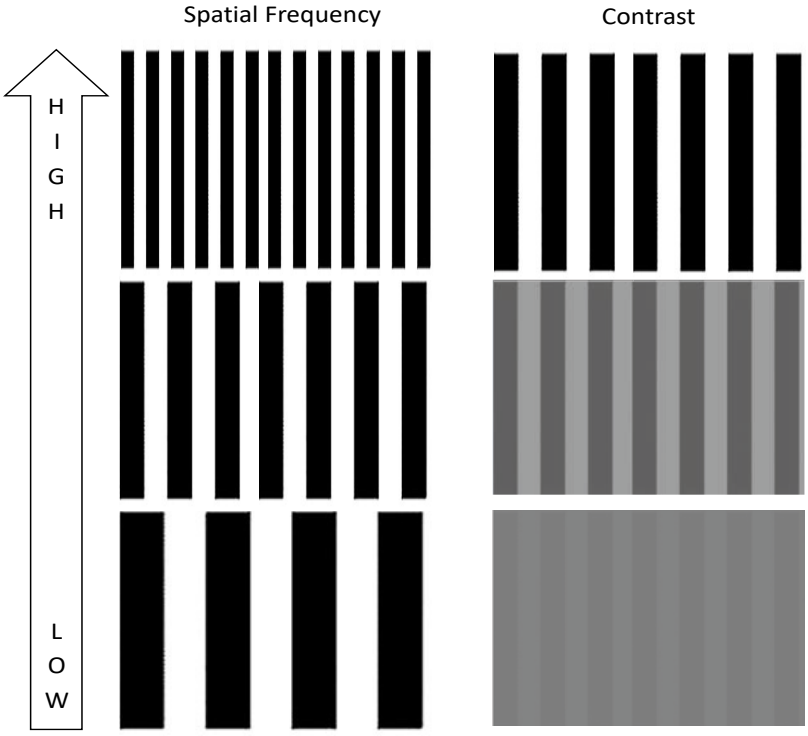

Note. The vertical gratings pictured here are solely for demonstration purposes. Horizontal gratings were used in the VEP stimuli in this study.

Figure 1b.

Square-Wave Grating Plotted as a Function of Luminance and Distance

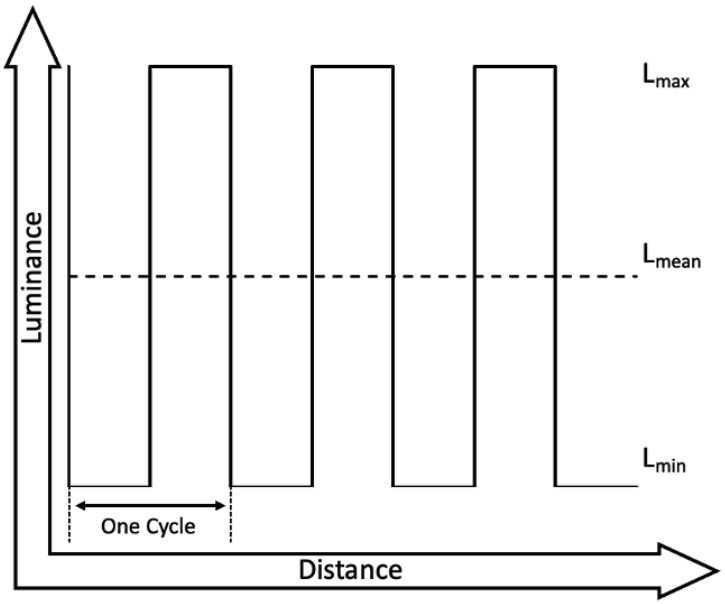

Visual Acuity Measurement

Visual acuity (VA) is the most commonly measured dimension of spatial vision, providing an estimate of the threshold of high contrast spatial resolution as a function of distance (Westheimer, 1965). Visual acuity reflects the highest spatial frequency that an individual can resolve at high contrast at a set distance. This is typically assessed with charts presenting a series of high contrast letters or shapes (referred to as optotypes) arranged serially in descending size. The Snellen acuity chart (Snellen, 1868), first introduced in 1862, remains one of the most widely used measures of acuity and has become a generic descriptor for optotype charts. The Snellen chart typically quantifies spatial resolution using the

"Snellen fraction," in which the numerator is the viewing distance (20 feet in the U.S.), and the denominator is the distance at which the height of the smallest readable letters would subtend 5 minutes of arc. 20/20 vision indicates that at a testing distance of 20 feet, the smallest letters an individual can resolve would subtend 5 minutes of arc at 20 feet (Bailey & Jackson, 2016).

There are numerous other optotypes and charts that have been introduced since the introduction of the Snellen chart, including the Bailey-Lovie Chart, the Sloan Letters used in the EDTRS chart (Group, 1991), Tumbling E, Landolt Rings (Landolt C), and Lea Symbols which are based on graphics instead of letters (Bailey & Jackson, 2016). Many newer VA assessment charts such as the Tumbling E and ETDRS are organized such that optotypes decrease in size logarithmically by 0.1 log unit from one line to the next. This was done to standardize and improve the accuracy of acuity assessment, as each line presents the same number of optotypes and the even spacing between symbols and lines allows for interpretation at nonstandard viewing distances. These types of charts are typically referred to as LogMAR charts as they quantify acuity as the logarithm (base 10) of the minimum angle of resolution (MAR). The MAR is a measure of the angle size (in minutes of arc) of the detail (or spatial frequency) in the smallest resolvable optotype. The MAR is equal to the reciprocal of the Snellen fraction (i.e., VA of 20/40 = 2 minute of arc), and conversion between Snellen and LogMAR values can be done easily (i.e., 20/20 Snellen = 1 minute of arc = MAR 1 = LogMAR 0) (Holladay, 2004).

Various optotypes are considered to measure two types of visual acuity: recognition acuity (i.e., reading a letter) and resolution or grating acuity (i.e., resolving a gap) (Kuo et al., 2011). Research comparing acuity derived from recognition- and resolution-based optotypes

has found that recognition-based measures like the ETDRS result in slightly higher VA estimates than resolution-based measures in individuals with logMAR acuity above +1.0 (Becker et al., 2007; Kuo et al., 2011). These findings suggest that differences in optotype presentation can impact the measurement of VA, specifically in individuals with deficits in spatial vision for whom these measures may be most important.

VA can also be measured electrophysiologically using visual evoked potentials (VEPs) (Hamilton et al., 2021a; Zemon et al., 1997), which reflects the neural response to spatial information. Grating acuity measured with VEPs can provide important information about associated neural activity and quantifies VA as the highest SF (in cpd) at which a measurable neural response occurs in the electroencephalogram (EEG) (Almoqbel et al., 2011; Hamilton et al., 2021b). Mechanistic differences and disparities in the expression of thresholds between electrophysiological and psychophysical assessments of VA can make a direct comparison of acuity estimates difficult. Additionally, variation among psychophysical optotypes and metrics of quantifying VA can also make it difficult to compare VA estimates across settings and studies. Although VA is the most ubiquitous measure of visual function, it only provides information about the visual system's ability to resolve spatial frequencies in ideal high luminance and contrast conditions and does not offer information about visual function under other conditions.

Contrast Vision Measurement

Contrast vision can also be measured psychophysically using charts similar to the Snellen and LogMAR charts used in the assessment of VA. In the assessment of contrast, however, contrast is decreased across the chart instead of spatial frequency. Charts like the

Pelli-Robson chart (Pelli & Robson, 1988) present Sloan letters (also used in the ETDRS chart) at a fixed size with contrast decreased progressively by a factor of $1/\sqrt{2}$ down the chart. The contrast threshold is taken as the lowest contrast level at which an individual can recognize two of the three letters in that contrast group. This type of contrast assessment provides a contrast threshold at a single letter size and can provide a single measurement of contrast sensitivity (CS), which is taken as the reciprocal of the contrast threshold (CT).

Contrast thresholds at a single spatial frequency are not often measured as they provide limited insight into visual function. More commonly, contrast vision is assessed as a function of spatial frequency to capture contrast sensitivity across a spectrum of spatial frequencies. This two-dimensional plot of the reciprocal of visual contrast thresholds across spatial frequency is represented as a contrast sensitivity function (CSF) (see Figure 2 for an example of a standard CSF). The CSF offers a more comprehensive description of spatial processing in the visual system than VA, which reflects spatial vision only at the highest contrast and finest detail. The CSF reflects visual function over a dynamic range of visual conditions that more fully reflect the complexity of real-world visual experiences. (Arden, 1978; Kelly, 1977; Owsley et al., 1983; Pelli & Bex, 2013; Richman et al., 2013).

Gustav Fechner, considered the father of psychophysics, in his pivotal 1860 report (Fechner, 1948) first described contrast thresholds and found CT to be as low as 1% contrast for a variety of stimuli and conditions (Solomon, 2011). The first CSF in humans was described by Otto Schade in 1956 (Schade, 1956). Since then, CS and the CSF have been extensively studied psychophysically and electrophysiologically in relation to healthy visual development as well as a number of visual, neurological, vascular, and metabolic disorders

Figure 2

Representative Example of a Contrast Sensitivity Function

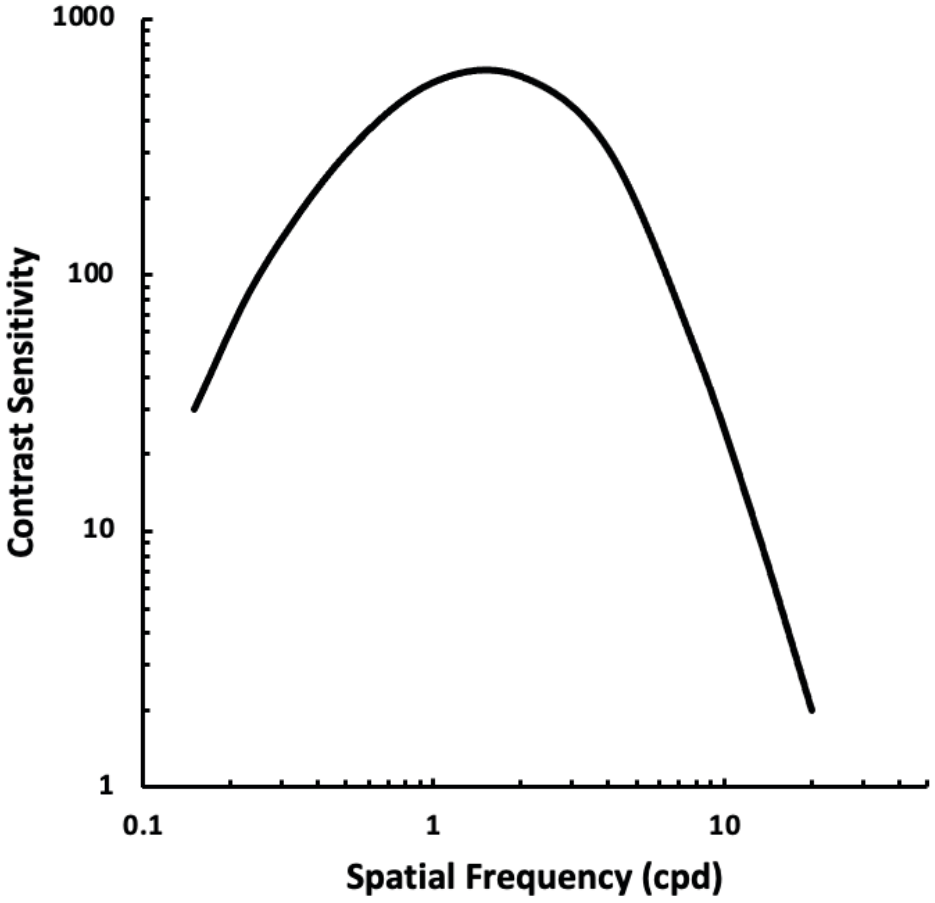

Note. CS is equal to 1/CT.

and diseases. Decades of research have found CS to be a much better measure of visual health and disease than simple acuity measures (Jindra & Zemon, 1989; Kelly, 1977; Legge & Rubin, 1986; Owsley, 2003; Storch & Bodis-Wollner, 1990; Xiong et al., 2020). CS impairment has been associated with a number of visual disorders like cataracts (Shandiz et al., 2011), glaucoma (Atkin et al., 1979; Hawkins et al., 2003; Ichhpujani et al., 2020; Richman et al., 2010), optic neuritis (Hoorbakht & Bagherkashi, 2012; Zimmern et al., 1979) and diabetic retinopathy (Durán et al., 2021; Sokol et al., 1985; Verrotti et al., 1998). CS has

also been associated with neurological disorders, including multiple sclerosis (MS) (M. Kupersmith et al., 1984; M. J. Kupersmith et al., 1984; Narayanan et al., 2019; Regan et al., 1977), Parkinson's disease (Bodis-Wollner et al., 1987; Ridder et al., 2017), schizophrenia (Butler et al., 2008; Zemon et al., 2021), Alzheimer's disease (Cormack et al., 2000; Hutton et al., 1993), and depression (Bubl et al., 2015; Fam et al., 2013; Morse, 2013). In many of these disorders, CS is impaired while acuity may remain intact, supporting the importance of CS assessment. Early identification of CS deficits can help to identify disease states like diabetes, Alzheimer's disease, and multiple sclerosis earlier.

Despite its acknowledged value, CS is not often evaluated in clinical settings due to the limitations of currently available psychophysical and electrophysiological methods. Traditional psychophysical methods of CS assessment have drawbacks that have limited their use in healthy populations. Paper or electronically viewed charts can be done relatively quickly but include a limited number of stimuli and have been found to offer inconsistent results (Pateras & Karioti, 2020). Forced-choice tasks are thought to be more reliable but are time-consuming and tedious. Additionally, all of these psychophysical measures require the cognitive and functional ability to attend to the stimuli and produce verbal and/or action-oriented responses. While these factors make it impractical to measure CS regularly in healthy populations, it makes it almost impossible in many disabled populations. CS measurement can be especially difficult to obtain for individuals with neurological impairment and young children, as there are often deficits in the motor functioning, verbal and nonverbal communication, and attentional and cognitive processing necessary to participate in standard behavioral and psychophysical measures of visual function.

Visual evoked potentials (VEPs) have been used to assess CS as well. The VEP measures electrophysiological cortical responses to visual stimuli and does not require verbal or behavioral responses. While this is a longstanding valid and reliable measure of visual function and contrast sensitivity (CS) and offers valuable neurophysiological information (Campbell & Maffei, 1970; Jindra & Zemon, 1989; Norcia et al., 1989; Zemon et al., 1997), there are limitations that make it challenging or impractical to use in clinical settings and in populations with certain patterns of impairment. Specifically, VEP recording requires the use of scalp electrodes placed on a stationary observer, a controlled dark environment, and sustained attention to repeatedly presented patterns, sometimes making it difficult to obtain accurate VEP recordings in observers who, due to age or impairment, are unable to participate or are intolerant of the methods.

The Curveball and Gradiate systems (Mooney et al., 2020; Mooney et al., 2018) are novel psychophysical tools designed to address some of the limitations of classic psychophysical measures to make it possible to evaluate visual function quickly and flexibly. These tasks measure contrast sensitivity through a smooth-pursuit eye movement tracking algorithm of a patch or multiple patches of continuously drifting visual noise that decreases in contrast or change in contrast and spatial frequency until no longer visible. The stimuli are presented on a portable LCD screen that can be used flexibly in hospital and clinical settings and the tasks have been found to provide consistent results across a variety of lighting conditions (Mooney et al., 2020; Mooney et al., 2018). Additionally, the tasks take five minutes or less to complete, can be completed without any instruction to the participant, and can accommodate interruptions in attention without sacrificing accuracy. These benefits can make the Curveball and Gradiate tasks invaluable in assessing visual function in populations

where traditional optotypes and electrophysiological methods may not be viable of practical options for accurate assessment.

There is a critical need for improved methods for assessing visual function in populations that are not candidates for evaluation using traditional optotypes or electrophysiological measures of visual function. Reliable, practical measures of visual function and CSFs can improve the diagnosis of neurological dysfunction as well as provide indicators of other disorders, as mentioned previously. Detection of visual deficits and accurate measurement of the parameters of an individual's visual function can improve interventions and potentially catch early signs of neurological and visual disorders. VEPs can provide accurate estimates of CSF and VA (Zemon et al., 1997; Zemon & Gordon, 2002) and can provide valuable information about the neural processes involved in vision (Zemon et al., 1988; Zemon & Ratliff, 1982; Zemon et al., 1986), but it can be an impractical tool in many clinical settings and in many clinical populations. The Curveball and Gradiate tasks can offer an additional method of evaluating visual function quickly, easily, and affordably in a wide range of clinical settings and in a wide range of clinical populations. In neurologically impaired, nonverbal, and very young populations, the CB and GR systems can make it possible to evaluate visual function, which to this point has been extremely limited due to limitations in currently available measurement tools.

Improved access to visual assessment is especially important in neurologically impaired individuals and children as it can be used to target rehabilitation more effectively as well as to establish better interventions and compensatory measures to improve daily functioning and quality of life. One in six children in the US has a developmental disability like autism, cerebral palsy, spina bifida, or fragile x syndrome (Boyle et al., 2011), and there

is evidence that neurodevelopmental disorders are associated with visual processing impairments (Laycock et al., 2007). Comprehensive visual assessment is often not available to children with severe physical and cognitive disabilities due to the limitations of their disorders and limitations of current assessment tools like eye charts and electrophysiological testing. The CS and GR systems can address this need and provide many children better access to comprehensive visual assessment.

Beyond its use in neurologically and developmentally impaired populations, the CB and GR systems can be employed in neurologically intact populations. Flexible, rapid, and affordable methods of evaluation can substantially improve access to contrast sensitivity assessment. This could potentially make it feasible to assess contrast sensitivity as part of standard ophthalmic examinations. CB and GR could be used as a screening measure to provide a more comprehensive evaluation of visual functioning, thereby improving diagnosis and remediation of visual deficits beyond what is currently available in standard refractive evaluations. Impaired visual function in non-disabled children can negatively impact development in all domains, including social, cognitive, motor, language, and emotional development (Zihl & Dutton, 2016). It is estimated that 5 to 10% of all preschoolers in the US have a visual impairment (Force, 2004) and given the potential negative developmental implications, better assessment of visual limitations earlier in life can lead to better interventions and long-term outcomes. The potential benefits of the CB and GR system are far-reaching, and validation and exploration of the systems using VEP as a reliable and validated objective measure is a necessary first step in exploring the clinical potential for these tasks.

Due to the recent and ongoing development of the CB and GR systems, they have yet to be validated against electrophysiological measures, and the neural correlates have not yet been investigated. The current study is the first to evaluate the agreement between CB and GR CSFs with objective electrophysiologically generated CSFs using a swept-parameter (sweep) VEP (swpVEP) technique. It is also the first study to evaluate the neurophysiological underpinnings of the Curveball and Gradiate tasks through comparison with well-validated VEP techniques known to reflect the activity of specific neurophysiological systems.

Chapter 2. Background and Study Aims

Overview of the Visual System

The human visual system is comprised of a complex network of integrated processing areas, beginning at the retina with optic tract extending to the lateral geniculate nucleus (LGN), followed by optic radiations projecting to the primary visual processing areas in the cortex, then to the extrastriate cortex which processes specific aspects of visual information, and ultimately to higher-order information processing centers in the brain (Felleman & Van Essen, 1991; Schwartz, 2009). Visual information enters this retino-geniculo-cortical pathway through cells in the retina of the eye. Visual information as light signals is processed by the retina and transduced by photoreceptors into electrochemical signals. There are two types of photoreceptors in the retina, rods, and cones, which function optimally under different lighting conditions. Rods process low-light (scotopic) vision, which is characterized by high sensitivity to low-light conditions, poor visual acuity, and an absence of color discrimination. Conversely, cones process high-luminance (photopic) vision, which is characterized by poor sensitivity to low-lighting conditions, excellent visual acuity, and color discrimination (Schwartz, 2009).

The retina is organized in layers, and photoreceptors transmit visual information in the form of electrical activity to bipolar cells, which in turn transmit signals to the ganglion cells that form the optic nerve that carries visual information to the brain. Horizontal and amacrine cells transmit information laterally within layers of the retina and act to modify

visual signals before they leave the retina via the optic nerve. The optic nerve carries visual information to the LGN of the thalamus, which functions as a relay center for visual information. At the level of the LGN, left and right visual field information is processed in the opposite hemispheres of this bilateral six-layered structure. Ipsilateral information is processed in layers 2, 3, and, 5 while contralateral information is processed in layers 1, 4, and 6 (Schwartz, 2009).

Visual Pathways

Visual information is organized and processed through a series of direct pathways carrying excitatory signals and lateral pathways carrying primarily inhibitory signals (Ratliff & Zemon, 1982; Zemon & Ratliff, 1982; Zemon & Ratliff, 1984). There are three distinct neural pathways that project to the LGN, each associated with one of three types of ganglion cells: M, P, and K cells. Each type of ganglion cell synapses at a different layer in the LGN. The two ventral layers receive input from M cells with large receptive fields and comprise the magnocellular (M) pathway. The four dorsal layers make up the parvocellular (P) pathway, which receives input from midget or P retinal ganglion cells. And finally, the koniocellular (K) pathway is formed at the boundaries between each layer (Felleman & Van Essen, 1991; Hendry & Reid, 2000; Kaplan, 2014; Morand et al., 2000).

The M and P pathways are considered parallel pathways in that they maintain distinct connections with disparate areas of the striate and extrastriate cortex, and they process different aspects of visual information received from the retina (Tootell et al., 1988; Tootell & Nasr, 2017). Each pathway carries information from its respective ganglion cell types and remain separate to the primary visual cortex (V1) and is believed to respond selectively to

different features of luminance, form, and motion, giving them distinct roles in the processing of visual information and visual perception (Kaplan & Shapley, 1986; Livingstone & Hubel, 1988; Merigan & Maunsell, 1993; Morand et al., 2000; Nassi & Callaway, 2009). The M pathway is involved in processing brightness, depth, and motion is sensitive to low-contrast stimuli, and has low spatial resolution. The M ganglion cells have large axons and receptive fields, allowing for faster conduction than P cells and higher temporal resolution, characterized by a transient response (Liu et al., 2006; Nassi & Callaway, 2009). The P pathway is involved in color vision, visual acuity, and form perception. It is characterized by sensitivity to high-contrast stimuli, high spatial resolution, low temporal resolution, and sustained responses, with projections to the ventral stream (Kaplan, 2014; Kaplan & Shapley, 1986; Liu et al., 2006).

Tootell et al. (1988) demonstrated in macaques that visual signals from magnocellular and parvocellular layers of the LGN remain largely segregated as they pass through the primary visual cortex. By evaluating the uptake of C2-deoxyglucose in subsections of the primary visual cortex in response to visual stimulation with gratings of varying contrast and spatial frequency, they found that low contrast (8%) gratings selectively stimulated layers of the striate cortex (4Ca, 4B, 6) receiving afferent signals from predominantly magnocellular layers of the LGN, but not layers associate with parvocellular projections (4Cb, 3, 5, 4A). The findings of Tootell et al. (1988) suggest that area V2 receives input primarily from parvocellular layers of the LGN, while area MT receives signals primarily from magnocellular layers. MT cells are believed to have a center-surround organization that makes them sensitive to contrast in space and time and consequently preferentially sensitive to motion and moving stimuli (Felleman & Van Essen, 1991).

In terms of contrast sensitivity, the findings of Tootell et al. (1988) are consistent with previous research that found magnocellular cells to have higher contrast sensitivity than parvocellular cells. Kaplan and Shapley (1982) recorded responses from M and P cells in the monkey LGN and found that M cells had significantly higher CS (82 ± 20) than P cells (11 ± 3). Their findings support the functional significance of the segregation of the two pathways. The CSF generated by each system shows variations in CS at higher and lower SFs. Several studies have shown that at lower SFs detection is mediated by the M pathway, and above this point detection is P pathway mediated. At SFs above the crossover point the M system is active but is not believed to mediate contrast detection (Skottun, 2000).

Visual Receptors

ON/OFF cells

The M and P pathways have subdivisions differentially involved in processing brightness and darkness information: ON/OFF subsystems that rely on activation of ON and OFF cells, respectively. ON cells respond selectively to positive contrast, whereas OFF cells respond selectively to negative contrast (Hartline, 1938; Zemon & Gordon, 2006; Zemon et al., 1988). Thus, the differential responses from these parallel pathways can be useful in identifying and understanding deficits in visual processing (Kaplan, 2014; Livingstone & Hubel, 1988; Schiller, 1982).

Visual Evoked Potentials

The visual evoked potential (VEP) is a measurement of cortically generated electrical activity recorded in response to light stimuli via electrodes placed on the scalp over areas

associated with visual processing, namely the occipital cortex (Colon & Visser, 1990). Visual evoked potentials (VEP) have been shown to be a reliable measure of visual function and contrast sensitivity in both children and adults (Campbell & Maffei, 1970; Norcia et al., 1989; Zemon et al., 1997) and are reflective of gross visual function as well as specific visual subsystems (Zemon et al., 1988; Zemon & Ratliff, 1984; Zemon et al., 1986) The sweep VEP (swpVEP) method, specifically, is a longstanding method for assessing sensitivity to both contrast and spatial frequency (Almoqbel et al., 2008; Norcia et al., 1989; Norcia & Tyler, 1985; Tyler et al., 1979). The contrast sweep VEP (C-swp VEP) stimuli that were used in the current study rapidly present incremental changes in the contrast of grating patterns while cortical responses are measured. This is done over a series of spatial frequencies to determine the contrast threshold or the minimum contrast at which each grating pattern can produce a significant response (National Research, 1985). Spatial frequency sweep VEPs were used to assess acuity (Arai et al., 1997).

Steady-State and Transient VEP

Various VEP stimuli can differentially elicit responses from different pathways and mechanisms in the visual system, including laterally inhibitory mechanisms, orientationally selective mechanisms, spatial frequency selective mechanisms, and contrast and luminance selective mechanisms (Jindra & Zemon, 1989; Ratliff & Zemon, 1982; Zemon & Gordon, 2006; Zemon et al., 1983; Zemon & Ratliff, 1984; Zemon & Gordon, 2002). There are two general types of VEPs classified based on the stimulus frequency and temporal waveform used to elicit them, referred to as *steady-state* and *transient* (Regan, 1966b).

Steady State VEP

Steady-state VEPs (ssVEP) are elicited by stimuli with contrast or luminance modulated at moderate to high temporal frequency (≥ 3.5 Hz) that does not allow sufficient time between stimulus presentations for the visual system to recover, resulting in overlapping, successive responses that yield a smooth oscillatory waveform (Regan, 1966a; Zemon & Ratliff, 1982). The power in ssVEPs is concentrated in the first few harmonic frequency components that are extracted from the ssVEP through Fourier analysis (Gutowitz et al., 1986; Regan, 1989). The contrast and spatial frequency swp VEPs in the current study are designed to elicit steady-state responses.

Transient VEP

The current study will also employ VEP stimuli designed to elicit a transient response. Transient VEPs (tVEP) are elicited by stimuli with modulations at a low temporal frequency, such that the response to one stimulus is complete by the time the next stimulus is presented, making each response distinct from the next (Regan, 1966b). This creates a discrete waveform with apparent positive and negative peaks in the first few hundred milliseconds following the stimulus change. These waveforms are typically analyzed using magnitude squared coherence (MSC), amplitude, and latency measures.

Contrast Sensitivity and Contrast Sensitivity Functions

The contrast threshold is defined as the minimum contrast needed to elicit a response, behavioral or electrophysiological. The reciprocal of the contrast threshold is the contrast

sensitivity (CS) and, when plotted against spatial frequency, generates a curve referred to as the contrast sensitivity function (CSF) (see Figure 2 for an example of a standard CSF).

Contrast sensitivity functions (CSFs) have been found to be a valuable measure of visual function (Arden, 1978; Jindra & Zemon, 1989; Lopes de Faria et al., 1998; Pelli & Bex, 2013). The CSF provides a more robust estimation of visual pathway integrity than does acuity alone (Ginsburg, 2003; Pelli & Bex, 2013). The CSF offers an accurate clinical evaluation of visual function over a wide range of spatial frequencies and is reflective of the individual's visual ability in complex, low contrast, real-world environments (Ginsburg, 2003; Lopes de Faria et al., 1998; Owsley et al., 1983). Individuals with 20/20 visual acuity can still experience loss of visual function that is not related to the ability to resolve fine details (Ginsburg, 2003).

CSFs can also be useful in diagnosing and treating multiple vision disorders such as glaucoma (Greenstein et al., 1998; Richman et al., 2010), macular degeneration, optic nerve lesions (Varinen et al., 1983), and cataracts (Elliott et al., 1989). Additionally, it is valuable in assessing potentially hidden visual deficits and early-stage cerebral visual impairment (CVI) in common and serious neurodegenerative disorders such as Alzheimer's disease (which is the leading cause of dementia worldwide) (Guo et al., 2017), multiple sclerosis (Kupersmith et al., 1984), and Parkinson's disease (Gooch et al., 2017). Contrast sensitivity has also been implicated in psychiatric disorders such as schizophrenia and depression (Butler et al., 2006; Butler et al., 2008) as well as metabolic disorders such as diabetes (Barber, 2003).

The CSF is also a useful tool in assessing CVI associated with acquired brain injury (Cockerham et al., 2009) and neurodevelopmental disorders (Laycock et al., 2007). CVI is

the leading cause of visual impairment in pediatric populations, associated with both trauma and developmental disorders, and it can impact cognitive functioning, learning, and attention, as well as social and motor development (Ospina, 2009). Improved visual assessment measures and better access to these measures could improve the diagnosis of visual impairment and treatment interventions for countless individuals.

Contrast Sensitivity in Electrophysiological and Psychophysical Tasks

Currently, the CSF, despite the superiority to simple acuity measurement, and wide-ranging potential benefits of its use, is not widely assessed due in large part to the limitations of the currently available measurement tools. Psychophysical measures of contrast sensitivity have several limitations. Printed charts lack sensitivity to the two-dimensional properties of the CSF, and forced-choice staircase tasks are extremely time-consuming, limiting their clinical feasibility. Adaptations to the staircase task have used algorithms to cut down on assessment time but have sacrificed accuracy due to the limitation in methods of computing the most relevant combinations of contrast and spatial frequency and offer only a limited estimation of the CSF (Lesmes et al., 2010). Newer computerized measures employ simultaneous two-dimensional Bayesian approaches to provide better estimates of CSF quickly and can be run on tablets (Dorr et al., 2017); however, these are still limited by their dependence on extended intervals of attention and active and subjective perceptual report.

All the available tools for assessment of the CSF are reliant on repeated presentation of visually uninteresting stimuli, and the adaptive nature of the assessment necessitates that most of the evaluation be spent at the threshold of vision, making the task difficult. These limitations, which make the task difficult for healthy adults, severely limit their use in

populations less tolerant to these drawbacks, such as children and neurologically impaired individuals, and render them almost useless in nonverbal and severely impaired populations where they may be most necessary and could provide the most useful diagnostic information.

VEPs have been used to address some of the limitations of psychophysical CSF measurement by eliminating the need for active responding and by providing an objective measure of contrast sensitivity, which can be done relatively quickly. VEP also has drawbacks that limit its clinical use, including reliance on intervals of sustained attention, the necessity of a controlled, dark testing environment, and the observers' ability to remain somewhat still and tolerate electrodes attached to the scalp. In neurologically impaired, severely physically disabled, and young populations, VEP recording is often difficult, as limitations in attention, intolerance of the methods, and impracticality of the testing conditions make it difficult to administer in some clinical settings.

The Curveball and Gradiate procedures are novel psychophysical tools recently developed at the Laboratory for Visual Disease and Therapy at the Burke Neurological Institute (Mooney et al., 2020; Mooney et al., 2018), in an effort to address the limitations of assessing contrast sensitivity in clinical settings and in previously underserved disabled populations, specifically children with disabilities and non-verbal individuals. These tasks make it possible to generate an objective measure of the CSF quickly and intuitively without the need for volitional or verbal responses, verbal instructions to the participant, or long periods of sustained attention.

A two-dimensional patch of band-limited visual noise (narrow range of spatial frequencies) is presented on a portable screen and continuously drifts around the screen, while an eye tracker and gaze algorithm monitor smooth pursuit eye movements in real-time,

reducing the contrast and/or spatial frequency of the noise patch until the participant is no longer able to smoothly track the stimulus. These systems can be used under any lighting conditions, and the screen can be easily moved to accommodate any patient, say in a hospital bed or doctor's office, and can be easily articulated and repositioned to accommodate individuals with physical limitations. These procedures can potentially make the assessment of contrast sensitivity and visual function more accessible to both physically and neurologically impaired populations as well as healthy individuals as part of a visual exam.

VEP evaluation of visual function and CS has been used reliably and successfully for years in many physically and neurologically impaired populations, including those with traumatic brain injury (Lachapelle et al., 2004; Padula et al., 1994), epilepsy (Conte & Victor, 2009; Porciatti et al., 2000), cerebral palsy (da Costa et al., 2004), Guillain-Barre syndrome (Wong, 1997), schizophrenia (Schechter et al., 2002), and non-verbal individuals (Almoqbel et al., 2008; Tyler et al., 1979). The Curveball and Gradiate tasks offer an alternative method with the benefit of potentially providing a quicker and more easily accessible estimate of CS. The Curveball and Gradiate tasks can also potentially be adapted and made game-like, making the task more engaging for individuals with attentional limitations. The Curveball and Gradiate systems can potentially help identify visual deficits beyond simple acuity more rapidly than other traditional psychophysical measures and can potentially improve diagnosis, interventions, and quality of life for people with complex retinal and cerebral visual impairments as well as potentially improve access to comprehensive visual assessment in general.

Curveball and Gradiate, as newly developed tools, have not yet been compared with electrophysiological measures of CS. This study will be the first to assess the validity of the

CSFs generated by the Curveball and Gradiate tasks with longstanding, validated electrophysiological VEP measures. The magnocellular visual pathway is hypothesized to be sensitive to low spatial frequency and low luminance contrast (Kaplan, 2014; Zemon & Gordon, 2006) and is also involved in the processing of motion (Krauzlis, 2004). As a result, low contrast, low SF stimuli presented by both the Curveball task and the VEP technique are expected to target the same visual pathways and are hypothesized to generate similar measurements of CS.

Contrast Definitions

The contrast of a target describes its relative difference in luminance from the background (Peli, 1990). The metric used to express this relationship can vary based on the type of stimuli being presented (Pelli & Bex, 2013). The most widely used contrast metrics and those applicable in this study are the Michelson contrast definition and the *root mean square* (RMS) contrast ratios.

Michelson Contrast

The Michelson contrast ratio defines contrast using the maximum and minimum luminance values as illustrated in the following formula:

$$C = \frac{Lmax - Lmin}{Lmax + Lmin}.$$

The Michelson contrast ratio is preferred for simple periodic patterns like those presented in the VEP recording. In this ratio, the contrast (*C)* of a periodic pattern such as square-wave or sinusoidal gratings is defined as the ratio of the difference to sum of maximum (*Lmax*) and minimum (*Lmin*) luminance values of the gratings. This reflects contrast as a dimensionless

ratio of change in periodic luminance and ranges from 0 to 1.0 (Peli, 1990; Pelli & Bex, 2013).

Weber Contrast

The Weber fraction of contrast refers to the relationship between a distinct target with uniform luminance and the uniform background it is presented on. This relationship is expressed as a Weber fraction as follows:

$$C = \frac{\Delta L}{L}$$

where contrast C is defined as the ratio of the change in the target luminance (ΔL) and the luminance of the uniform background (L) (Peli, 1990). This contrast ratio is ideal in situations where a circumscribed target is presented against a larger background, and can be useful in assessing detection of difference thresholds in research, often referred to as the just noticeable difference (Schwartz, 2009). Weber contrast can range from -1.0 to $+\infty$ (Peli, 1990).

RMS Contrast

The *root mean square* (RMS) contrast ratio defines contrast using the standard deviation of the luminance levels in the stimuli (Kukkonen et al., 1993) and is preferred for natural images and noise targets (Peli, 1990; Pelli & Farell, 1999). For Curveball and Gradiate, contrast is defined and calculated using the RMS contrast ratio metric, which is based on the standard deviation of luminance levels (per pixel) in the stimulus noise pattern. The RMS contrast ratio used in the calculation of Curveball and Gradiate CSs is as follows:

$$C = \frac{\sqrt{\frac{1}{N}\ \Sigma_x \Sigma_y (L(x, y,) - \ L_\mu)^2}}{L_\mu}$$

where mean luminance was calculated to be 63.512 cd/m^2 in the testing environment (Mooney et al., 2020; Mooney et al., 2018). The RMS contrast definition does not depend on the spatial frequency content of the target image or the spatial distribution of contrast (Peli, 1990) and uses the standard deviation of the luminance levels to account for variability in the complex noise pattern stimuli.

Preliminary Studies

Curveball

The Curveball task was developed by Dr. Scott Mooney and Dr. Jeremy Hill at the Laboratory for Visual Disease and Therapy at the Burke Neurological Institute under the direction of Dr. Glen Prusky. Curveball is a novel psychophysical tool introduced in 2018 (Mooney et al., 2018) that infers CS based on the participant's ability to smoothly track a continuously wandering target of a set spatial frequency as it is decreased in contrast (see Measures section, “Curveball Task” for a full explanation of the task). A single filtered noise patch with a center spatial frequency of 0.25, 0.5, 1, 2, 4, or 8 cpd was presented in each trial and moved continuously around the screen. The contrast was reduced as the participant smoothly tracked the patch within a set degree of accuracy until they were no longer able to maintain smooth pursuit of the stimulus. The contrast threshold was identified as the contrast level where an individual was no longer able to track the stimulus based on frame-by-frame gaze tracking.

Their introductory study examined CSFs generated by the Curveball task in thirty-five healthy adults with normal or corrected-to-normal vision over two sessions and under several conditions (far, close, light, dark). Participants also completed a standard 4AFC staircase task to compare with the Curveball results. To assess repeatability, the Curveball task was also administered under standard lighting and distance conditions (well-lit room at 62 cm) a total of three times over two sessions. Eighteen participants with visual correction completed an additional run of Curveball without their corrective eyewear. The CSFs generated during the task were compared with CSFs generated using a conventional psychophysical four-alternative forced-choice (4AFC) staircase task presented under both static and moving conditions. The staircase task used in this study employed six static gratings at the same spatial frequencies as the Curveball task and five moving gratings at lower spatial frequencies due to aliasing effects.

Mooney et al. (2018) found the CSFs generated by the Curveball task to be well-correlated with those generated through standard, well-validated, psychophysical forced-choice measures. For static gratings, an affine transformation was applied to the 4AFC CSF to account for systematic differences in threshold estimates. Based on this transformation the mean correlation across participants for the static condition was .790 ± .154, $t(27) = 4.044$, $p < .001$. The moving gratings in the 4AFC task could not be filtered to avoid aliasing in the same way as the larger Curveball stimuli. As a result, the moving gratings presented were a lower and more restricted range of spatial frequencies than those in Curveball (0.125, 0.25, 0.5, 1 and 2 cpd). To account for the difference in SFs presented and allow for comparison of CS at each SF, the Curveball contrast sensitivities were translated to the left by one log unit, and the highest Curveball spatial frequency was dropped. The mean correlation based on this

transformation for moving gratings was .907 ± .074, $t(28) = -1.116$, $p = .274$. Participants took between 15 and 25 minutes to complete the full set of interleaved staircase runs necessary to generate a CSF. For standard Curveball runs, the average task completion time was 5 minutes and 15 seconds (SD = 37 s). Repeatability was assessed using the coefficient of repeatability (CoR), which reflects the value at which the absolute differences between two measurements would fall below with 0.95 probability. It is calculated by multiplying the Standard Error or Measurement by 2.77 ($\sqrt{2}$ x 1.96) and quantified in the same units as the assessment tool. It is considered an ideal methods to compare two measures (Vaz et al., 2013). Repeatability was found to be high for same-day (CoR = 0.275) and different day (CoR = 0.227) Curveball CSFs generated under standard viewing conditions.

In terms of viewing distance, they found that there was a significant decrease in pursuit score (the observer's ability to accurately maintain smooth pursuit within the margin of error allowed by the Curveball algorithm) between the standard (62 cm) and far (77 cm) conditions ($t(21) = 3.536$, $p = .002$) and no significant difference between the standard and close (47 cm) conditions. These results suggest that at greater distances, the increased noise in the gaze data obtained by the eye tracker can shift observers' eye-tracking ability below the threshold required for the algorithm to estimate a contrast threshold. There was no significant change in mean CS between standard and close conditions, but a significant decrease in the far condition (0.135 log RMS, $F(1,20) = 38.981$, $p < .001$). They found a significant interaction between distance and spatial frequency for the close condition ($F(5,130) = 3.036$, $p = .013$) but not the far condition. Moving closer to the display increases the degrees of visual angle and results in a CSF shifted to the left. This effect may have been obscured in the far condition due to increases in noise in eye tracker data at greater distances. Regarding

the impact of ambient illumination, there was a minimal significant positive impact on mean sensitivity in the dark condition relative to the standard lighting conditions ($F(1,26) = 4.679$, $p = .040$), suggesting that a decrease ($10cd/m^2$) in screen luminance has a minimal impact on Curveball performance.

They also compared two Curveball results obtained from the same individuals with and without visual correction as a preliminary assessment of sensitivity to impairment. Their analyses found the Curveball task to be highly sensitive to improvements in refraction ($r(18) = -.890$, $p < .001$). This analysis was based on the evaluation of the shear parameter of an affine transformation, with more negative shear associated with greater impairment in visual acuity with the removal of corrective eyewear.

Taken together, these results provide initial support for the validity, reliability, and efficiency of the Curveball task. Some limitations exist with this task, including a high false-negative rate in individuals who were not able to track the stimuli quickly enough or maintain smooth pursuit adequately to reach their contrast threshold prior to the trial timing out. The average length of each trail was around five minutes. While this is significantly improved from standard measures, it was found in unpublished qualitative pilot trials with children with CVI that this was too lengthy a trial for them to adequately maintain engagement in the task.

Gradiate

The Gradiate task was designed as a follow-up to the Curveball task. Mooney et al. (2020) designed Gradiate to address some limitations identified in the initial study of Curveball and to improve upon the efficiency and accuracy of the psychophysical evaluation

of CS. The Gradiate task shares many similarities to Curveball in the basic principles of the task. An eye-tracking device is employed in the frame-by-frame analysis of smooth pursuit eye tracking to infer thresholds of vision for noise patches at a variety of spatial frequencies and contrast levels. There are several key differences between the two tasks. In the Gradiate task, five noise patch stimuli are presented simultaneously, and with successful tracking, each patch changes in both spatial frequency and contrast (see Measures section, "Gradiate Task" for a full explanation of the task). To make the task more engaging than the original Curveball task, a soundtrack was added, and a musical note was played as feedback to the observer with each successfully tracked step in the stimulus. These changes are intended to decrease the duration required to generate a CSF as well as generate a more robust estimation of the CSF by including more data points generated by the vector-based stimulus presentation.

In the introductory Gradiate study (Mooney et al., 2020) sixty healthy participants completed two experimental sessions, each consisting of two repeats of the full 15 point CSF Gradiate task and one trial of the low-contrast acuity (LCA) variation of the task. In the LCA variation trial, the contrast was constant at 0.06 RMS contrast, and only spatial frequency was varied in steps from 0.5 to 16.0 cpd. Thirty-eight participants with refractive correction completed two additional experimental sessions without corrective lenses. Six participants also completed a computer-based 4AFC staircase task, in which eight of the 15 radial sweeps used in the Gradiate tasks were presented at one of four cardinal points around a central fixation point on the screen. The stimuli used were the same size as those presented in the Gradiate task, presented on the same grey background, and scrolled within the fixed location on the screen at the same speed (5° per second) to capture the effects of motion in Gradiate.

They found the repeatability of the CSF to be high between sessions for all observers (CoR = 0.0562 $\log_{10}$ cpd). Repeatability was also found to be high between LCA thresholds and interpolated CSF thresholds (CoR = 0.055 $\log_{10}$ cpd), suggesting that the two methods of measurement are in good agreement. Gradiate was sensitive to visual impairment, especially in participants with more severe deficits in acuity. Overall, Gradiate generated normal and corrected to normal CSF curves with peaks around 1cpd, which falls between values produced by traditional psychophysical tasks (~0.6 cpd in moving tasks and ~2 cpd in static tasks).

Consistent with results from the initial Curveball study (Mooney et al., 2018), there were differences in the thresholds generated in the Gradiate and 4AFC task with higher CSs generated in the 4AFC task. Because the stimuli used in both tasks were the same, the authors suggest that this difference in CS may be largely related to the eye-tracking and smooth pursuit methodology in the Gradiate task. The authors suggest that it may be easier for observers to discriminate targets from the background than to track them reliably and smoothly. An affine transformation applied to the 4AFC results eliminated most of the difference between the results and reduced the correlation of repeatability from 0.0575 to 0.0473 in units of normalized sweep length, suggesting that the two tasks are measuring comparable visual abilities. It should also be noted that the 4AFC task took an average of 10 minutes and 15 seconds to generate a full CSF, while the Gradiate task took an average of 2 minutes and 14 seconds to generate a CSF.

Principal component analyses identified two orthogonal components related to CSF size (radius and slope) and two orthogonal components related to CSF shape (aspect ratio and curvature). Size-based components, radius and slope accounted for most of the variance in

the Gradiate CSFs. These two components accounted for 96.4% of the variance in peak CS and 97.3% of the variance in peak spatial frequency. Radius accounted for 73.6% of the variance in acuity and 47.3% of the variance in age in a linear regression. Radius was reported to be well correlated with sweeps that moved toward higher spatial frequencies and peaked with the 14th sweep (r = .973, p < .001), suggesting that in healthy participants, this single sweep could potentially provide an estimate of the overall CSF. Slope, unlike radius, was not correlated with age or acuity and accounted for 10% of the variance in participants with and without refractive error, suggesting that the slope of the CSF may be specifically sensitive to contrast sensitivity. Additionally, when taken together, the 1st, 3rd, and 14th sweeps predicted the slope factor with a correlation of .946.

Analysis of normalized CSF sweep length showed that shape-based components accounted for less overall variance than size-based components. Aspect ratio, which refers to the width-to-height ratio of the CSF, explained 55.41% of the variance and curvature, which refers to where along the CSF radius peaks, accounted for 10.84%, and both were correlated significantly with CSF radius and slope. Taken together, aspect ratio and curvature accounted for 67.0% of the variance in acuity. These components were also predicted by a small number of vector sweeps; aspect ratio was predicted by the 3rd and 14th sweeps (r = .953, p < .001), and curvature by the 2nd, 6th, 7th, and 14th sweeps (r = .932, p < .001).

Mooney et al.'s (2020) results suggest that the radial-vector based approach to CS measurement can reduce the time a participant must remain engaged in the task to generate a reliable CSF as compared with the Curveball task (15-point Gradiate CSF average time = 2 min, 14 s, 6-point Curveball CSF average time = 5 min, 15 s). No observers were eliminated due to insufficient tracking, suggesting that Gradiate can accommodate observers who

employ more frequent saccades in tracking moving targets. After accounting for the systematic variation in tracking versus discrimination-based tasks, the high level of agreement between Gradiate and the staircase task suggest that Gradiate provides a reliable estimate of CS. The identified size and shape-based CSF factors could be predicted with good accuracy from just a few of the vectors derived from the full curve, suggesting that accurate CS information could potentially be derived from an abbreviated version of the task in the future. The flexibility and reliability of the data will be especially relevant as the task is studied in impaired populations in the future and modified to better meet the needs and functional capacity of visually, physically, developmentally, and cognitively compromised individuals.

VEP Pilot Data

Pilot data evaluating preliminary agreement of Curveball with contrast-reversing (CR) and appearance-disappearance (AD) contrast sweep VEP responses were obtained from three observers. Results from VEP data revealed that the AD stimuli generally generated a low pass function and CR stimuli generated a more consistent peak. The peak CS for AD stimuli differed between all three observers ranging from 1.6 to 6.4 cpd. However, for all three observers, there was a sharp decline in CS from 12.5 to 25.6 cpd, and lower CS values at the highest SF than recorded in the CR condition. In the CR condition, peak CS was at 1.6 cpd for two observer's and at 3.2 cpd for the third observer. All three observers showed a steady decline in CS after peak CS had been achieved in the CR condition. Visual inspection of the CSFs revealed that CS estimates generated in the Curveball task were higher than

those obtained in either VEP condition across all three observers. The CSFs for the three participants can be seen in Figure 3.

Over the range of 6.4 to 25.6 cpd, two observers showed good agreement between CR and AD CSFs. However, this was not found for the third observer. Curveball CS estimates were consistently higher across all SFs for all observers, possibly due in part to the impact of higher luminance on the Curveball display and systematic differences between the two tasks. For all three observers, peak CS was found at lower SF in the Curveball condition than in either VEP condition. The range of spatial frequencies presented in the Curveball stimuli is limited to lower spatial frequencies than those presented in the VEP stimuli. However, in general, the peak CS in the CR condition was closer to that of the Curveball CS peak values than that of the AD condition. Additionally, the overall shape of the Curveball CSF appears to be more closely related to that of the CR condition than AD. Both Curveball and CR CSF have a bandpass shape.

Additionally, the CS values obtained under the CR VEP condition were generally higher than those obtained under the AD VEP condition at low SFs. These measurements, as well as the Curveball CS measurements at low SFs, appear to reflect involvement of a *transient* psychophysical mechanism that cuts off at low SF and is thought to implicate magnocellular pathway activity (Breitmeyer & Ganz, 1976; Merigan et al., 1991).

As a pilot study, these results suggest that CR stimuli may be more appropriate for use in comparison with CS generated by the Curveball task and in further evaluation of the mechanisms underlying the CSF generated by the Curveball task. There are a number of potential factors contributing to these observed differences in Curveball and VEP CSFs,

Figure 3

Pilot Data from Three Observers Comparing Contrast Sensitivity Functions from Curveball and Two Presentations of Contrast Sweep VEP Stimuli

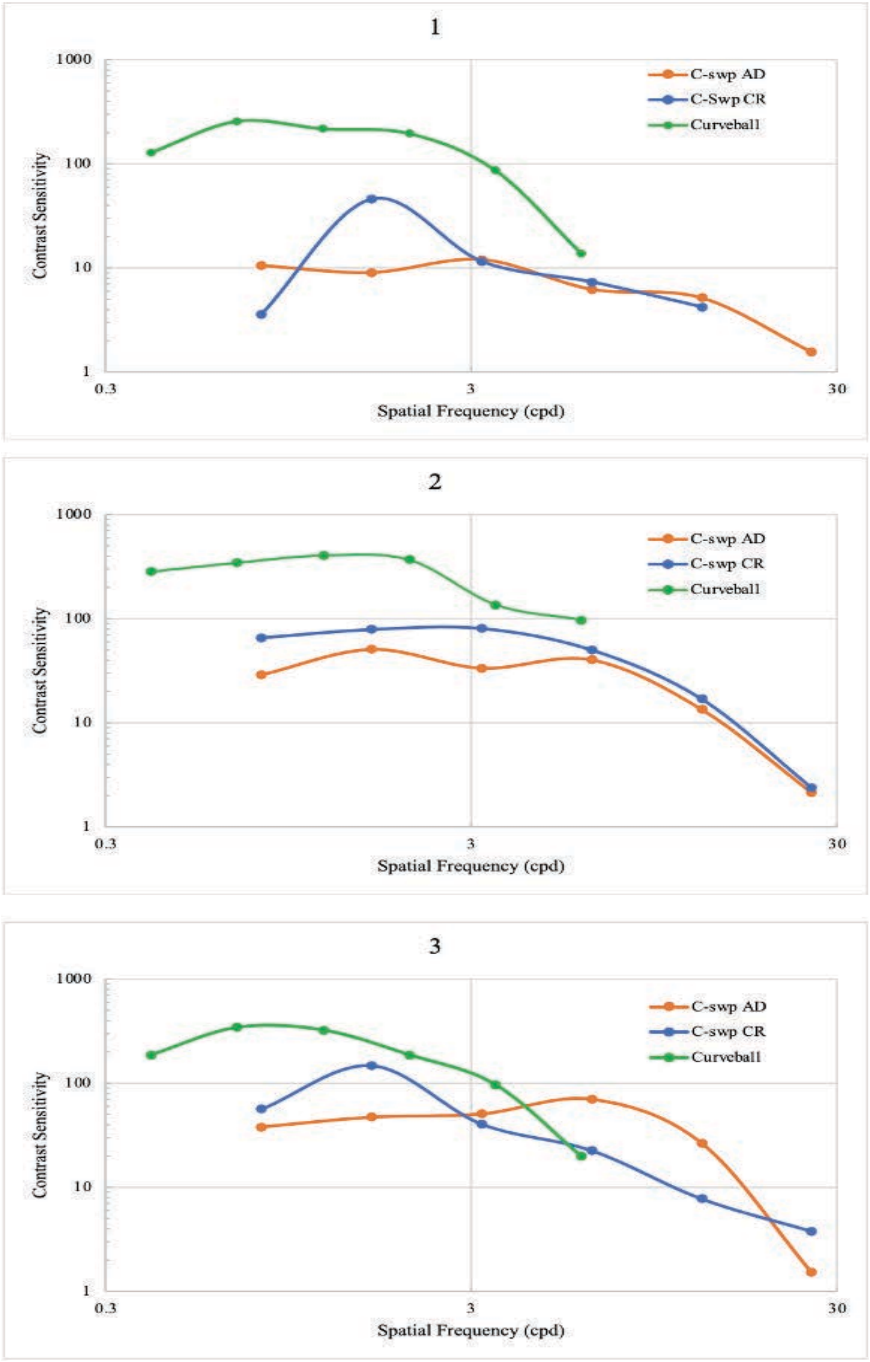

Note. AD = Appearance-Disappearance; CR = Contrast-Reversing: CR stimuli were determined to be preferable for CSF comparison with Curveball.

including background and surround stimulus luminance (Kelly, 1977; McCann & Hall, 1980), stimulus structure and presentation, varying definitions of contrast (Kukkonen et al., 1993), and fundamental differences between behavioral and electrophysiological response mechanisms.

The current study will expand on this to further explore the factors contributing to observed similarities and differences between Curveball, Gradiate, and VEP CSFs in a larger sample. This will allow for a more comprehensive exploration of the neurophysiological mechanisms involved in the Curveball and Gradiate tasks.

Rationale and Study Aims

The current study builds on this initial evidence supporting the viability of the Curveball and Gradiate tasks to further explore the potential of this innovative technology and validate its use in the assessment of contrast sensitivity and visual impairment. Specifically, the use of objective electrophysiological measures in the current study will provide a reliable evaluation of the parameters of visual function to compare with the Curveball and Gradiate psychophysical tasks used by Mooney et al. (Mooney et al., 2020; 2018), which can be limited by variability in response style, constraints associated with technology including eye-tracking devices and screen limitations, and the effects of environmental conditions on perception. Additionally, the use of VEPs in the current study will provide valuable information regarding the underlying neurophysiological mechanisms involved in the Curveball and Gradiate tasks that have not yet been assessed.

The goal of the current study is to measure and evaluate the agreement of CSFs using a steady-state contrast sweep VEP (swpVEP) and transient VEP (tVEP) techniques and the Curveball and Gradiate tasks in neurologically intact adults with normal and corrected-to-normal vision ($N = 15$). swpVEP is a validated method of measuring contrast sensitivity (CS) (Almoqbel et al., 2017; Lopes de Faria et al., 1998) and comparison with the psychophysically generated Curveball and Gradiate CSFs will offer insight into the differences of each system and serve to further validate Curveball and Gradiate, as well as highlight discrepancies between results generated with the two methods to explore underlying neurophysiological mechanisms. Specifically, the current study proposes to:

1. Aim 1: Evaluate the level of agreement between contrast sensitivity functions generated by contrast reversing swpVEP and the Curveball and Gradiate tasks as a means of exploring the underlying neurophysiological mechanisms implicated in the tasks as well as to assesses preliminary criterion validity of the Curveball and Gradiate procedures.

    Hypothesis 1: The CSF derived from steady-state swpVEP responses and the Curveball and Gradiate systems in participants with normal and corrected-to-normal vision are hypothesized to show good agreement at low spatial frequency as measured with Lin's concordance correlation coefficient ($\rho_c >$ .90, based on McBride (2005)), as both responses are hypothesized to be mediated by the magnocellular pathway at low spatial frequencies.

2. Aim 2: Compare visual acuity estimates generated from a Spatial Frequency Sweep VEP and the Gradiate task to further explore the neural pathways implicated in the Gradiate task.

Chapter 3. Methods

This study was conducted through a collaboration between the Laboratory for Visual Disease and Therapy at the Burke Neurological Institute (BNI) in White Plains, NY, an affiliate of Weill Cornell Medicine, and the Systems Neuroscience Laboratory at Ferkauf Graduate School of Psychology, Yeshiva University in the Bronx, NY, under the direction of Glen Prusky, Ph.D. and Vance Zemon, Ph.D. An ethical review of study protocols and procedures was conducted by the Biomedical Research Alliance of New York (BRANY) Institutional Review Board. The Institutional Review Board of the participating university (Ferkauf Graduate School of Psychology, Yeshiva University) granted approval to conduct this study and has approved the Biomedical Research Alliance of New York (BRANY) Institutional Review Board to oversee this study (Protocol BRC-452). All data were collected at BNI.

Screening/Recruitment

Participants ($N = 15$) were recruited through the Burke Neurological Institute. Due to BNI restrictions related to the COVID-19 pandemic, only institute faculty and staff working in person at the time of recruitment were permitted to participate in the study. Faculty and staff of the institution were invited to participate via email. All interested participants were asked screening questions to assess exclusion criteria prior to scheduling testing. Care was taken to protect the privacy of participants and adhere to all Health Insurance Portability and Accountability Act (HIPAA) regulations. All collected personal health information (PHI)

was stored in a locked cabinet in the Laboratory for Visual Disease and Therapy, accessible only via key card. Appropriate participants were scheduled for a single testing session.

Inclusion/Exclusion Criteria

All participants were required to be: 1) adults aged 18-70 years, with no history of neurological injury or impairment or neurodegenerative disease as assessed through self-report; 2) generally healthy; individuals with major or chronic illness, including metabolic disorders, cancer, cardiovascular disorders or neurodegenerative disease, were excluded; 3) have normal and corrected-to-normal vision; 4) excluded if taking psychotropic medications or with major mental illness as assessed by self-report; 5) excluded based on self-reported regular recreational drug use. Due to institutional COVID-19 safety policies, only BNI employees working in person at the time of recruitment were permitted to participate in the study.

COVID-19 Impact and Precautions

Due to the COVID-19 Pandemic, data collection for the current study was delayed significantly (~ 7 months), as BNI was closed to clinical work. The current study was the first human research study to take place after the reopening of the Institute and was used as a test of the implementation and efficacy of BNI COVID-19 safety protocols. COVID-19 symptom and exposure screening questions were asked at the time of scheduling and again the day prior to testing. Before entering the testing room, participants' temporal artery temperatures were taken using a no-touch infrared thermometer. Participants were required to complete a COVID-19 symptom and exposure screening form, hand sanitizer was

administered, and they were provided with an N-95 mask that was required to be worn at all times throughout the study.

Researchers wore a surgical gown, N-95 mask, face shield, and gloves at all times. All testing materials, pens, surfaces, chairs, and screens were disinfected before and after each testing session. Hand sanitizer and gloves were made available to all participants. All necessary contact information was collected for contact tracing. A two-week follow-up was conducted to assess for any potential COVID-19 symptoms after to the testing session. No participants reported experiencing COVID-19 symptoms or testing positive for COVID-19 at the two-week post-study follow-up.

Ethics and Data Security

Informed written consent was obtained from all participants. Prior to participation, all aspects of the study, including the purpose of the experiment, experimental procedures, and potential risks and benefits, were described in detail, and all questions were answered. Participants were informed of their rights and reminded that they were free to withdraw from the study at any time. All data were de-identified through the assignment of a number code unique to each participant. All protected health and personal information were stored in RedCAP, a secure online database, and any paper copies containing any PHI were stored in a locked cabinet only accessible to the study's principal investigators via keycard and key.

Risks and Benefits for Participants

There is minimal risk to participants in this study as both the VEP and Curveball/Gradiate procedures are noninvasive. The primary risk was possible slight scalp

irritation during the preparation of scalp sites for electrode placement. This was minimized by communication with participants, and administrators were trained in appropriate electrode placement procedures. There was potential for minor eye fatigue, which was minimized by frequent breaks and ensuring that testing was paced according to the participant's comfort level.

No direct benefits to the participants were gained from this study. Results were provided to individuals with some information regarding their visual functioning upon request. The primary benefit from this study is that it may provide preliminary support for greater use of eye-tracking tasks such as Curveball and Gradiate in the clinical evaluation of visual functioning, which could have the potential benefit of improving access to contrast sensitivity testing for participants in the future.

Equipment

Electrophysiological Recording of Visual Evoked Potentials

VEP stimulus presentation, recording, and analysis was done using the Neucodia system, Version 3.24 (VeriSci Corp., USA). Stimuli were presented on a 17-inch IBM 6737 C170 cathode ray tube (CRT) monitor powered by an Nvidia graphics card, with a refresh rate of 120 Hz, a spatial resolution of 800 x 600 pixels, and a mean display luminance of ~50 cd/m^2 (nits). Screen gamma was calibrated using an ILT1700 radiometer (International Light Technologies, Peabody, MA, USA). The overall stimulus field was 20 x 20 cm (512 x 512 pixels), which subtends a 10° x 10° visual angle at a viewing distance of 114 cm. An optically-isolated differential amplifier with a gain of 20K was used to prevent back current

and amplify the VEP signal, with a bandpass filter of 0.5 – 100 Hz. The Neucodia program was run from a desktop computer with a Windows 7 operating system.

Electrodes were placed at standard locations indicated by the ISCEV standards for recording of visual evoked potentials (Odom et al., 2016), and in accordance with the International 10/20 system. Three standard gold cup electrodes were used with the active electrode placed over the occipital cortex at Oz, a reference electrode placed at the vertex at position Cz, and a ground electrode at the front of the head at position Fz (Odom et al., 2016). Electrode locations were prepared with an alcohol swab and abrasive gel to lower the impedance, and electrodes were attached using a water-soluble electroconductive paste. Recording took place under dark conditions with no light disturbance, and electrical interference was minimized. Stimuli were presented binocularly to match the binocular presentation in the Curveball and Gradiate tasks.

Psychophysical Curveball and Gradiate Tasks

The Curveball and Gradiate tasks were administered using a 27-inch LCD Dell widescreen all-in-one computer mounted on a wheeled stand with an articulating arm. Screen luminance under average lighting conditions (well-lit room, fluorescent lighting) range ~10 cd/m^2 (black screen) to 221 cd/m^2 (maximum screen luminance). The computer was equipped with a display-mounted USB Tobii 4C eye tracker (Tobii Technology, Stockholm Sweden), which samples average gaze position at 90 Hz by combining binocular eye data. The stimuli were programmed in Python using the Shady graphics toolbox (Hill et al., 2019) and audiomath (Hill et al., 2021) and rendered at a frame rate of 60 Hz.

Gaze data were analyzed in real-time using the novel Curveball and Gradiate algorithms, "which measure the similarity between gaze and stimulus trajectories to infer stimulus visibility on a frame-by-frame basis" (Mooney et al., 2018). Participants were positioned at approximately 620 mm from the screen. The Tobii 4C eye tracker tolerates head movements, and the software was configured to pause the trial and display a warning message if participants were detected to be closer than 520 mm or further than 720 mm, or if their gaze strayed from the screen.

Stimuli

Electrophysiological Stimuli

For all VEP stimuli, recording continues until ten valid runs (no artifacts, interruptions, or unusual noise) were recorded for each spatial frequency, contrast level, or stimuli. The Neucodia system automatically detects and rejects runs in which noise or large electrical artifacts are above a threshold level. Participants were instructed to remain still and fixate on the crosshairs at the center of the display through each run. Participants were asked to do their best to refrain from blinking during stimulus presentations and were given time to rest their eyes between stimuli presentations to minimize eye strain and fatigue.

All VEP stimuli were presented binocularly to match the binocular presentation in the Curveball Task. For the periodic grating stimulus used in this study, the Michelson contrast metric is used. The Michelson contrast ratio defines contrast using the maximum and minimum luminance values as illustrated in the following formula:

$$\frac{Lmax - Lmin}{Lmax + Lmin}.$$

Contrast-Reversing Stimuli: A contrast sweep VEP paradigm was used to present square-wave contrast-reversing horizontal gratings of six spatial frequencies. The gratings were contrasted-reversed at a temporal frequency of 6.0 Hz, and contrast was increased over seven successive steps at the following values: 1, 2, 4, 8, 16, 32, and 64% (see Figure 4a). Spatial frequencies presented were 0.8, 1.6, 3.2, 6.4, 12.8 and 25.6 cycles per degree (cpd). Each of the seven contrast levels was presented for 160 frames, for a total recording time of 9.33 seconds per run at each spatial frequency.

Figure 4a

Example of C-swp VEP Stimuli Used in the Current Study

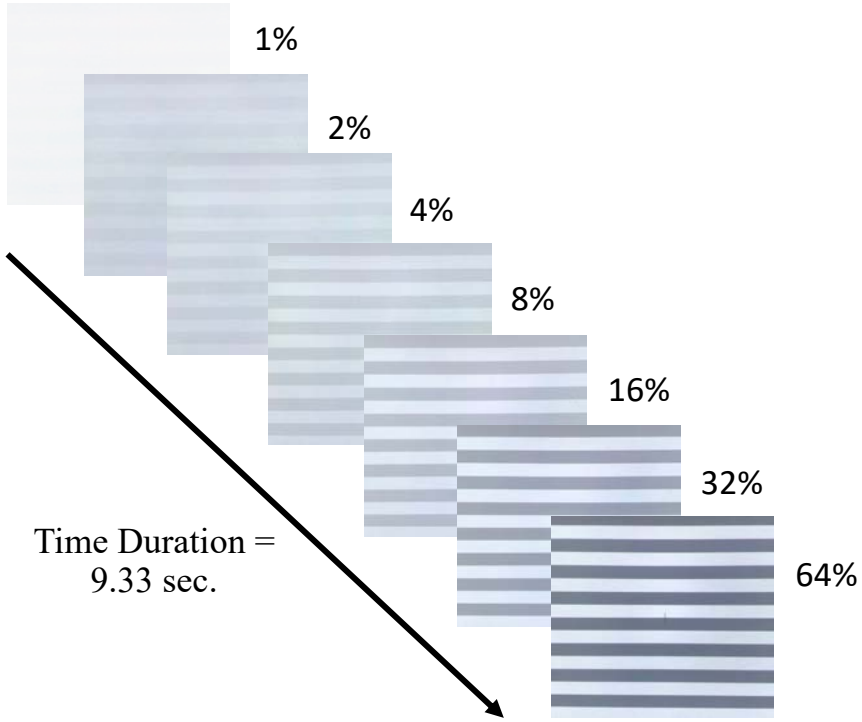

Note. Spatial frequency of 8 cycles per frame is shown.

Figure 4b.

Example of SF-swp VEP Stimuli Used in the Current Study

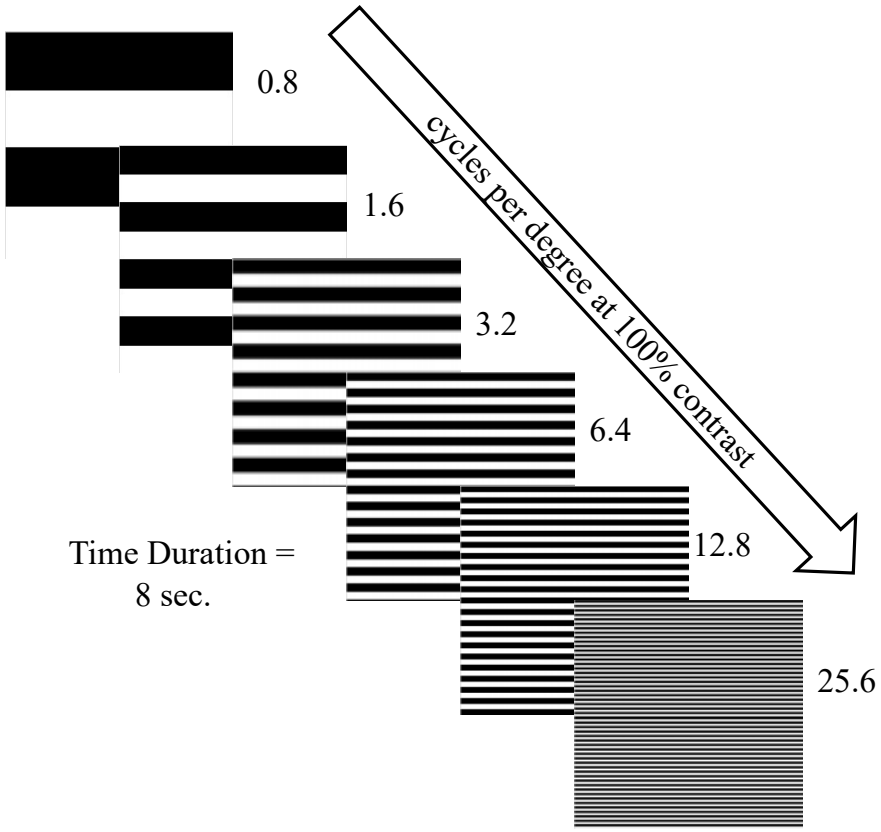

Spatial Frequency Sweep Stimuli: A contrast-reversing, spatial frequency-sweep, horizontal square-wave grating pattern was presented from coarse (low spatial frequency) to fine (high spatial frequency). The contrast was reversed at 6.0 Hz with a square-wave temporal signal and Michelson contrast (see formula above) fixed at 100%. During a single sweep, the spatial frequency of the horizontal gratings was varied in the following six octave steps, 0.8, 1.6, 3.2, 6.4, 12.8, and 25.6 cpd (see Figure 4b) Each step was presented for eight cycles for a total recording time of eight seconds per run.

Psychophysical Stimuli

Curveball. In each trial, a noise patch of narrow-band spatial frequencies is presented on a screen with a uniform grey background with 0.5 normalized display luminance (63.5 cd/m^2). The noise patches are generated by the application of a circular-symmetric Hann window to a filtered noise pattern, subtending 12° of visual angle and appeared at a random location on the screen (see Figure 5). The patch then moved smoothly and randomly around the screen at a fixed speed of 10° per second, which Dakin and Turnbull (2016) have found to be the optimal speed for smooth pursuit tracking. To eliminate the effects of temporal aliasing at high spatial frequencies, the patch is filtered with an anisotropic filter. The

Figure 5

Example of Curveball Stimulus

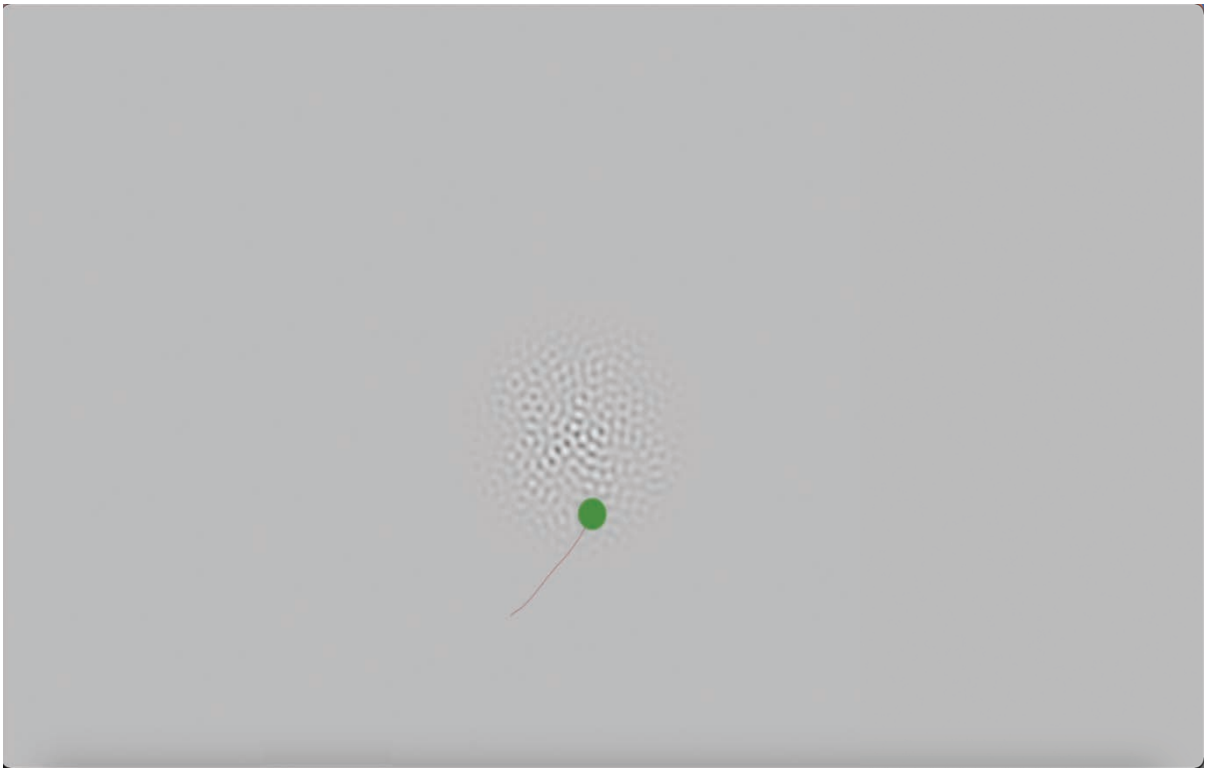

Note. The green dot and red line show the gaze position and gaze trajectory of the observer.

anisotropic filter removes Fourier components with horizontal spatial frequencies greater than 5.7 cpd. Additionally, the stimuli were continuously rotated to keep this anti-aliasing filter consistent with the direction of motion.

At the start of each trial, a cartoon ghost appears over the noise target as means of quickly drawing the participant's attention to the new target location without the need for instructions. Once the participant's gaze comes within 5° of the target, the ghost fades out, and the algorithm begins evaluating for smooth pursuits by continuously comparing the participants gaze trajectory with that of the moving noise target, which must fall within 5° of the outside edge of the target to be accepted as tracking, after five consecutive frames of successful tracking, the contrast of the noise target will begin to reduce logarithmically for as long as the smooth pursuit continues. If there is an interruption in smooth pursuit for even one frame, the contrast reduction is discontinued, and the algorithm waits for another five frames of successful pursuit before continuing to decrease contrast.

The contrast is reduced until the participant is no longer able to follow the target. The trial is terminated when the participant is no longer able to pursue the target for at least one of every seven frames. The reciprocal of the noise target's final *root mean squared* (RMS) contrast is recorded as the contrast sensitivity at the target's spatial frequency. The next trial begins immediately with a new stimulus and cartoon ghost.

In each Curveball run employed in this study, seven spatial frequencies were presented: 0.25, 0.5, 1, 2, 4, 8, and 10 cpd, with each repeated twice. The mean contrast threshold of the two trials was used to determine contrast threshold estimates. A total of 14 noise patches were presented.

Gradiate Single and Gradiate Full. As in Curveball, the Gradiate Single (GR-S) and Gradiate Full (GR-F) tasks also employ patches of filtered noise which are moved smoothly and randomly around the screen with a uniform grey background with normalized display luminance of 0.5. Figures 6a and 6b show examples of the stimulus presentation in the GR-1 and GR-F tasks. The GR-1 task presents noise patches one at a time, while the GR-F present five noise patches simultaneously.

Figure 6a

Example of Gradiate – Single (GR-1) Stimulus

Note. The green dot and red line show the gaze position and gaze trajectory of the observer.

Figure 6b

Example of Gradiate – Full (GR-F) Stimuli

Note. The green dot and red line show the gaze position and gaze trajectory of the observer.

Like Curveball, the noise patches presented in the Gradiate tasks are created using a circular-symmetric Hann window applied to a noise pattern (1/*f* amplitude spectrum and random phase). Each noise pattern is filtered with a band-pass filter centered on the target spatial frequency with a constant width of 0.34 octaves. As with Curveball, to eliminate the effects of aliasing, the patch is filtered and continuously rotated to keep this anti-aliasing filter facing the direction of motion. In both Gradiate tasks, the stimuli presented are smaller than those presented in the Curveball tasks, subtending 6° of visual angle at the same viewing distance of 620 mm.

The most significant difference between the Gradiate tasks and Curveball is the way contrast and spatial frequency are presented. In Gradiate, the noise patches change concurrently in both contrast and SF in discrete steps with successful smooth pursuit, and it

continues to decrease in contrast and increase in SF until the observer is no longer able to track the patch smoothly. SF cannot be smoothly transitioned as contrast can, and as such, the SF of the noise patches is changed in steps. Tracking behavior in the split-second steps between changes in SF and/or contrast is excluded from the evaluation of contrast thresholds.

Stimuli spatial frequency and contrast content are determined and progress along with a set of predefined radial vectors that originate from a common point. The vectors extend at equal angles from the common starting point within a linear transformation of the log-log CSF space, determined through unpublished pilot testing to fit a normative CSF with a circle radius of 0.5. The parameters of the space were defined such that point (0,0) reflects the log-log value of (0.25 cpd, CS = 5), and point (1,1) reflects the log-log value of (12 cpd, $10^{3.5}$ CS). Within this space 15 sweep vectors were defined, with all vectors starting at the point corresponding to (SF = 1 cpd, CS = 5) or a starting RMS contrast ratio of 0.2. The 15 vectors are spaced evenly between polar angles of 109.703° and 0° with an interval of 7.836°. Each of the 15 radial sweep vectors was divided into 16 steps, each corresponding with a set spatial frequency and contrast of a single narrow-band noise stimulus, produced using the process described above. Figure 7a shows a representative GR-F output. Each vector line reflects the stepwise changes in SF and C for a noise patch and the threshold determined for that stimulus along the vector. This can be compared with representative CB output seen in Figure 7b, wherein the CSF is based on CS at a set of predetermined SFs.

Figure 7a

Representative Example of a Gradiate – Full Output.

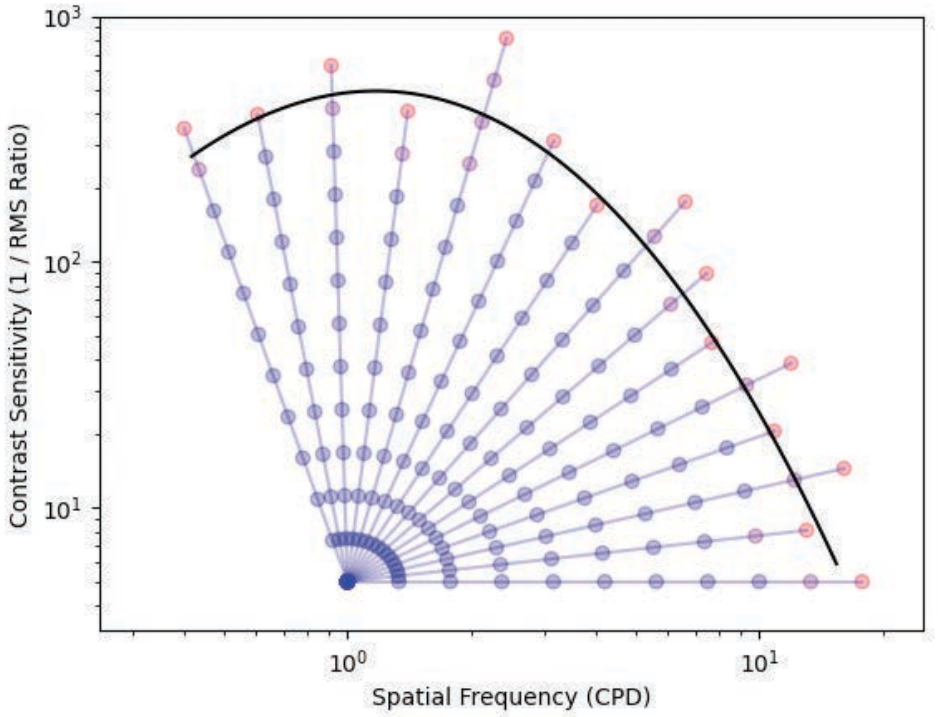

Note. Each blue line reflects a vector at a set angle. The points along the vector reflect a change in SF and C of the noise patch. The blue points are successfully tracked stimuli and the red points are unsuccessfully tracked stimuli. The CS for each vector is calculated as the mean of the value of the last blue and first red point on each vector. The black line reflects the CSF curve fit to the CS estimates determined along each vector.

Figure 7b

Representative Example of a Curveball Output

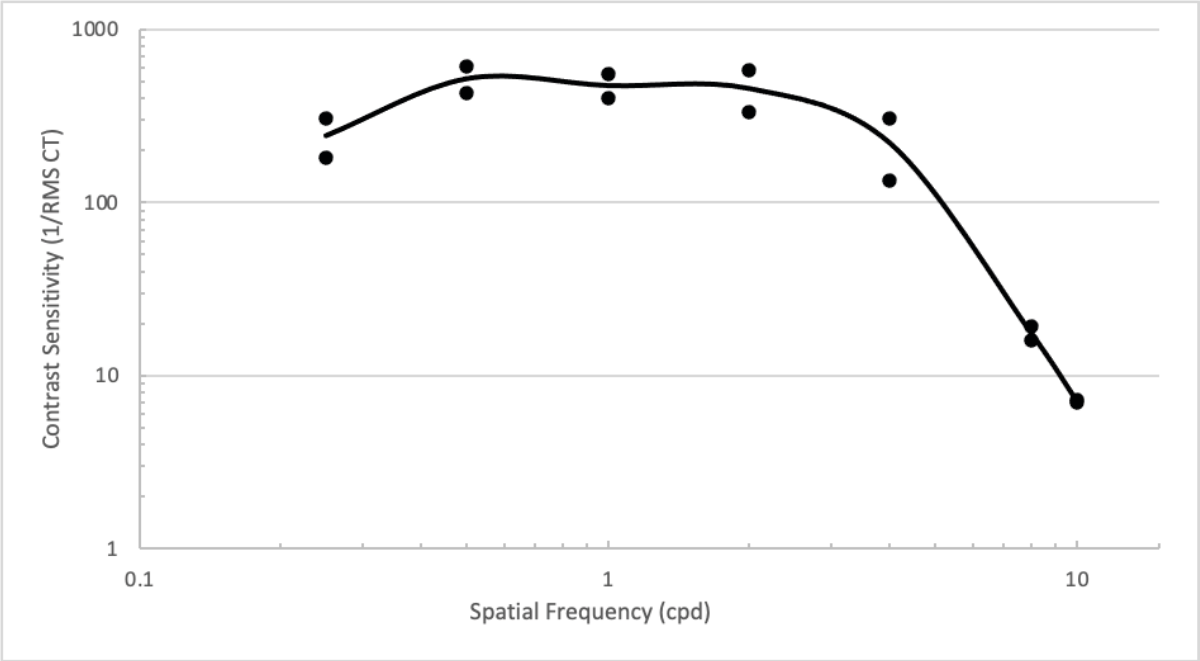

Note. The points at each SF reflect the CS estimate generated in each trial. The CSF curve is determined as the mean of the linear CS of both trials.

In the GR-F task (the same task described by (Mooney et al., 2020) five noise patches are presented simultaneously at the outset of each trial. The observer can choose any one of the five patches to start tracking and can move between noise patches at will. The motion of the five target noise patches is coordinated by a grid motion system which rules set to ensure that targets do not overlap or obscure one another, repeating movements, or moving synchronously. Each target moved around the grid, making 90° turns at semi-random intervals. If no movement was possible for a given target, it remained still until movement was possible, and no tracking was recorded until motion resumed. A trial is concluded when the observer has successfully tracked all five targets to the point where they are no longer visible. In GR-1, one patch of noise is presented on the screen at a time, following the same

movement rules utilized in GR-F. The participant must track that single noise patch until a threshold is generated before the next noise patch will be displayed.

The algorithm for inferring stimulus visibility is changed in the Gradiate task to accommodate observers who employ more frequent saccades in maintaining smooth pursuit to address the difficulties with the high false-negative rate in the original Curveball task. Target visibility was inferred in real-time by a continuously updating evidence counter tracking the relationship between the position of the target and the observer's gaze point. The threshold for error in gaze position was the radius of the stimuli (3°) with an additional 2° region surrounding the stimulus. Positional tracking error was calculated as the sum of the relative difference between the target and the gaze point over eight frames. Trajectory tracking error was calculated as the sum of the distance between the gaze point and target over the same eight frames after subtracting the previous gaze-target differences from each of the eight gaze points. This creates a much stricter trajectory-based error threshold of 0.4°. The combination of a strict trajectory detection and more liberal position detection increases the tolerance for eye tracker calibration and differences in tracking style.

Smooth tracking was inferred if gaze samples met both positional and trajectory conditions. An evidence counter kept track of whether criteria were met for smooth tracking on a frame-by-frame basis. For each frame that met positional and trajectory criteria the evidence counter banked five units or points. These points have no unitary value other than to keep a running tab of smooth tracking progress for each patch of noise. The evidence counter was progressed by five units per frame until 100 units of evidence were collected as evidence of the visibility of a specific target. If neither condition for smooth tracking was evident, the evidence counter decayed by 1 unit per frame to a minimum of zero. Once the evidence

counter reached 100 units, the appearance of the target was immediately updated by altering its spatial frequency and/or contrast by one step along the predetermined vector in CSF space. The evidence counter for that target was reset to zero, and the process began again. A separate global evidence counter concurrently tracked gaze to determine when no stimulus was visible to the observer, and the trial was terminated when the global evidence counter reached -300.

Contrast thresholds were determined for each target as the point halfway between the point representing the last successfully tracked spatial frequency and contrast and the current unsuccessfully tracked step along the vector in log-log space.

Gradiate also incorporates audio feedback and a points system to promote engagement. Successful tracking at each step of the SF and contrast vector is followed by a random note sound to indicate successful completion, and this makes the task more engaging for observers. When an observer has tracked each patch of noise to the point where it is no longer visible, they will then begin tracking another of the five noise patches until all five noise patches are no longer visible on the screen and the trial ends. At the end of each trial, the observer is shown how many “notes” they achieved as a reflection of how accurately they were able to track the stimulus as a motivating factor (see Figure 8).

Figure 8

Example of Feedback and Score Presented Following the Gradiate Tasks

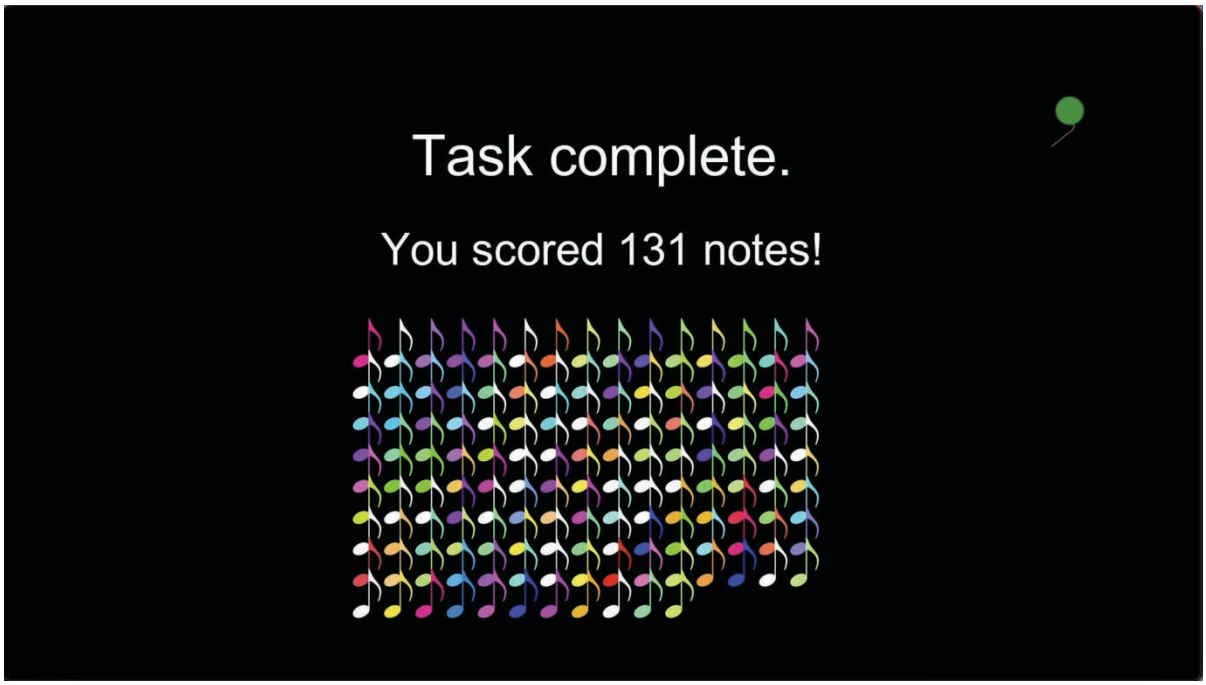

Note The number of notes earned reflects the number of successfully tracked stimuli.

Testing Procedure

All testing took place at the Burke Neurological Institute (BNI), and all testing materials, supplies, and equipment have been provided by the Prusky Laboratory for Visual Disease and Therapy at BNI. Prusky lab employees and graduate students were exclusively involved in recruiting, screening, obtaining informed consent, collecting demographic information, and administrating the VEP battery and Curveball and Gradiate tasks. COVID-19 contact tracing was maintained, and all participants completed a follow-up COVID screener at two weeks post participation. Participants came for a single testing session that lasted approximately 90 minutes. Participants completed a COVID screener at the time of

scheduling and were informed of all necessary COVID precautions and requirements for the testing session.

Testing took place in a quiet room at the BNI, under appropriate lighting conditions for each task (lights off for VEP; lights on for Curveball and Gradiate). The session was begun by obtaining fully informed consent and completion of a screener to collect additional demographic information and ensure that they still meet inclusion criteria. Participants were provided with a copy of their signed consent form and COVID-19 screening form. LogMAR (log of the minimum angle of resolution) visual acuity was assessed binocularly at the start of both the VEP and CB/GR testing as the two tasks are performed at different distances. Visual correction for participants requiring it was worn during testing. Participants first completed a modified Tumbling E (Taylor, 1978) acuity measure, viewed at 62 cm to ensure normal or corrected-to-normal vision, before performing the psychophysical tasks. Participants completed the Curveball task first, followed by Gradiate – Single and then Gradiate – Full. All participants were instructed to look and follow only at whatever appears on the screen.

After a short break, scalp electrodes were placed, and participants completed a second acuity measure using an onscreen modified Snellen eye chart available through the Neucodia system, viewed at a distance of 114 cm. The VEP battery was conducted in the following order: contrast-reversing horizontal grating contrast sweep, contrast-reversing horizontal grating spatial frequency sweep, appearance-disappearance horizontal grating transient. VEP recording was paced according to the participant's comfort and ability to remain focused on the stimuli. Participants were given breaks whenever necessary to reduce eye fatigue. Following VEP recording, electrodes were removed, and alcohol and water wipes were used

to remove residual electrode gel from the participant's scalp, and they were given the opportunity to ask any additional questions.

Data Analysis

CSFs were generated using data from steady-state contrast swpVEP and transient VEP recordings as well as with Curveball and Gradiate tasks. Acuity estimates were derived from SF swpVEP, contrast swpVEP, and Gradiate. Results from all measures were analyzed as outlined below.

VEP-determined CS

The Neucodia system performs a discrete Fourier transform (DFT) on the collected VEP data. The DFT was applied to extract the harmonic frequency component of interest. In the case of the contrast-reversal ssVEPs, this was the second-harmonic component in the swpVEP response. In the case of appearance-disappearance transient VEPs, a particular frequency band of interest was used. Statistical analyses (T^2circ, magnitude-squared coherence (MSC), and *F* tests) were performed to test for significant responses and for measures of the relative strength of response (Zemon et al., 1997).

The ten individual responses obtained during each VEP test were analyzed by calculating the sine and cosine coefficients, and a vector-mean amplitude and phase was derived. In addition, the T^2circ statistic was used to obtain a 95% confidence circle around the vector-mean response, and it was used to specify an estimate of the variability in amplitude (amplitude error) and phase (phase error). Signal-to-noise ratios (SNR) were

calculated by taking the ratio of vector-mean amplitude to the radius of the 95% confidence circle.

From the SS Cswp responses for each individual, VEP contrast thresholds at each SF were estimated by interpolating the contrast response function to an SNR = 1. The interpolation was completed using the following formula:

$$CT = \frac{C_{low} + (C_{high} - C_{low})(1 - SNR_{low)}}{SNR_{high} - SNR_{low}}$$

Contrast sensitivity (reciprocal of contrast threshold) was plotted as a function of SF to generate CSFs for all participants. In cases where there was no contrast step response with a SNR above 1 for a particular SF, that SF was omitted from analysis.

VEP Acuity Estimates

Grating acuity estimates were obtained from the spatial frequency swpVEPs through linear interpolation (or, if necessary, linear extrapolation using the two highest spatial frequency points) to an SNR = 1 (criterion for significant response at .05 level) done in the Neucodia system (See Figure 9 for an example response output). Grating acuity estimates were also calculated from the contrast swpVEP through linear extrapolation of the CSF to a CS of 1. In cases where the C-swp VEP generated a signal at all six spatial frequencies, SF_x = 12.8 and SF_y = 25.6, and their corresponding CS values were used in the linear extrapolation. In cases where the highest SF (25.6 cpd) did not generate a response, values were shifted to the two preceding highest SFs (6.4 and 12.8 cpd) and their corresponding CSs.

Figure 9.

Representative SF-swp VEP Output

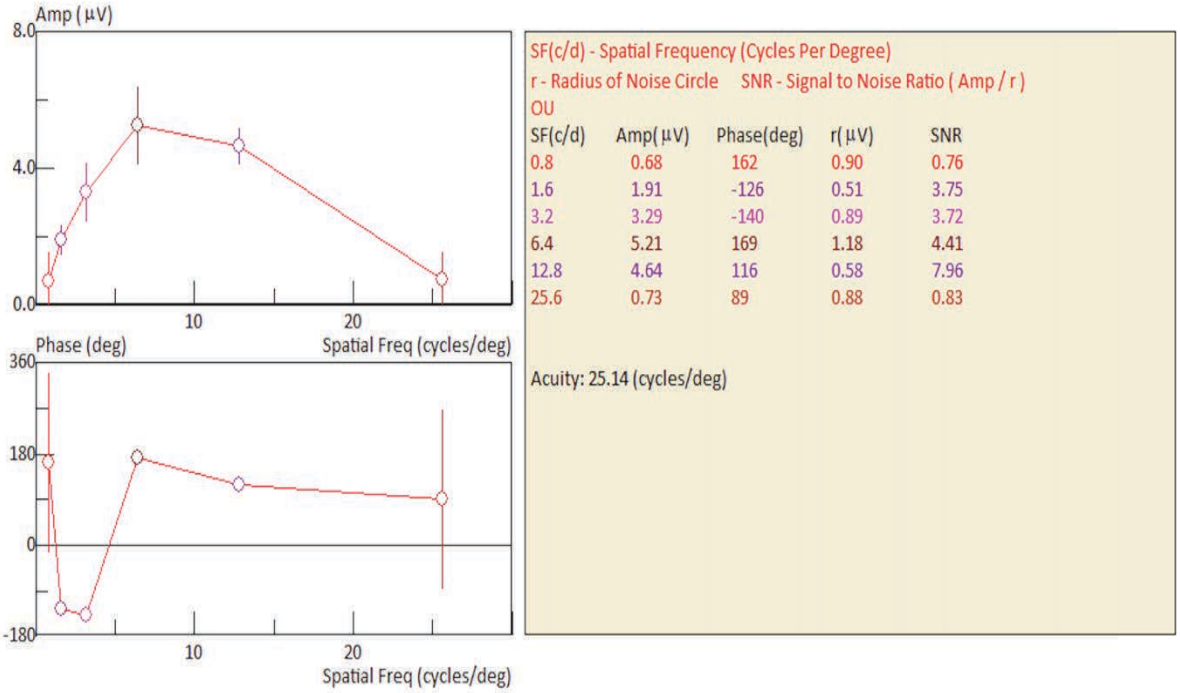

Note. The SNR is shown at each SF step. The response amplitude is plotted by SF in the top graph. The lower graph is a plot of the signal phase by SF. The grating acuity estimate shown on the right is generated based on extrapolation of the response to a SNR of 1.

Curveball and Gradiate Analysis of CSFs

The Curveball algorithm calculates CS at each spatial frequency as the mean of the two lowest contrast thresholds. The Gradiate system calculates CS as the mean of the last successfully tracked stimuli and the subsequent failed stimuli. The contrast ratio determined by the CB and GR algorithms is corrected to account for the physical luminance properties of the screen by applying the following correction:

$$C^i = \frac{c\ x\ b}{b + \frac{m}{M - m}}$$

, where C^i equals the adjusted contrast ratio, c is the calculated contrast ratio, b is equal to the normalized background luminance of 0.5 (63.5 cd/m^2), m is the minimum luminance of the screen, which was determined to be 10.0 nits, and M is the maximum luminance of the screen, determined to be 221.0 nits (1 nit = 1 cd/m^2) At the end of all runs, the algorithm automatically compiles the data to generate a CSF based on contrast thresholds calculated at each spatial frequency (Mooney et al., 2020; Mooney et al., 2018).

All Curveball and Gradiate CTs were converted from RMS contrast to Michelson contrast (MC) to allow for easier comparison to VEP results. This was done using the following conversion:

$$CS_{mc} = \frac{CS_{rms}}{\sqrt{2}}$$

as done in by Kukkonen et al. (Kukkonen et al., 1993). As seen in Kukkonen et al. (1993), this conversion did not alter the shape of the curve but simply translates RMS values down by a factor of $\sqrt{2}$, as is illustrated in Figure 10. All CB and GR values used in the analysis were converted to MC for consistency and to reduce the impact of differences in contrast definition on results.

Figure 10

Demonstration of RMS to Michelson Contrast Conversion

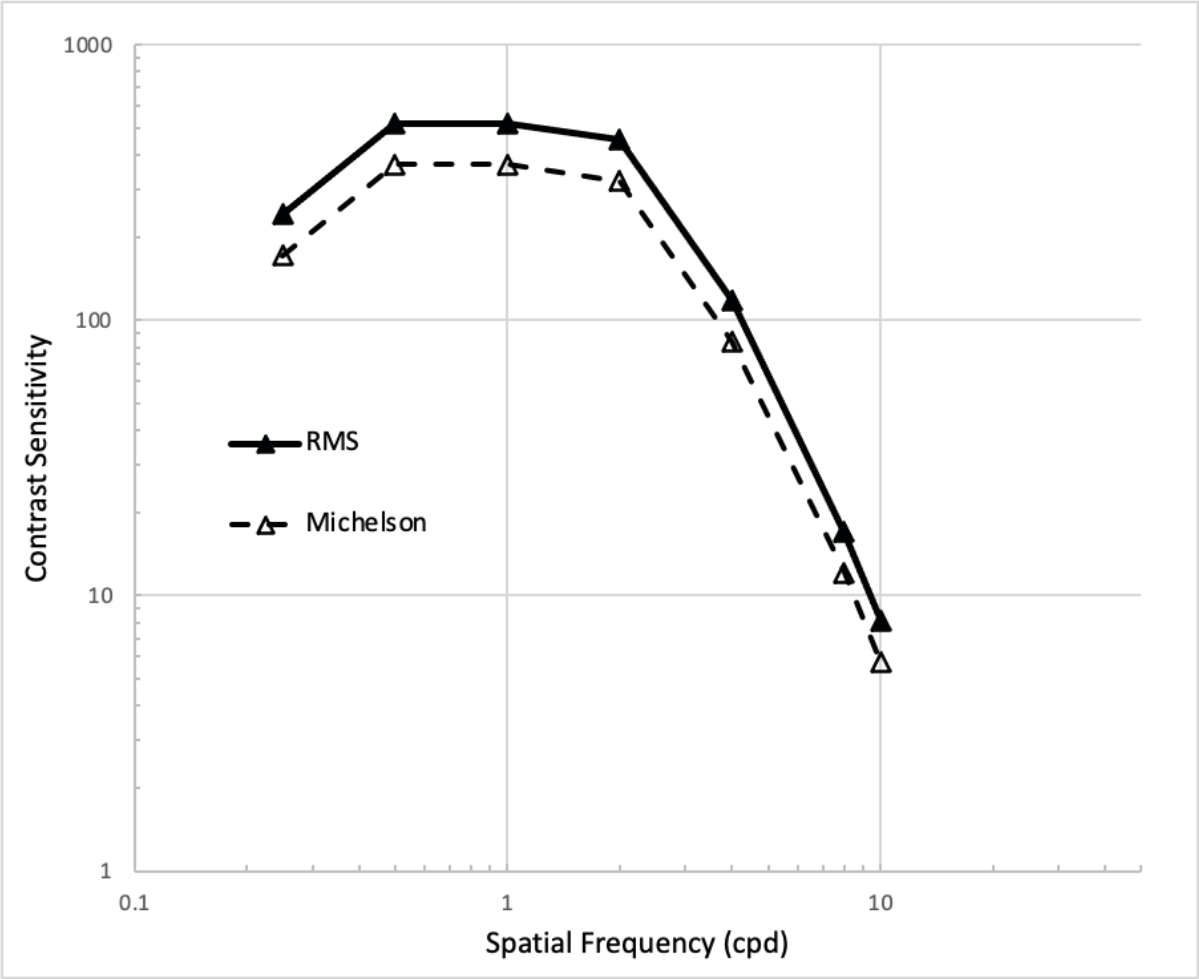

Note. The RMS curve is shifted up by a factor of $\sqrt{2}$.

Aims and Hypotheses

Aim 1: Evaluation of agreement between CSFs generated by swpVEP and Curveball and Gradiate tasks.

Descriptive statistics, including means, standard deviations, frequencies, and normality measures, were collected for all variables of interest and calculated across the

sample. Correlational analysis was completed using SPSS and Jamovi. Normality and linearity were assessed and corrected for prior to analysis. Lin's concordance correlation coefficients were calculated using syntax created in Excel (Lin & Torbeck, 1998; Watson & Petrie, 2010).

$$r_c = \frac{2r\, s_x\, s_y}{(\bar{x} - \bar{y})^2 + s_x^2 + s_y^2}$$

Bivariate correlational analysis was conducted, and Pearson's *r* statistic was evaluated for closely matched spatial frequencies. Although this method is not ideal for assessing agreement, it is included based on its use by Mooney et al. (2018) and multiple previous studies evaluating the agreement between CSFs generated by VEP and other psychophysical measures (Allen et al., 1986; Cannon Jr, 1983; Souza et al., 2007).

Aim 2: Evaluation of agreement between acuity estimates derived from the electrophysiological response and the Gradiate task.

Descriptive statistics, including means, standard deviations, frequencies, and normality measures, were collected for all variables of interest and calculated across the sample. Differences between acuity estimates derived from each task were calculated for all participants. t-tests were conducted to assess relationships between difference scores for each measure across the sample. Bland-Altman plots (Bland & Altman, 1986) were generated as well, using SPSS Chart editor and Jamovi, by calculating the difference scores between the CS values measured by each system at each spatial frequency as well as the mean of all measurements and plotting the difference as a function of the mean. This method of analysis reflects the level of agreement of the two methods and offers a more comprehensive evaluation than correlational measures alone. Additionally, Lin's concordance coefficient

was calculated for each of the measures. This is believed to provide a better estimate of relationships in small sample sizes.

Power Analysis

G*Power software was used to determine an adequate sample size based on bivariate correlation analysis. Alpha was set at .05, two-tailed, with an effect size of $r = .50$ as suggested by Cohen (1992) as typical for a large effect size. Power was set to .80 as a conservative estimation of power, with a sample size of $n = 24$ necessary to achieve this. Similar studies utilizing VEP responses to explore psychophysical measures have done so successfully with as few as three participants (Campbell & Maffei, 1970).

Chapter 4. Results

Study Sample

Of the 21 participants recruited for this study, 19 completed all electrophysiological and psychophysical measures. One participant's data were excluded due to meeting exclusion criteria post study, two were excluded due to equipment failure that corrupted the VEP recordings, and one additional participant was excluded due to insufficient response data. Data from 15 participants were included in the final analysis. Demographics information for included participants can be found in Table 1. Binocular visual acuity was measured at 114 cm and 62 cm for all participants, and all participants were found to have 20/20 acuity or better at both viewing distances.

Aim 1: Evaluate level of agreement between contrast sensitivity functions generated by contrast-reversing swpVEP and the Curveball and Gradiate tasks.

Steady-State Contrast-Reversing Contrast Sweep VEP

A representative VEP output for a single SF can be seen in Figure 11. Second harmonic SNR values were used to interpolate CTs and calculate CS at each SF for each participant. The $\log_{10}$ of the CS value was calculated and used in all analyses to maintain consistency with CB and GR values. Table 2 displays the mean, median, standard deviation, and range for the $\log_{10}$ CSs extrapolated from the C-swp VEP for all participants at each of

the included SFs. All participants generated interpretable responses for SFs of 0.8, 1.6, 3.2, 6.4, and 12.8 cpd. At 25.6 cpd only seven participants generated responses with a SNR above 1. CTs were interpolated for these participants at 25.6 cpd and this SF was omitted from the CSF for the remaining eight participants.

Visual examination of individual C-swp VEP CSFs revealed sizeable variability among participants, which is expected in VEP recording. Table 3 displays normality statistics for the C-swp measures. Based on these statistical analyses and visual examination of the frequency distribution and assessment of normality, it was determined that the data are within acceptable limits and the VEP measures represent valid data and are appropriate for further analyses.

Figure 11

Representative Example of C-swp VEP Output at 6.4 cpd

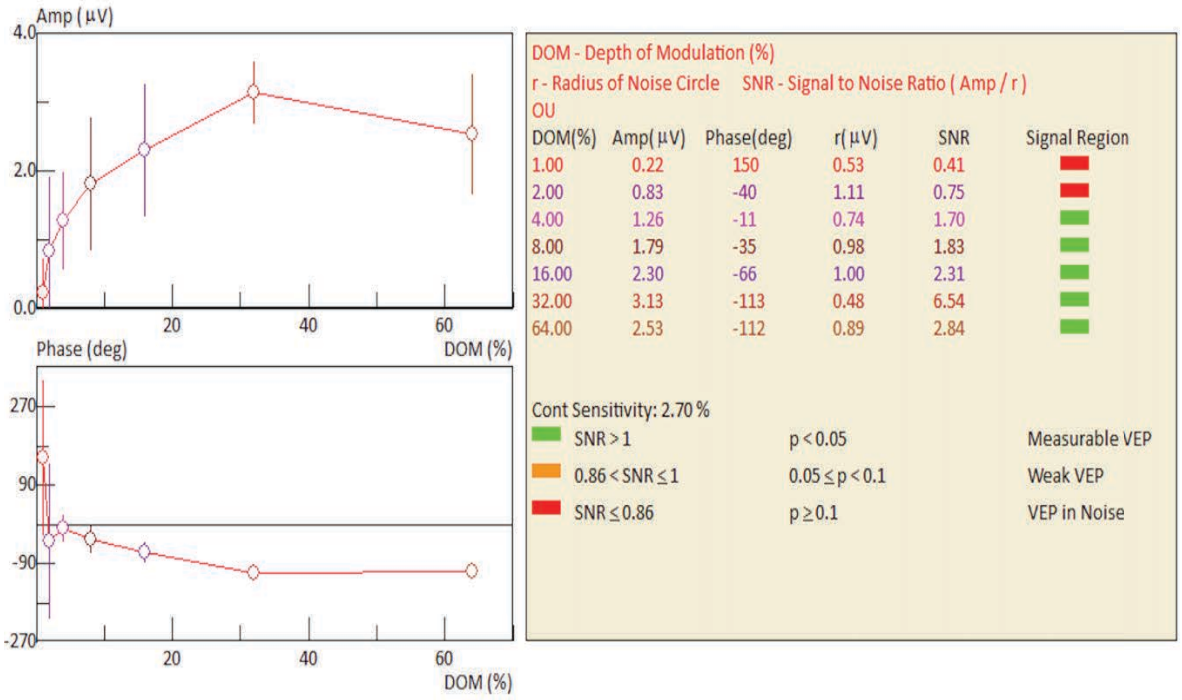

Figure 12

Boxplot of C-swp VEP Contrast Sensitivity Estimates by Spatial Frequency for 15 Participants

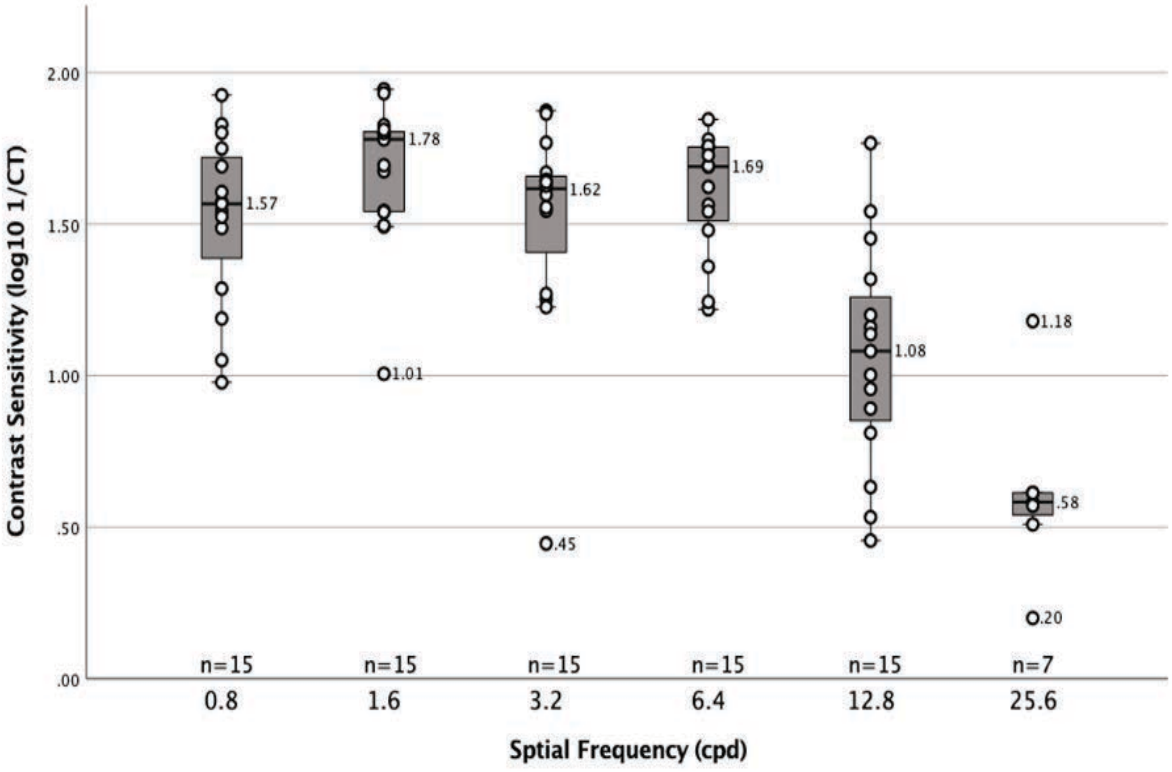

Figure 12 shows the $\log_{10}$ CS for each participant at each SF displayed as a boxplot to highlight the individual variability and median responses of the C-swp CSFs. The overall shape of the responses is similar to that seen in Figure 2, where the slope of the curve is flatter between 0.8 and 6.4 cpd and then drops sharply between 6.4 and 25.6 cpd. There was one outlier at 1.6 cpd and one at 3.2 cpd from different participants. Given that the other points for these participants were within normal limits, these points likely reflect aberrant responses. At 25.6 cpd only seven participants generated responses distinguishable from noise. Of these, there were two outliers. One participant generated a significantly higher $\log_{10}$ CS than expected and one significantly lower. At the highest spatial frequency, 25.6 cpd,

many individuals are beyond or near their limit of spatial vision and as such the VEP response is weaker at this point. This suggests that the two points with higher and lower responses are likely impacted by noise.

Curveball Task

Curveball CS estimates were generated for all participants at each of the seven SF steps. CS estimates for all observers at each SF can be seen in Figure 13. The boxplot reflects the overall shape of the CSF curve across all participants. Outlier points are labeled with their log CS value. The CS estimates generated by the Curveball algorithm were converted to MC contrast and the $\log_{10}$ of this CS was used in all analyses. Table 4 displays the mean, median, standard deviation, range, and normality and distribution for the $\log_{10}$ CS for all participants at each of the included SFs.

Figure 13

Boxplot of Curveball Contrast Sensitivity by Spatial Frequency for 15 Participants

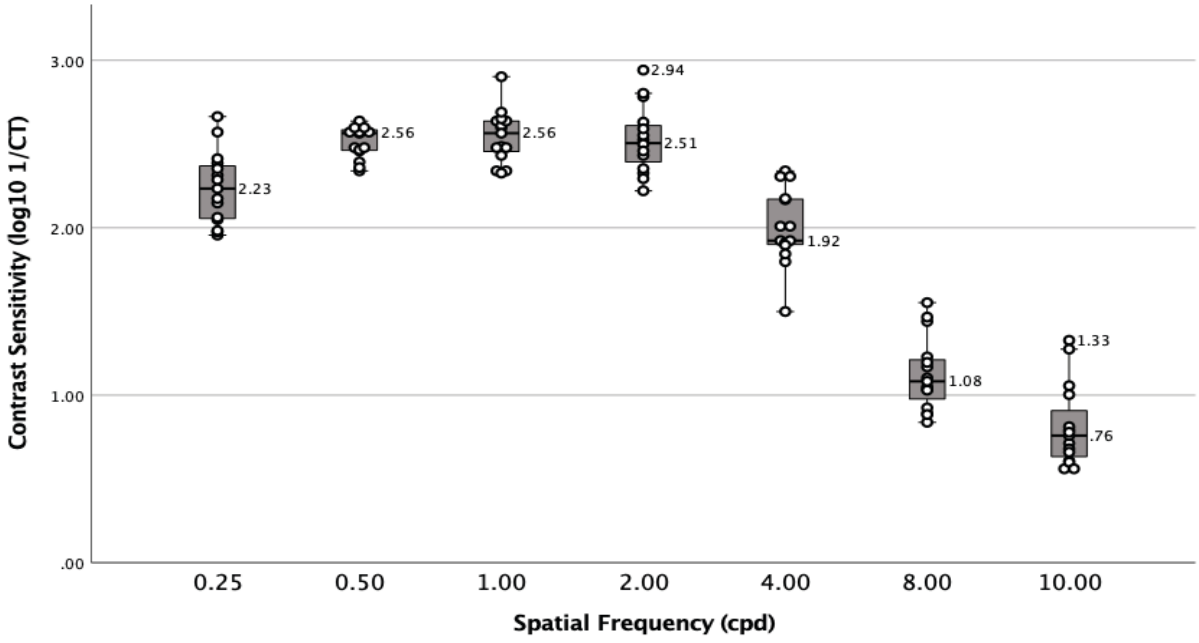

Gradiate Single and Full

CS estimates were generated by the Gradiate tasks based on the 7 or 15 vector angles that comprise the GR-S and GR-F tasks respectively. The vector angle was consistent across participants for each task. The SF and CS generated for each participant at each vector was determined based on their performance and how they progressed along a given vector. The SF and CS at each vector angle varied from participant to participant based on the point at which they were not able to successfully track the stimuli. The variation in CSF SF points made it difficult to compare individual CSs across participants. Figures 14a and 14b show the variation in SFs defined for each vector for all participants. The 0.00° angle represents the horizontal axis along which only SF is altered from step to step. This vector reflects the threshold of spatial resolution and greater variability is expected as stimuli approach threshold levels. As was illustrated in Figure 7a, increase in vector angle indicates that the stimuli contain increasingly high contrast and low SF content and are likely to be more readily tracked. This is seen in Figures 14a and 14b; as vector angle increased variation in CS decreased.

Figure 14a

Boxplot of GR-1 Spatial Frequency Thresholds by Vector Angle for 15 Participants

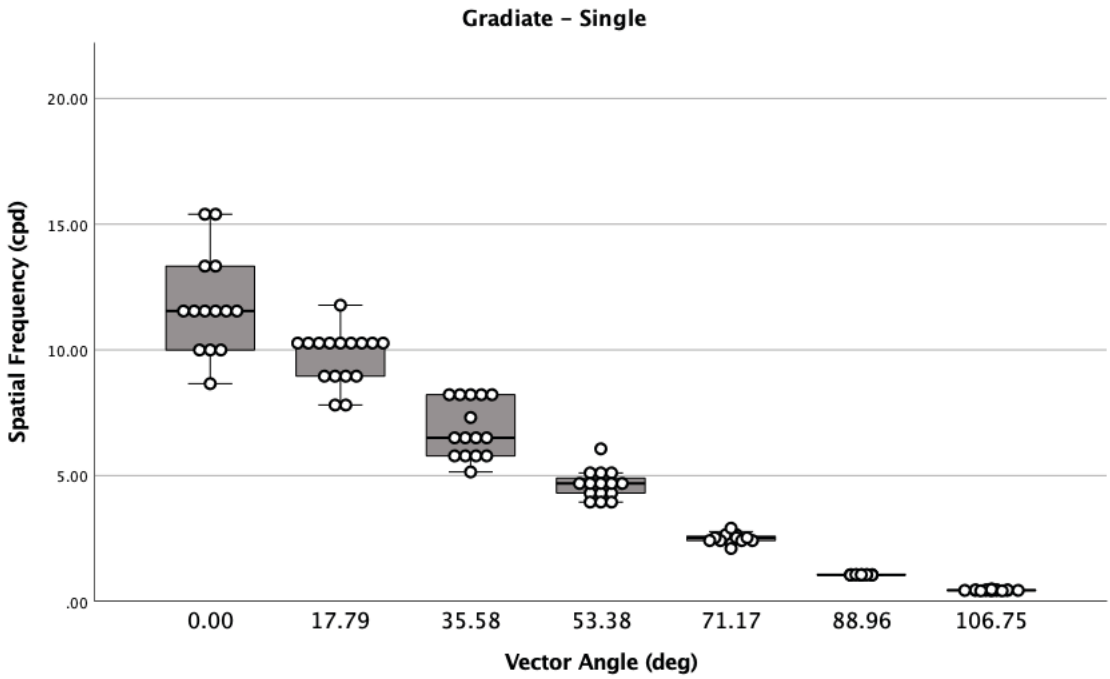

Figure 14b

Boxplot of GR-F Spatial Frequency Thresholds by Vector Angle for 15 Participants

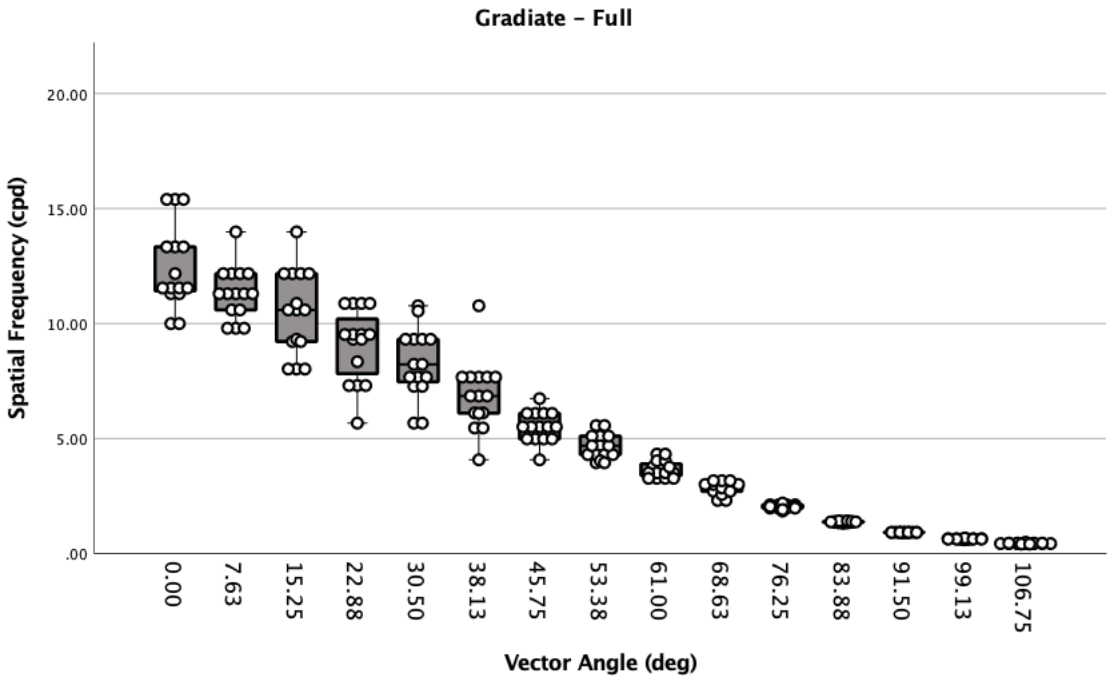

Figure 15 shows CSFs derived from GR-S and GR-F tasks for all 15 participants. As expected, the curves generated by both versions of the task show good agreement. The GR-1 CSF has seven points while the GR-F has 15 and there are few SFs that repeat exactly in both tasks for each individual. This makes it difficult to compare CS directly at a given SF. To address this, the peak CS was calculated for each task. The peak CS derived for each participant for both tasks is marked on the graphs. Bivariate correlation between peak CSs in the two measures yielded moderate albeit not significant results (r^2 = .439, p = .116) as illustrated in Figure 16a.

Figure 15

GR-1 and GR-F Contrast Sensitivity Functions for 15 Participants

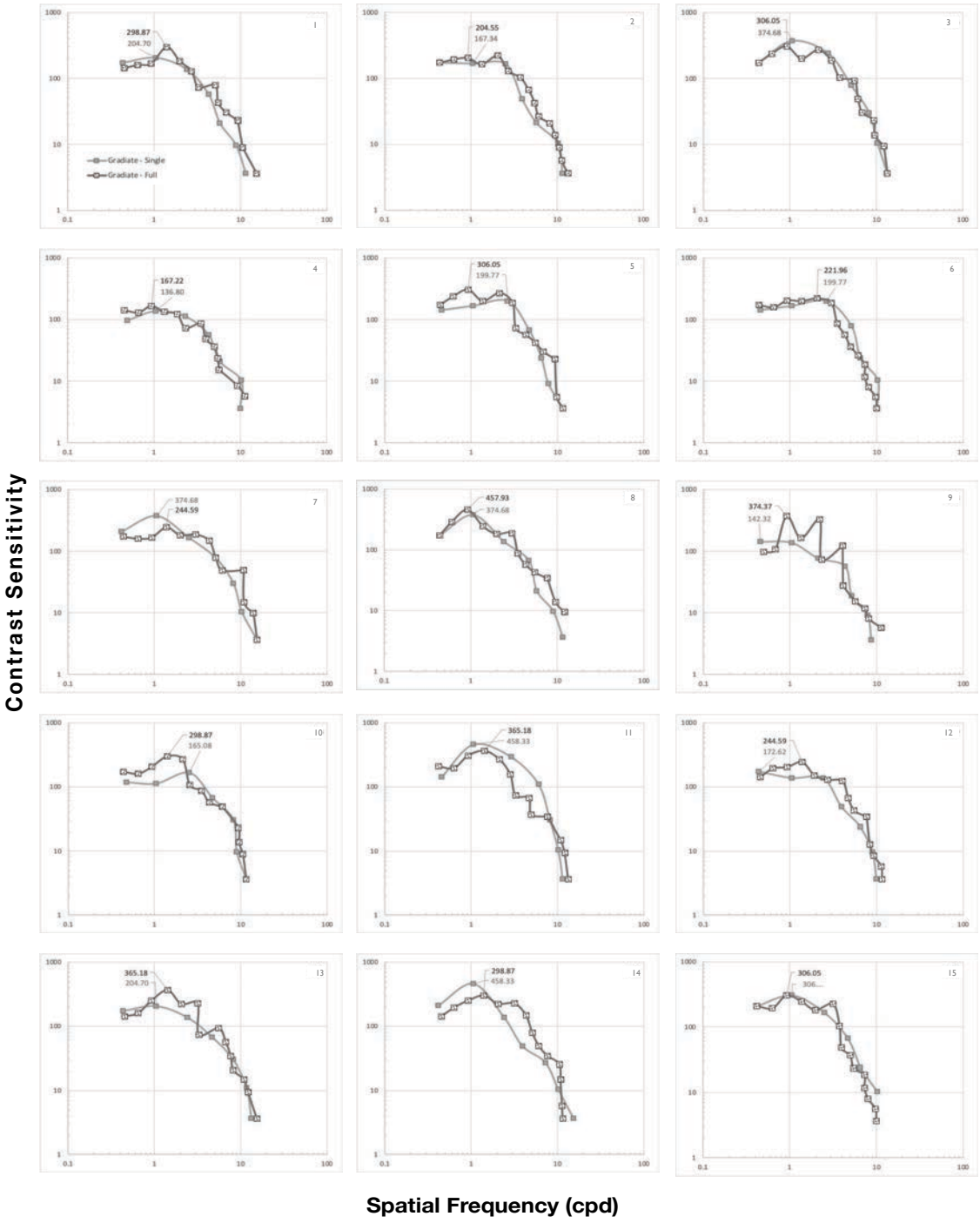

Note. Peak CS is labeled for both tasks. GR-1 peak CS is below the value for GR-F peak CS.

Figure 16a

Scatter Plot of Peak Contrast Sensitivity for GR-1 Plotted Against GR-F

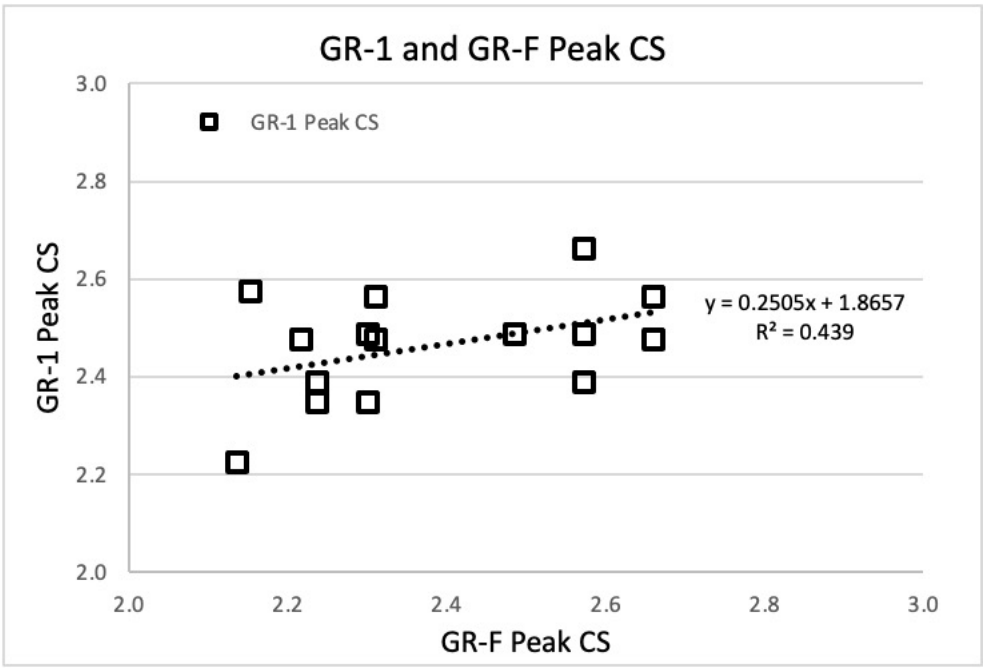

Figure 16b

Scatter Plot of Area Under the Curve for Contrast Sensitivity Functions For GR-1 Plotted Against GR-F

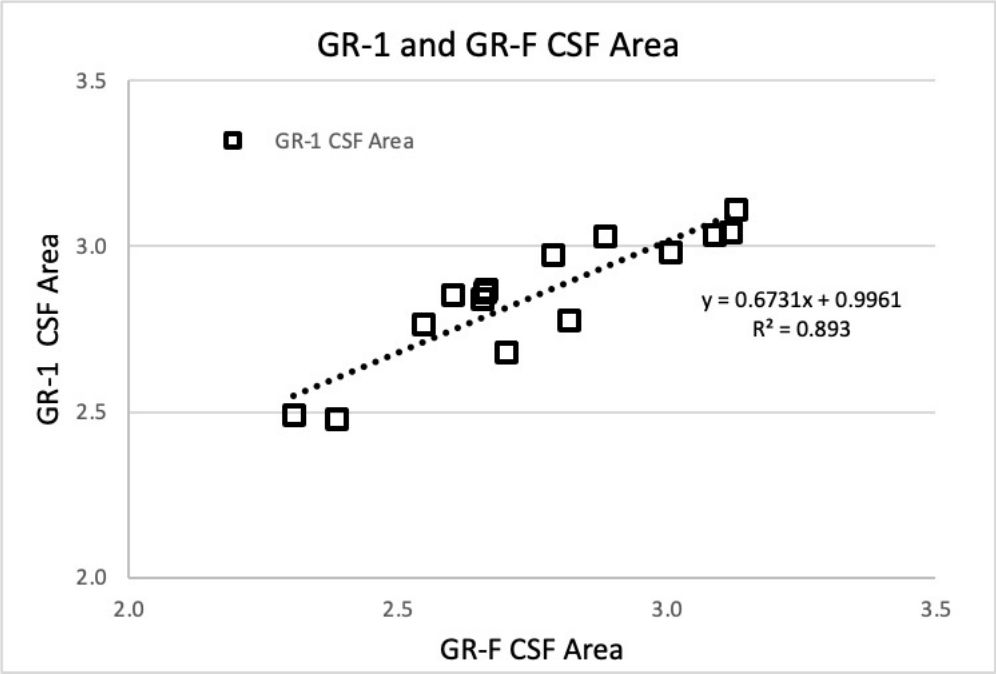

To evaluate overall curve shape, the area under the curve (AUC) was calculated for the CSFs for each participant. Bivariate correlation between GR-1 and GR-F AUCs revealed a significant result (r^2 = .893, < .001) as illustrated in Figure 16b. This indicates that while there is some variability in the peak CS estimated in each version of the task, having fewer points on the curve does not greatly change the overall shape of the CSF. This is supported by visual inspection of the CSF curves for each participant seen in Figure 15.

Figure 17

Contrast Sensitivity Functions Derived from CB, GR-F and C-swp VEP for 15 Participants

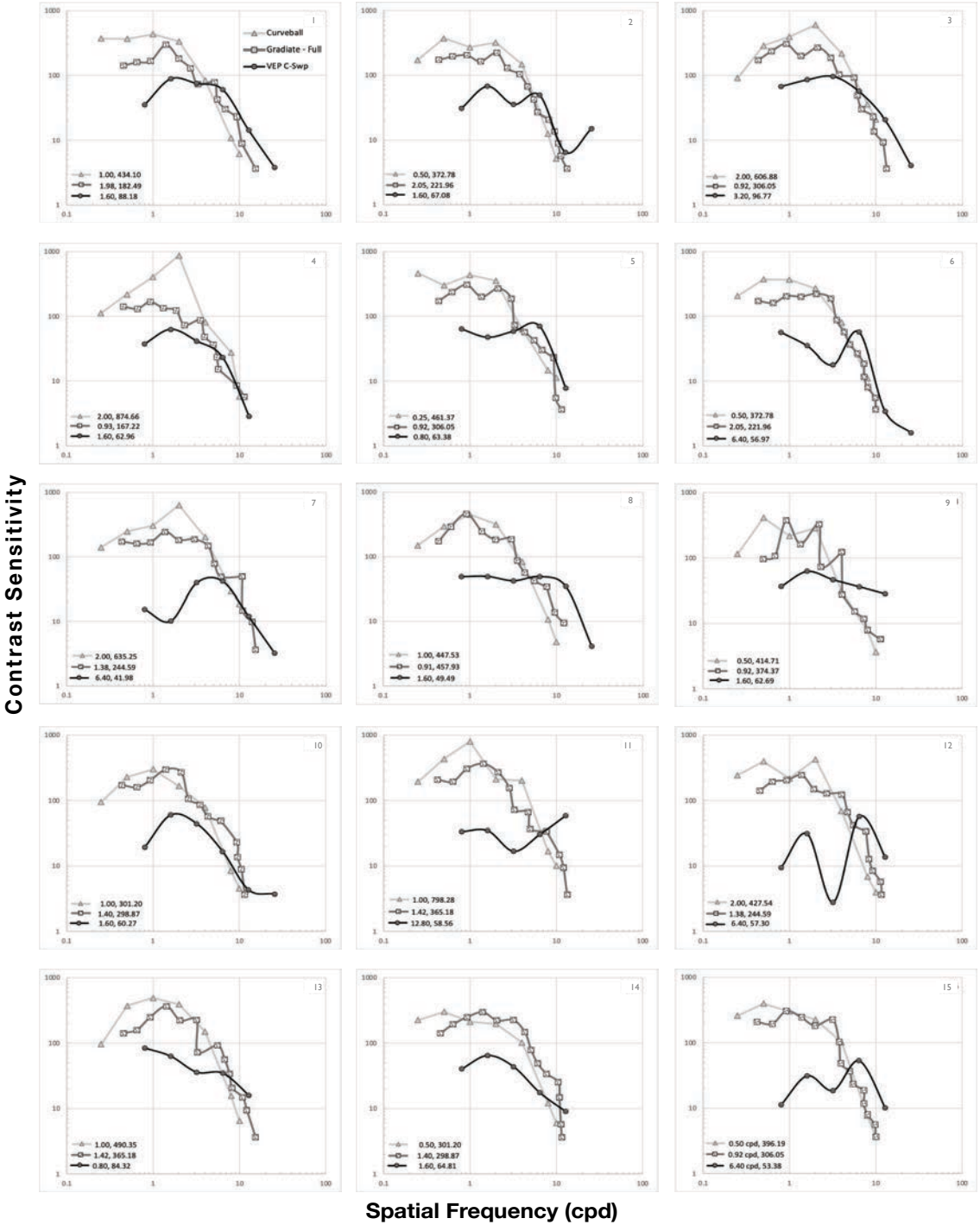

Note. The lower legend indicates the peak CS derived from each measure, represented as the x and y value of the peak point in SF (cpd) and CS (i.e., SF (cpd), CS).

Comparison of VEP, CB and GR CSFs

Figure 17 shows the CSFs derived from CB, GR-F and Cswp VEP for all 15 participants. GR-1 was excluded from this figure as the curves are similar to those generated by GR-F. Additionally, the GR-F task is the primary task and the one being investigated further in the Laboratory for Visual Disease and Therapy and is identical to the task used in Mooney et al. (2020). Visual inspection of these curves show that the CB and GR-F curves are similar in overall shape with some variability between individuals. The peak CS is varied, and CB appears to generate higher CS estimates at low SF than GR-F. This is potentially a result of the increased aperture size of the stimuli. Larger stimulus size has been shown to increase CS (Vassilev, 1973) as the image occupies a greater visual angle. At low SFs, the CB and GR-F tasks appear to agree more closely, and the CSF shape is maintained.

The VEP CSF shows a significantly different overall curve shape. The VEP CSF reflects a low-pass function with more variability among individuals than is seen in the psychophysical tasks. At low SFs, the VEP CS estimates are significantly lower than those produced by either of the psychophysical tasks. This is consistent with results from previous studies comparing VEP and psychophysically derived CS that have found that the VEP CS estimate is often lower than psychophysical estimates particularly at lower SF (Cannon Jr, 1983; Souza et al., 2007).

At higher SFs, the VEP responses generated higher CS estimates than the psychophysical tasks. Figure 17 shows that at 6.4 cpd the VEP CSFs begin to intersect with the CB and GR CSFs for some participants, and in some cases exceed psychophysical CS estimates. At 12.8 and 25.6 cpd the VEP response was generally higher than both the CB and GR tasks across participants. Due to limitations associated with properties of the screen, SFs

above 19.143 cpd could not be displayed in the psychophysical tasks and thus limited the range of SFs that could be included. The VEP extended to 25.6 cpd, and seven participants generated responses at this SF. For the seven participants that generated responses at 25.6 cpd, the slope of the VEP CSF was significantly shallower and generated a much higher acuity estimate than in the CB and GR tasks.

This overall trend in the data is illustrated in Figure 18, which shows mean CB, GR-F and C-swp VEP CSFs for all participants derived from the individual results seen in Figure 17.

Figure 18

Mean Contrast Sensitivity Functions Derived from CB, GR-F and C-swp VEP for 15 Participants

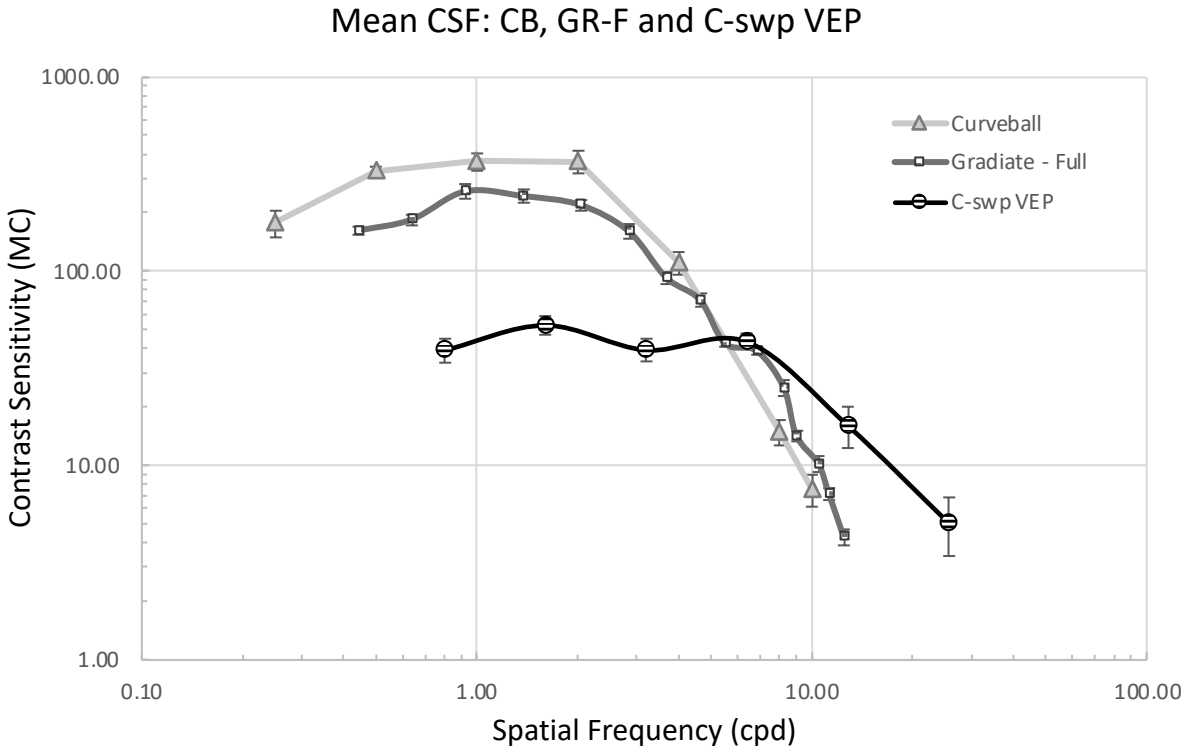

The averaged VEP function is not considered an ideal means of understanding the data as it can produce a curve that is inconsistent with any of the individual functions and obscure individual variability in the VEP response. In this dataset, however, the averaged VEP CSF is consistent with the overall shape of the individual data displayed in Figure 17. Additionally, the error bars seen in the mean VEP curve in Figure 18 demonstrate that variability in the scores was not extreme and highlights the increased variability at higher SFs. The averaged CB and GR-F CSFs are also consistent with individual responses and the error bars indicate that there was minimal variation among individuals, especially in the GR-F task.

Because each task generated CS estimates at different SFs it was difficult to assess agreement based on SF. To evaluate the level of agreement between the CSFs derived from the psychophysical and electrophysiological measures, two alternative variables were used: peak CS, and area under the curve. Peak CS values reflect the point on the CSF curve where CS was determined to be highest. The area under the curve provides a general measure of the size and shape of the CSF, and a general estimation of the area of the CSF that reflects the spectrum of visibility for each individual. The area under the curve metric was used in accordance with methods employed by Mooney et al. (2020).

Analysis of Peak CS

Descriptive statistics of peak CS for each measure can be found in Table 5. Peak CS estimates were highest in the CB task (M = 2.68, SD = 0.13), slightly lower in the GR-1(M = 2.38, SD = 0.19) and GR-F tasks (M = 2.46, SD = 0.11) and lowest in the C-swp VEP (M = 1.80, SD = 0.10). A one-way repeated measures ANOVA was conducted to determine

whether there were statistically significant differences in peak CS between the four measures. There were no outliers, and the data were normally distributed, as assessed by boxplot and the Shapiro-Wilk test ($p > .05$), respectively. The assumption of sphericity was not violated, as assessed by Mauchly's test of sphericity, $\chi2(5) = 6.56$, $p = .257$. Peak CS was significantly different between measures, $F(3,42) = 118.77$, $p < .001$, partial $\eta2 = .895$. Post hoc analysis with a Bonferroni adjustment revealed that peak CS was significantly lower in the C-swp VEP condition than CB (M = -0.88, 95% CI [-1.01, -0.74], p < .001), GR-1 (M = -0.58, 95% CI [-0.76, -0.40], p < .001), and GR-F (M = -0.66, 95% CI [-0.77, -0.55], p < .001). CB peak CS was significantly higher than both versions of the GR-1 (M = 0.30, 95% CI [0.12, 0.47], p = .001) and GR-F (M = 0.22, 95% CI [0.06, 0.37], p = .005). There was no significant difference in peak CS between the two versions of GR (M = 0.80, 95% CI [-0.22, 0.55], p = .547).

Figures 19a, 19b, and 19c show the Bland-Altman comparisons of the psychophysical and VEP derived peak CS. The Bland-Altman graph plots the difference between two measurements against the mean of those two measurements for each observer. In Figures 19a, 19b, and 19c, the mean of the two measures in each analysis is shown on the horizontal axis and the difference on the vertical axis. All values are expressed in $\log_{10}$. The mean difference across observers (also referred to as bias) is represented by the solid black line. The solid grey lines show the upper and lower bounds of the 95% limits of agreement. The blue line shows the proportional bias line, and the surrounding shaded area shows the 95% confidence intervals of this line. Bias refers to the average of the differences between the two measures across all subjects. The proportional bias reflects the consistency in bias across the range of measures (Bland & Altman, 1986; Ludbrook, 2010).

Figure 19a

Bland-Altman Plot of Peak Contrast Sensitivity Measured by CB and C-swp VEP

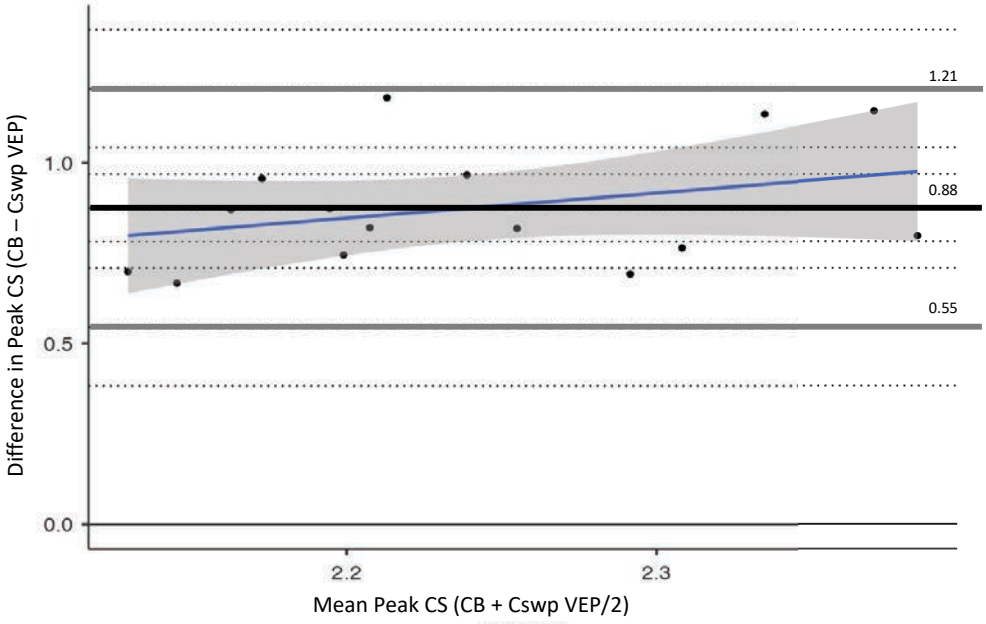

Figure 19b

Bland-Altman Plot of Peak Contrast Sensitivity Measured by GR-1 and C-swp VEP

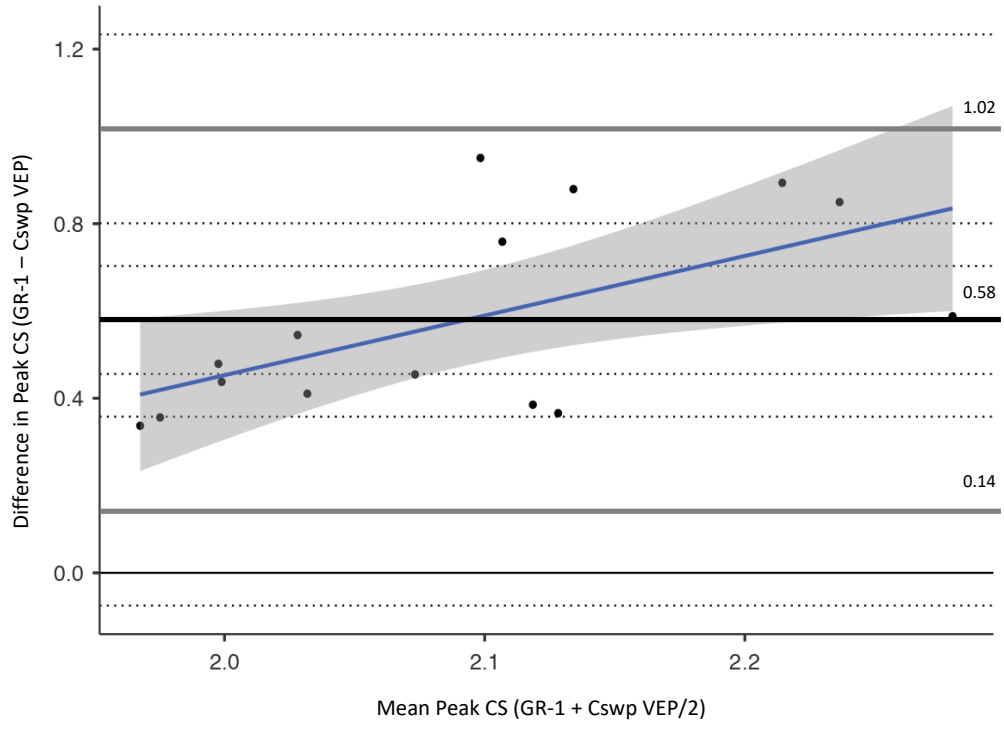

Figure 19c

Bland-Altman Plot of Peak Contrast Sensitivity Measured by GR-F and C-swp VEP

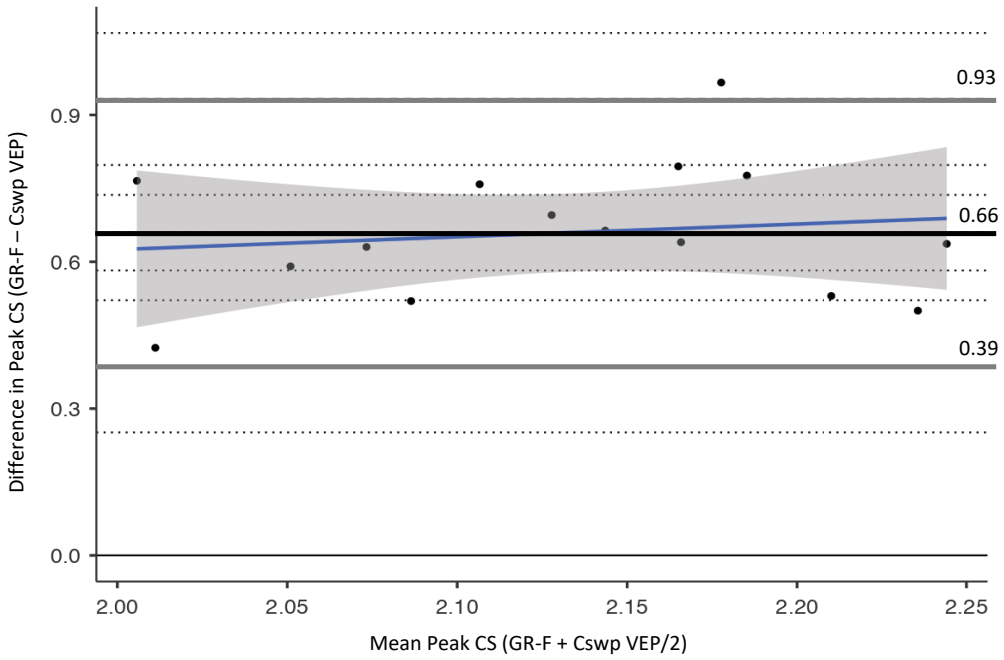

The difference scores were consistently above zero in all three comparisons, suggesting that the psychophysical tasks generated consistently higher CS estimates than did the VEP. Figures 19a, 19b and 19c show that the CB, GR-1, and GR-F peak CSs were an average of 0.88, 0.58 and 0.66 log units higher respectively than those derived from the VEP, as indicated by the bias line in each figure. The proportional bias lines in all three comparisons suggests that although the peak CS is consistently higher in the psychophysical tasks, they are not higher by a consistent value. The differences between the psychophysical and VEP tasks are not consistent across the range of measures and are not interchangeable.

Analysis of Area Under the CSF Curve

Descriptive statistics of the area under the CSF curve for each measure can be found in Table 6. CSF AUC was highest in the CB task ($M = 3.49$, $SD = 0.16$), slightly lower in the GR-1 ($M = 2.76$, $SD = 0.25$) and GR-F tasks ($M = 2.85$, $SD = 0.19$) and lowest in the C-swp VEP ($M = 1.95$, $SD = 0.28$). Figure 20 depicts the relationships between the CSF AUC derived from C-swp VEP with those derived from the three psychophysical measures.

Figure 20

Scatter Plot of Area Under the Curve of CB, GR-1, and GR-F Plotted Against C-swp VEP for 15 Participants

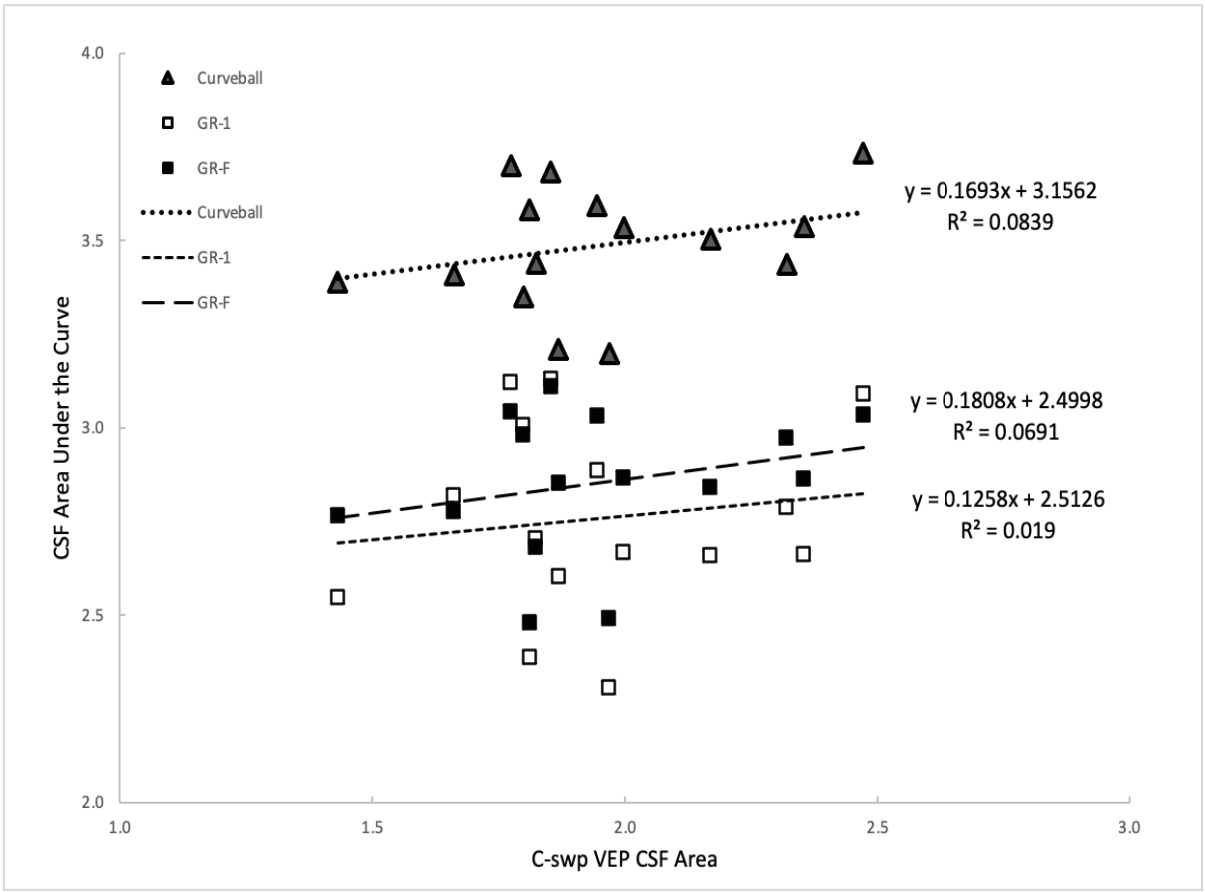

The CSF area of the VEP was significantly different from all psychophysical measures. The results of the regression indicated that CB explained 1% of the variance (r^2 = .01, $F(1,13) = 1.91$, $p = .295$), GR-1 was associated with 2% of the variance ((r^2 = .02, $F(1,13) = 0.252$, $p = .624$) and GR-F was associated with 7% of the variance (r^2 = .07, $F(1,13) = 0.964$, $p = .344$). Bivariate correlational analysis revealed no significant correlation between VEP CSF area and CB ($r(15) = .290$, $p = .295$), GR-1($r(15) = .138$, $p = .624$) and GR-F ($r(15) = .263$, $p = .344$).

Aim 2: Compare visual acuity estimates generated from a Spatial Frequency Sweep VEP, Contrast Sweep VEP, and the Gradiate task to further explore the neural pathways implicated in the Gradiate task.

Descriptive statistics for acuity estimates generated by each measure are displayed in Table 7. A representative example of SF-swp output from which grating acuity estimates are derived is pictured in Figure 9. The VEP response is interpolated to a SNR of 1 to derive acuity estimates. Acuity estimates were derived from C-swp responses through linear extrapolation of the response function to 1. C-swp acuity could not be accurately extrapolated for two participants due to deviations in the responses at high SFs, and as such these two were removed from analysis. In the GR tasks, VA estimates are derived from the SF thresholds obtained along the 0° vector. Figure 21 depicts the VA estimates from the four measures included (GR-1, GR-F, SF-swp VEP and C-swp VEP). Visual inspection of the data revealed that the electrophysiological measures generated higher acuity estimates than the psychophysical tasks in all 15 participants (13 in the C-swp condition).

Figure 21

Visual Acuity Estimates by Measure for 15 Participants

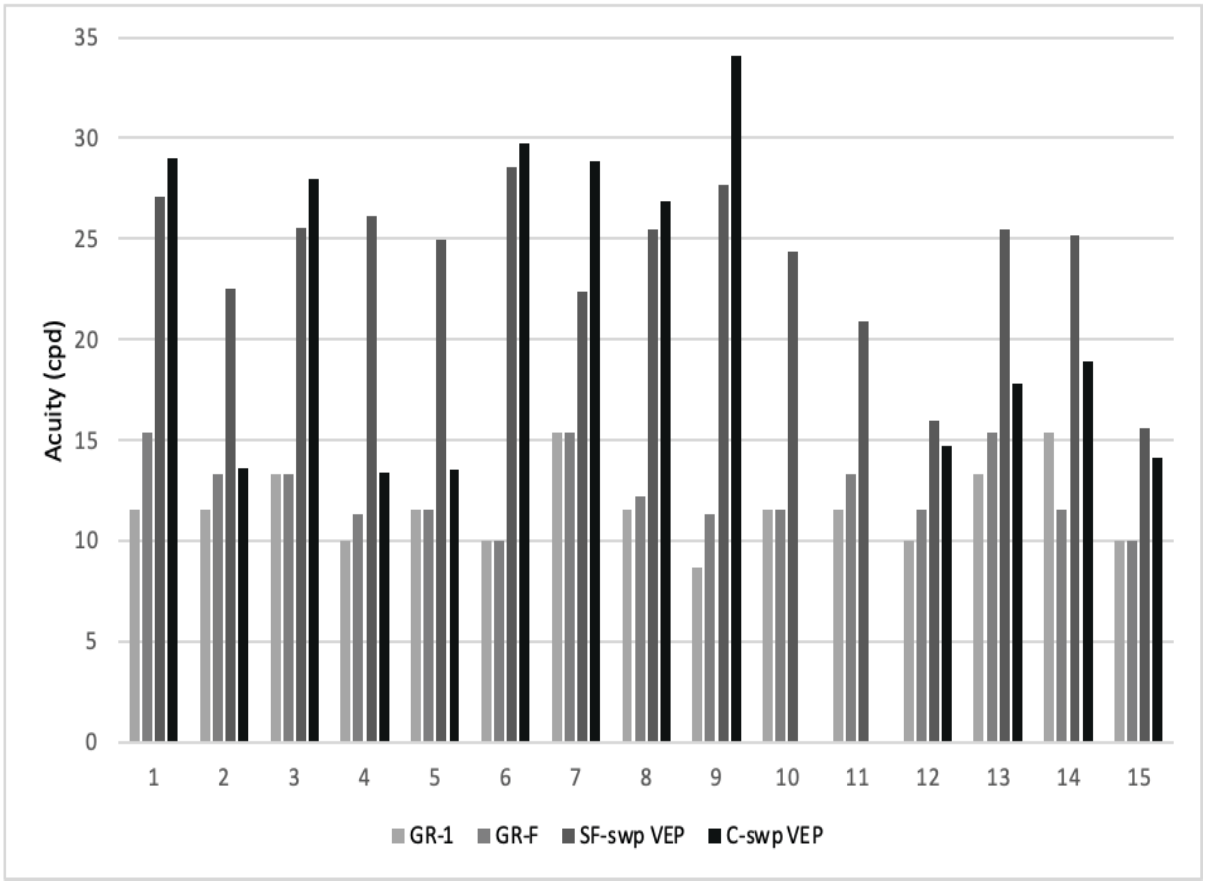

A one-way repeated measures ANOVA was conducted to determine whether there were significant differences in VA estimates between the four measures. Mauchly's test of sphericity indicated that the assumption of sphericity had been violated, $\chi 2(5) = 22.25$, $p = .001$. Epsilon (ε) was 0.514, as calculated according to Greenhouse and Geisser (1959) and was used to correct the one-way repeated measures ANOVA. Acuity estimates derived from the four measures were significantly different, $F(1.54, 18.51) = 30.59$, $p < .001$, partial $\eta 2 = .72$, with both GR tasks generating significantly lower VA estimates than the VEP tasks.

Post hoc analysis with a Bonferroni adjustment revealed that there was a significant mean decrease in VA between GR-1 and SF-swp VEP estimates of 12.32 cpd, 95% CI [-16.20, -8.45], $p < .001$, and between GR-1 and C-swp VEP estimates of 10.01 cpd, 95% CI [-16.96, -3.07], $p = .004$. This was also true for GR-F, with a significant mean decrease in VA of 11.56 cpd, 95% CI [-15.22, -7.90], $p < .001$ from SF-swp VEP and 9.25 cpd, 95% CI [-15.86, -2.63], $p = .005$ from C-swp VEP. There was no significant difference between VA estimates between GR-1 and GR-F ($p = .962$), or between SF-swp and C-swp VEP VA estimates ($p = 1.0$).

Bivariate correlational analysis between estimates derived from the four measures revealed that there was a significant, moderate positive correlation between the two psychophysical tasks, $r(13) = .58$, $p = .025$, with 33% of the variation accounted for between tasks. This relationship is illustrated in Figure 22. There was a moderate positive, but not significant, correlation between SF-swp and C-swp VEP, $r(11) = .55$, $p = .051$, with 30% of the variance accounted for by this model. There was no significant correlation between SF-swp VEP and GR-1 ($r(13) = .08$, $p = .777$) or GR-F ($r(13) = .14$, $p = .626$), with 1% or less shared variance in both tasks, as illustrated in Figure 23. The same was true for the C-swp VEP (see Figure 24), with no significant correlation found with GR-1 ($r(11) = .41$, $p = .894$) or GR-F ($r(11) = .22$, $p = .481$).

Figure 22

Scatter Plot of Visual Acuity Estimates from GR-1 Plotted Against GR-F

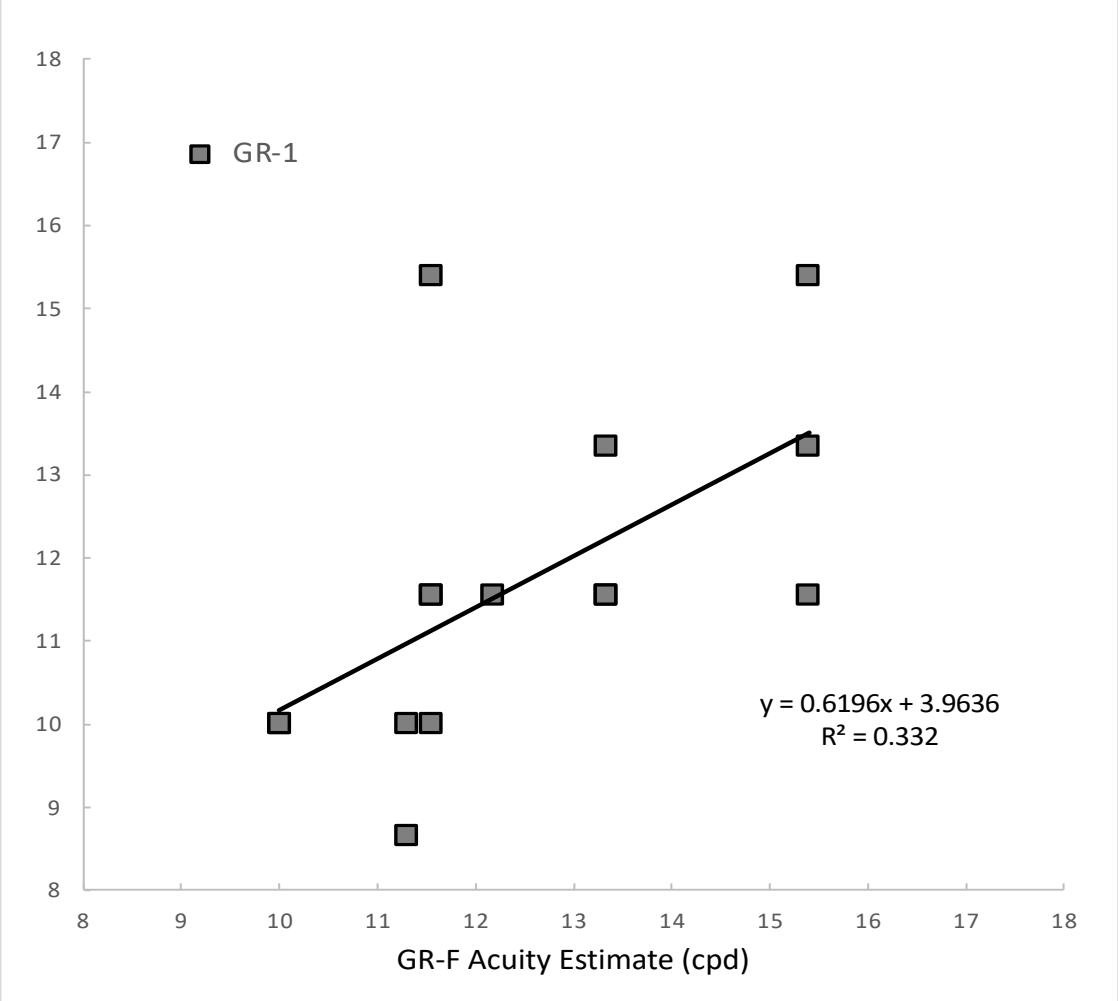

Figure 23

Scatter Plot of Visual Acuity Estimates from GR-1, GR-F and C-swp VEP Plotted Against SF-swp VEP

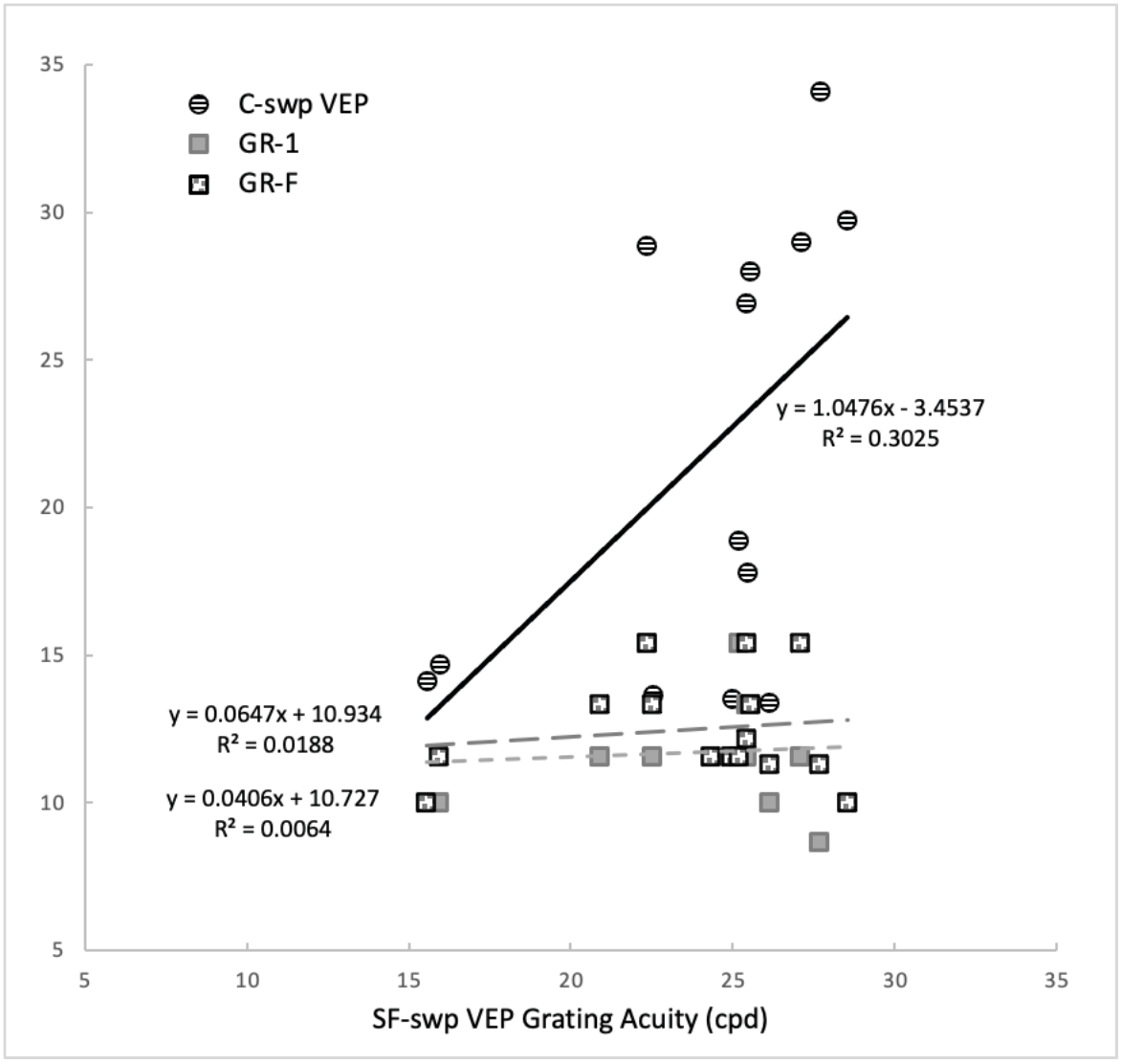

Figure 24

Scatter Plot of Visual Acuity Estimates from GR-1, GR-F and SF-swp VEP Plotted Against C-swp VEP

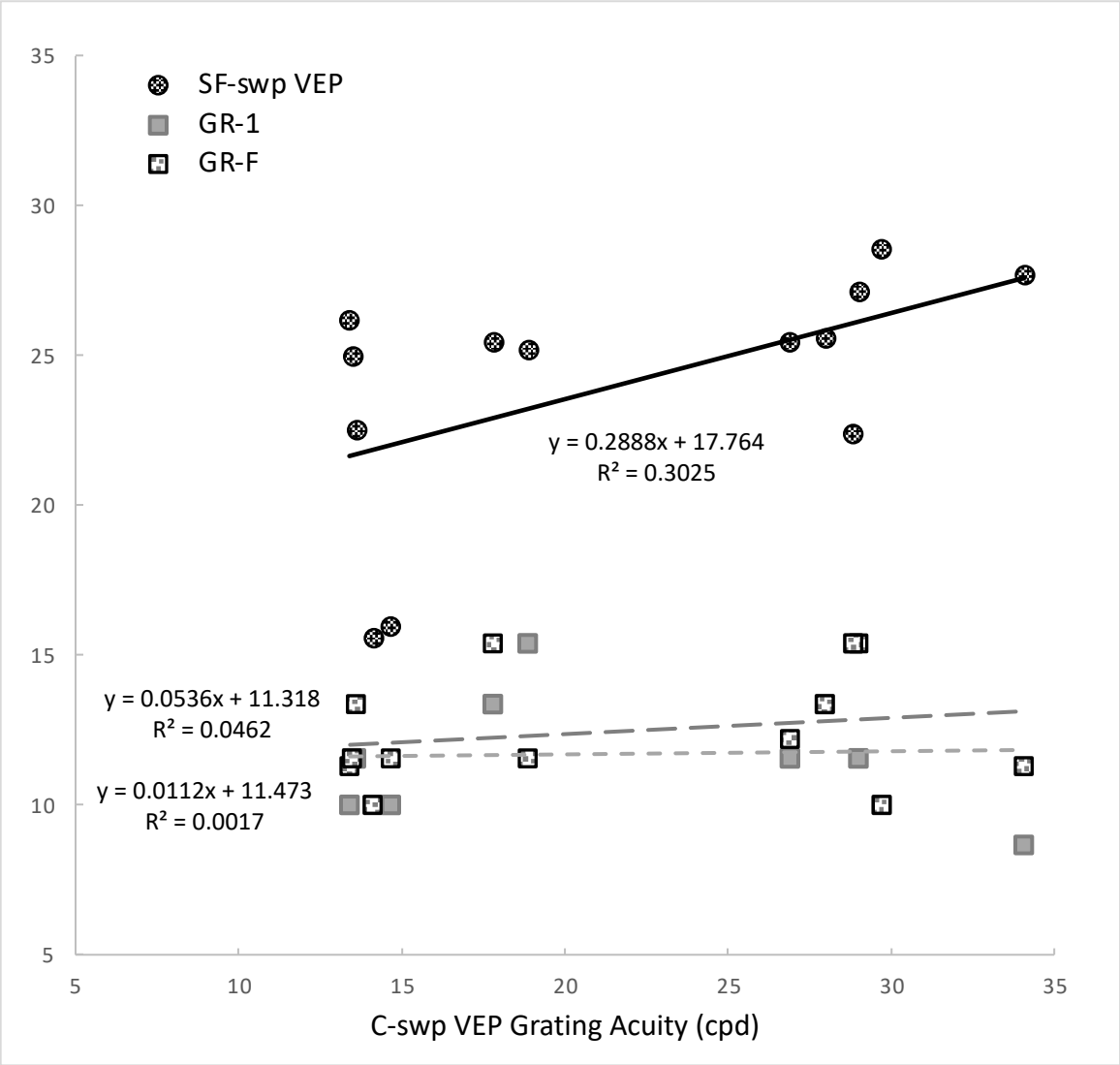

Chapter 5. Discussion

The current study has attempted to describe and analyze the relationship between CSFs and acuity estimates derived from electrophysiological sweep VEP measures and psychophysical smooth pursuit eye-tracking based measures, in an effort to use what is known about VEP stimuli and response patterns in specific visual pathways to investigate the neural pathways implicated in the psychophysical eye-tracking tasks. The goal of this study is to investigate the relationship between data derived from each measure to make inferences about which visual pathways are targeted in the CB and GR tasks to improve interpretation of the results generated by these tasks. This section will summarize these results and relate them to previous work to understand patterns of variation between the two systems and make interpretations. It will discuss potential implications of these findings in terms of underlying functional mechanisms.

Comparison of Contrast Response Functions

Contrast swpVEPs have been found to be a reliable objective measure of CS in humans (Almoqbel et al., 2008; Campbell & Maffei, 1970; García-Quispe et al., 2009; Kelly, 1977; Norcia et al., 1989; Rentschler, 1996; Tyler et al., 1979) and have been used repeatedly to investigate psychophysical CS as was done in the current study. The results presented here reflect substantial differences between the C-swp VEP and the CB and GR tasks. There were differences in the VEP responses among participants which is consistent with previous

studies (Joost & Bach, 1990). Despite these differences, patterns emerged in the relationships between the electrophysiological and psychophysical CSFs.

Overall, the VEP CS estimates were significantly lower than those derived from CB or GR at SFs below 3.2 (seen in 6/15 participants) and 6.4 cpd (seen in 9/15 participants). At SFs above 3.2 to 6.4 cpd the VEP CS estimates were generally higher than the CB and GR estimates. CB and GR CSs decreased noticeably at 3-4 cpd and continued to decrease sharply with increased SF. The VEP CSF curve decreased along a much more gradual slope, generating higher CS estimates than CB and GR at SFs above 6.4 cpd (seen in 9/15 participants) and 12.8 cpd (seen in 6/15 participants).

Previous research comparing contrast sensitivities derived from VEP and psychophysical stimuli have shown good agreement in overall CSF shape (Allen et al., 1986; Cannon Jr, 1983; Conte, 1995; Lopes de Faria et al., 1998). Results of the current study found differences in CSF shape between the electrophysiological and psychophysically derived curves. This discrepancy in overall CSF shape may be related to several factors that have been found to impact CS, including methodological differences in stimuli and response criteria and differences in neural generators of these responses. Evaluation of the impact of these factors on the variation in CSF curve shape and the observed crossover point in contrast sensitivity at high and low SFs between the two methods may reflect differential contributions of the M and P systems in CS estimates.

As previously discussed, the M and P pathways are considered parallel pathways and are selectively sensitive to different stimuli, The contributions of the M and P systems in the current results depend on the spatial, temporal, and contrast characteristics of the stimulus as well as the overlap in M and P pathway response to aspects of spatial and temporal

frequencies (Tobimatsu et al., 1995). The differences between CS at low and high SFs seen in the current results may be related to contributions of the M and P pathways in the CB and GR tasks and at different points in the VEP response. The M pathway is believed to have high CS, responding optimally to stimuli with high temporal frequency, and is implicated in excitatory responses to motion (Shapley, 1990). In contrast, the P pathway is believed to have lower CS, with P pathway CTs found at approximately 10% contrast (Tootell et al., 1988). The P pathway responds preferentially to high SF stimuli, with lower temporal resolution than M cells. The CSF often reflects the combined activity of theses pathways to reflect whichever of the two systems is more sensitive at a given SF and temporal frequency.

Previous research has suggested that there is a transition point in a typical CSF where detection mediation is switched from M dominant to P dominant. This transition from M to P pathways has been found to occur between 1.5 (Legge, 1978) and 3 to 5 cpd (Ellemberg et al., 2001; Green, 1981; Schütz et al., 2009; Strasburger et al., 1993; Strasburger et al., 1996). This is consistent with the crossover point observed between the VEP and psychophysical CSs in our results, suggesting that our results reflect different contributions of M and P activity in each task. The CB and GR tasks may reflect M pathway activity while the VEP CSF which produced higher CS estimates at SFs above 3.2 to 6.4 cpd, may reflect that the P pathway is mediating thresholds at these SFs. In the CB and GR tasks, M pathway responses may dominate throughout the CSF, resulting in the lower CS at SFs above about 5 cpd seen in the current results.

The effects of stimulus motion and smooth pursuit eye tracking also likely play an important role in understanding our results. Magnocellular contributions to the CSFs derived from the CB and GR tasks are likely strengthened by stimulus motion. Spering et al. (2005)

found that stimulus velocity significantly impacted CS estimates in a smooth pursuit task. Their results demonstrate that stimulus velocity between 8 and 15 deg/s resulted in a sharp decrease in CS at SFs above 1cpd. The CB and GR stimuli were presented at 10 and 5 deg/s respectively due to differences in stimulus size. The increased velocity of the CB stimuli relative to GR stimuli may have contributed to the increased CS in the CB task at low SFs. Kelly (Kelly, 1979) found that stimulus velocity increases from 3 deg/s to 11 deg/s improved CS at low SF. These results suggest that increased velocity improves CS at low, but not high SFs which is consistent with the current results. It is likely that the velocity of CB and GR stimuli are sufficiently high to target the M pathway, particularly at low SF.

Schutz et al. (2009) presented conflicting data that showed CS at SFs above 3 cpd was improved during smooth pursuit relative to fixation. However, this and other studies that evaluated smooth pursuit did so with stimulus presentations of 1 s or less (Burr & Ross, 1986; Burr & Thompson, 2011; Green, 1981) or evaluated motion onset responses (Bach & Ullrich, 1997; Kubová et al., 1995) which may not be analogous to the sustained pursuit employed in the current study. Previous research has suggested that smooth pursuit initiation and maintenance are not interchangeable and may reflect different mechanisms (Tavassoli & Ringach, 2009). Smooth pursuit maintenance, as is required for completion of the CB and GR tasks, may reflect mechanisms similar to those involved in gaze stabilization (Krauzlis, 2004; Tavassoli & Ringach, 2009).

The C-swp VEP stimuli used in the current study have been found to target the P pathway at high SFs (Nelson & Seiple, 1992; Strasburger et al., 1993; Tobimatsu et al., 1995). The crossover seen in the VEP and psychophysically derived CSFs at SFs above 6.4 cpd suggests that the P dominance observed in the VEP response is not present in the CB and

GR CS estimates. In the CB and GR tasks, it is possible that, at higher SFs, the velocity of the stimuli may function to desensitize the P system such that the M system governs the response. This could also reflect a desensitized P response which could limit CS at higher SFs, as is seen in the CB and GR CSFs.

There are also other factors that may be contributing to the observed differences in the VEP and psychophysical data obtained in this study. Studies comparing C-swp VEP and psychophysical CSFs derived from static or sinusoidally modulated stimuli have found that CSFs derived from swpVEPs are systematically lower than psychophysical CSFs derived from static and sinusoidally-modulated stimuli (Cannon Jr, 1983; Lopes de Faria et al., 1998; Strasburger et al., 1996). These studies have found the swpVEP CS to be reduced by a factor of 0.24 log units (Strasburger et al., 1996) to 0.62-0.79 log units (Lopes de Faria et al., 1998) compared to CSs derived from psychophysical forced-choice or method of adjustment tasks employing sinusoidally-modulated stimuli. Although the reduction in VEP-derived CS relative to psychophysical CS seen in the current study was not systematic across SFs, the same methodological influences found in these studies may have contributed to the differences seen at low SF. The lower CSs generated with the VEP responses is thought to be related to differences in criterion responses between the types of measures. The VEP requires a sizeable neural signal to generate evident electrical potentials in the cortex that can be recorded from the scalp. Alternatively, the psychophysical thresholds reflect perception that can be based on the activation of far fewer neurons (Cannon Jr, 1983; Conte, 1995; Lopes de Faria et al., 1998).

Additionally, the cortical generators of the VEP response differ from those involved in the psychophysical tasks. The VEP is primarily a foveal/macular measure and reflects the

summation of cortical signals averaged mainly over the primary visual cortex. The measured VEP response is also impacted by excitatory and inhibitory activity from other areas of the visual cortex, including V2, V3, V6 and V5 (Vanni et al., 2004). While these are some of the same cortical areas believed to be involved in smooth pursuit eye movements (Krauzlis, 2004), behavioral smooth pursuit CTs are not directly impacted by the electrophysiological inhibitory interactions that can limit VEP response magnitude. The neuronal response to luminance may also have contributed to the higher CB and GR CSs in the current study. The psychophysical tasks in the current study were completed in a lit environment while the VEP was obtained in dark conditions, which may be related to the higher CS estimates derived by the CB and GR tasks, as increased luminance has been shown to generate higher psychophysical CS estimates (Bühren et al., 2006).

The information presented here supports magnocellular dominance in CB and GR derived CTs, particularly at low SFs. The CSF generated by smooth pursuit behavioral mechanisms may reflect functioning of the M pathway and its projections to temporal and parietal brain regions. The MT/V5 area has been shown to be activated in both smooth pursuit (Krauzlis, 2004; Merigan & Maunsell, 1993) and low SF CS (Di Russo et al., 2005; Merigan et al., 1991) and as such is likely to be implicated in the CB and GR responses. Based on the spatial and temporal properties of the CB and GR systems, there is evidence that the CSs generated in these tasks may reflect activity in afferent projections from the visual cortex to several other cortical areas. Analysis of the M pathway and smooth pursuit eye motion pathways suggest that the current tasks may involve MT/V5 in pursuit initiation and MST for pursuit maintenance (Krauzlis, 2004). The frontal eye field (FEF) has been identified as a cortical area that exerts substantial control in smooth pursuit maintenance,

specifically the smooth eye movement subregion of the FEF. This region receives direct input form the MST and makes direct connections with premotor nuclei in the brainstem (Felleman & Van Essen, 1991; Krauzlis, 2004; Van Essen et al., 1990). There are many other connections and areas involved in this system, and those discussed here are only the most dominant cortical regions involved in the M pathway.

Most of the current analyses were based on comparisons of peak CS and CSF shape across SFs. Area under the curve was also used compare CSF size and shape. Given that the psychophysical and VEP measures use different criteria for responses, area under the curve (AUC) is not an ideal metric to compare functions. The size and shape of the CSFs generated by each measure are dependent on arbitrary criteria to establish response thresholds. The VEP criterion to establish CS is a SNR of 1 and the psychophysical criterion is based on a proportional measure of correct responses or smoothly tracked frames. Both the SNR and proportion correct criterion can be arbitrarily changed and as such the size and shape of the curves can be altered based on alteration of the response criterion. Despite these drawbacks the area under the curve was used in the absence of an alternative metric for direct comparison.

AUC can be a useful measure in comparing tasks with comparable threshold criteria like the two GR tasks. The CS estimates generated by the two tasks are also represented by values in the same log vector space which gives them the same scale. The AUC for GR-1 and GR-F were strongly correlated. While there are benefits to having a more comprehensive estimate of the CSF in the 15-point GR-F task, these findings suggest that the GR-1 task offers a comparable estimation of the CSF. This suggests that the GR-1 tasks could offer an

alternative method of administration for individuals who struggle with the simultaneous stimulus presentation in the GR-F task.

Comparison of Acuity Estimates

The SF-swp VEP is a broadly accepted objective measure of VA (Hamilton et al., 2021a)**.** VA estimates from the SF-swp were compared with VA estimates derived from two versions of the Gradiate task, and estimates extrapolated from C-swp VEP data. We found that VA estimates were consistently higher in the VEP tasks than the GR tasks across all 15 participants. This was a robust significant finding and suggests that the SF-swp VEP and the GR tasks may be measuring different aspects of acuity and likely reflect different underlying neural mechanisms. The VA estimates generated by the SF-swp VEP are thought to be generated from activation of P cells with high VA, suggesting that these cells were not implicated in the VA estimates generated by the GR tasks. This is consistent with findings from the CSF data that suggest that the GR task may predominantly reflect activity of the M pathway.

Analysis of VAs between the two types of VEP measures and between the two types of psychophysical measures was somewhat less informative, showing moderate positive correlations between VEP measures and between GR measures. This suggests that each kind of measure (electrophysiological and psychophysical) had good consistency. The strong correlation between GR tasks suggests that the alternative single ball version of Gradiate may offer a good alternative in situations where the five-ball presentation is too cognitively or visually overwhelming.

Potential Clinical Implications

These results suggest that the CB and GR tasks are likely mediated by M dominant visual pathway responses, particularly at low SFs. The current findings are the first to explore the underlying mechanisms involved in these tasks and should be considered preliminary evidence for M pathway dominance. If these findings can be supported in future research, there are a variety of clinical implications that may come from understanding the neural mechanisms. A clear understanding of the visual pathway associated with results from this measure can help to clarify variations, deficits or improvements, in performance. This can add qualitative neurological information to quantitative CS estimates that can inform rehabilitation. As mentioned previously, there are many disorders that selectively impact M pathway processes, including Alzheimer's disease, schizophrenia, optic neuritis, autism, and dyslexia. If CB and GR are confirmed to differentially measure M pathway function, the tasks could potentially provide information to help inform diagnosis and potentially identify deficits and disease markers earlier. This study offers preliminary evidence related to interpretation of the CSF generated in the CB and GR tasks and potential underlying neural mechanisms. This is a necessary first step in the development of an accessible measure of CS in multiple clinical and general populations.

Limitations and Future Directions

There are several limitations to the current study. Due to the COVID-19 pandemic and institutional safety restrictions, only employees of BNI were eligible to participate in the study thereby significantly reducing the potential participant pool and limiting demographic diversity in the sample as well as limiting the sample size. In addition, because this is a

preliminary study, only non-randomized healthy participants were included, and the results are not generalizable to other populations. Additionally, the small sample size impacts the generalizability of these results.

This study is also limited by the available technology. Eye tracking devices and screens are imperfect, and although the Curveball and Gradiate algorithm accounts for this, the study is still limited somewhat by the technology used. Future research will be necessary to evaluate the validity of the Curveball and Gradiate tasks in neurologically impaired individuals and children, as well as find ways to integrate advancements in eye tracking technology. In addition, eye tracking based task are not optimally suited for all conditions, including individuals with eye movement disorders who may not be able to complete the task or produce smooth pursuit eye movements. Based on the current findings, future research will be needed to further explore the underlying neural mechanisms in a larger, more representative sample, as well as to clarify M and P pathway contributions at high SF.

References

Allen, D., Norcia, A. M., & Tyler, C. W. (1986). Comparative study of electrophysiological and psychophysical measurement of the contrast sensitivity function in humans. *American Journal of Optometry and Physiological Optics*, *63*(6), 442-449.

Almoqbel, F., Leat, S. J., & Irving, E. (2008). The technique, validity and clinical use of the sweep VEP. *Ophthalmic and Physiological Optics*, *28*(5), 393-403.

Almoqbel, F. M., Irving, E. L., & Leat, S. J. (2017). Visual acuity and contrast sensitivity development in children: sweep visually evoked potential and psychophysics. *Optometry and Vision Science*, *94*(8), 830-837.

Almoqbel, F. M., Yadav, N. K., Leat, S. J., Head, L. M., & Irving, E. L. (2011). Effects of sweep VEP parameters on visual acuity and contrast thresholds in children and adults. *Graefe's Archive for Clinical and Experimental Ophthalmology*, *249*(4), 613-623.

Arai, M., Katsumi, O., Paranhos, F. R. L., De Faria, J. M. L., & Hirose, T. (1997). Comparison of Snellen acuity and objective assessment using the spatial frequency sweep PVER. *Graefe's archive for clinical and experimental ophthalmology*, *235*(7), 442-447.

Arden, G. B. (1978). The importance of measuring contrast sensitivity in cases of visual disturbance. *British Journal of Ophthalmology*, *62*(4), 198-209.

Atkin, A., Bodis-Wollner, I., Wolkstein, M., Moss, A., & Podos, S. M. (1979). Abnormalities of central contrast sensitivity in glaucoma. *American journal of ophthalmology*, *88*(2), 205-211.

Bach, M., & Ullrich, D. (1997). Contrast dependency of motion-onset and pattern-reversal VEPs: interaction of stimulus type, recording site and response component. *Vision research*, *37*(13), 1845-1849.

Bailey, I., & Jackson, A. (2016). Changes in the clinical measurement of visual acuity. Journal of Physics: Conference Series, *772*(1), 12-46.

Barber, A. J. (2003). A new view of diabetic retinopathy: a neurodegenerative disease of the eye. *Progress in Neuro-Psychopharmacology and Biological Psychiatry*, *27*(2), 283-290.

Becker, R., Teichler, G., & Graf, M. (2007). Comparison of Landolt-C and ETDRS-Visual Acuity in Healthy Subjects and Patients With Different Eye Diseases. *Investigative Ophthalmology & Visual Science*, *48*(13), 4887-4887.

Bex, P. J., & Makous, W. (2002). Spatial frequency, phase, and the contrast of natural images. *JOSA A*, *19*(6), 1096-1106.

Bland, J. M., & Altman, D. G. (1986). Statistical methods for assessing agreement between two methods of clinical measurement. *Lancet (London, England)*, *1*(8476), 307-310.

Bodis-Wollner, I., Marx, M. S., Mitra, S., Bobak, P., Mylin, L., & Yahr, M. (1987). Visual dysfunction in Parkinson's disease: Loss in spatiotemporal contrast sensitivity. *Brain*, *110*(6), 1675-1698.

Boyle, C. A., Boulet, S., Schieve, L. A., Cohen, R. A., Blumberg, S. J., Yeargin-Allsopp, M., Kogan, M. D. (2011). Trends in the prevalence of developmental disabilities in US children, 1997-2008. *Pediatrics*, *127*(6), 1034-1042.

Breitmeyer, B. G., & Ganz, L. (1976). Implications of sustained and transient channels for theories of visual pattern masking, saccadic suppression, and information processing. *Psychological review*, *83*(1), 1.

Bubl, E., Kern, E., Ebert, D., Riedel, A., van Elst, L. T., & Bach, M. (2015). Retinal dysfunction of contrast processing in major depression also apparent in cortical activity. *European archives of psychiatry and clinical neuroscience*, *265*(4), 343-350.

Burr, D., & Ross, J. (1986). Visual processing of motion. *Trends in Neurosciences*, *9*, 304-307.

Burr, D., & Thompson, P. (2011). Motion psychophysics: 1985–2010. *Vision research*, *51*(13), 1431-1456.

Butler, P. D., Martinez, A., Foxe, J. J., Kim, D., Zemon, V., Silipo, G., . . . Javitt, D. C. (2006). Subcortical visual dysfunction in schizophrenia drives secondary cortical impairments. *Brain*, *130*(2), 417-430.

Butler, P. D., Silverstein, S. M., & Dakin, S. C. (2008). Visual perception and its impairment in schizophrenia. *Biological psychiatry*, *64*(1), 40-47.

Bühren, J., Terzi, E., Bach, M., Wesemann, W., & Kohnen, T. (2006). Measuring contrast sensitivity under different lighting conditions: comparison of three tests. *Optometry and Vision Science*, *83*(5), 290-298.

Campbell, F. W., & Maffei, L. (1970). Electrophysiological evidence for the existence of orientation and size detectors in the human visual system. *The Journal of physiology*, *207*(3), 635-652.

Campbell, F. W., & Maffei, L. (1974). Contrast and spatial frequency. *Scientific American*, *231*(5), 106-115.

Cannon Jr, M. W. (1983). Contrast sensitivity: Psychophysical and evoked potential methods compared. *Vision research*, *23*(1), 87-95.

Cockerham, G. C., Weichel, E. D., Orcutt, J. C., Rizzo, J. F., & Bower, K. S. (2009). Eye and visual function in traumatic brain injury. *Journal of rehabilitation research and development*, *46*(6), 811.

Cohen, J. (1992). A power primer. *Psychological bulletin*, *112*(1), 155.

Colon, E., & Visser, S. L. (1990). *Evoked potential manual: a practical guide to clinical applications* (2 ed.). Springer Science & Business Media.

Conte, M. M. (1995). *Comparisons between electrophysiologically and psychophysically determined contrast sensitivity functions in humans* City University of New York].

Conte, M. M., & Victor, J. D. (2009). VEP indices of cortical lateral interactions in epilepsy treatment. *Vision research*, *49*(9), 898-906.

Cormack, F. K., Tovee, M., & Ballard, C. (2000). Contrast sensitivity and visual acuity in patients with Alzheimer's disease. *International Journal of Geriatric Psychiatry*, *15*(7), 614-620.

da Costa, M. F., Salomão, S. R., Berezovsky, A., de Haro, F. M., & Ventura, D. F. (2004). Relationship between vision and motor impairment in children with spastic cerebral palsy: new evidence from electrophysiology. *Behavioural brain research*, *149*(2), 145-150.

Dakin, S. C., & Turnbull, P. R. K. (2016). Similar contrast sensitivity functions measured using psychophysics and optokinetic nystagmus. *Scientific reports*, *6*, 34514.

Di Russo, F., Pitzalis, S., Spitoni, G., Aprile, T., Patria, F., Spinelli, D., & Hillyard, S. A. (2005). Identification of the neural sources of the pattern-reversal VEP. *Neuroimage*, *24*(3), 874-886.

Dorr, M., Lesmes, L. A., Elze, T., Wang, H., Lu, Z.-L., & Bex, P. J. (2017). Evaluation of the precision of contrast sensitivity function assessment on a tablet device. *Scientific Reports*, *7*, 46706.

Durán, T. L., García-Ben, A., Méndez, V. R., Alcázar, L. G., García-Ben, E., & García-Campos, J. M. (2021). Study of visual acuity and contrast sensitivity in diabetic patients with and without non-proliferative diabetic retinopathy. *International Ophthalmology*, 1-6.

Ellemberg, D., Hammarrenger, B., Lepore, F., Roy, M.-S., & Guillemot, J.-P. (2001). Contrast dependency of VEPs as a function of spatial frequency: the parvocellular and magnocellular contributions to human VEPs. *Spatial vision*, *15*(1), 99-112.

Elliott, D. B., Gilchrist, J., & Whitaker, D. (1989). Contrast sensitivity and glare sensitivity changes with three types of cataract morphology: are these techniques necessary in a clinical evaluation of cataract? *Ophthalmic and Physiological Optics*, *9*(1), 25-30.

Fam, J., Rush, A. J., Haaland, B., Barbier, S., & Luu, C. (2013). Visual contrast sensitivity in major depressive disorder. In (Vol. 75, pp. 83-86).

Fechner, G. T. (1948). Elements of psychophysics, 1860.

Felleman, D. J., & Van Essen, D. C. (1991). Distributed hierarchical processing in the primate cerebral cortex. *Cerebral cortex (New York, NY: 1991)*, *1*(1), 1-47.

Force, U. S. P. S. T. (2004). Screening for visual impairment in children younger than age 5 years: recommendation statement. *Annals of family medicine*, *2*(3), 263-266.

García-Quispe, L. A., Gordon, J., & Zemon, V. (2009). Development of contrast mechanisms in humans: a VEP study. *Optometry and vision science: official publication of the American Academy of Optometry*, *86*(6), 708.

Ginsburg, A. P. (2003). Contrast sensitivity and functional vision. *International ophthalmology clinics*, *43*(2), 5-15.

Gooch, C. L., Pracht, E., & Borenstein, A. R. (2017). The burden of neurological disease in the U nited S tates: A summary report and call to action. *Annals of Neurology*, *81*(4), 479-484.

Green, M. (1981). Psychophysical relationships among mechanisms sensitive to pattern, motion and flicker. *Vision Research*, *21*(7), 971-983.

Greenhouse, S. W., & Geisser, S. (1959). On methods in the analysis of profile data. *Psychometrika*, *24*(2), 95-112.

Greenstein, V. C., Seliger, S., Zemon, V., & Ritch, R. (1998). Visual evoked potential assessment of the effects of glaucoma on visual subsystems. *Vision research*, *38*(12), 1901-1911.

Group, E. T. D. R. S. R. (1991). Early Treatment Diabetic Retinopathy Study design and baseline patient characteristics: ETDRS report number 7. *Ophthalmology*, *98*(5), 741-756.

Guo, L., Pahlitzsch, M., Javaid, F., & Cordeiro, M. F. (2017). Retinal Neurodegeneration in Alzheimer's Disease. *Frontiers in Clinical Drug Research-Alzheimer Disorders*, *6*, 56.

Gutowitz, H., Zemon, V., Victor, J., & Knight, B. W. (1986). Source geometry and dynamics of the visual evoked potential. *Electroencephalography and clinical neurophysiology*, *64*(4), 308-327.

Guzzetta, A., Mercuri, E., & Cioni, G. (2001). Visual disorders in children with brain lesions: 2. Visual impairment associated with cerebral palsy. *European journal of paediatric neurology : EJPN : official journal of the European Paediatric Neurology Society*, *5*(3), 115-119.

Hamilton, R., Bach, M., Heinrich, S. P., Hoffmann, M. B., Odom, J. V., McCulloch, D. L., & Thompson, D. A. (2021a). ISCEV extended protocol for VEP methods of estimation of visual acuity. *Documenta Ophthalmologica*, *142*(1), 17-24.

Hamilton, R., Bach, M., Heinrich, S. P., Hoffmann, M. B., Odom, J. V., McCulloch, D. L., & Thompson, D. A. (2021b). VEP estimation of visual acuity: a systematic review. *Documenta Ophthalmologica*, *142*, 25-74.

Hartline, H. K. (1938). The response of single optic nerve fibers of the vertebrate eye to illumination of the retina. *American Journal of Physiology-Legacy Content*, *121*(2), 400-415.

Hawkins, A. S., Szlyk, J. P., Ardickas, Z., Alexander, K. R., & Wilensky, J. T. (2003). Comparison of contrast sensitivity, visual acuity, and Humphrey visual field testing in patients with glaucoma. *Journal of glaucoma*, *12*(2), 134-138.

Hendry, S. H., & Reid, R. C. (2000). The koniocellular pathway in primate vision. *Annual review of neuroscience*, *23*(1), 127-153.

Hill, N. J., Mooney, S. W., & Prusky, G. T. (2021). audiomath: A neuroscientist's sound toolkit. *Heliyon*, *7*(2), e06236.

Hill, N. J., Mooney, S. W. J., Ryklin, E. B., & Prusky, G. T. (2019). Shady: A software engine for real-time visual stimulus manipulation. *Journal of neuroscience methods*, *320*, 79-86.

Holladay, J. T. (2004). Visual acuity measurements. *Journal of Cataract & Refractive Surgery*, *30*(2), 287-290.

Hoorbakht, H., & Bagherkashi, F. (2012). Optic neuritis, its differential diagnosis and management. *The open ophthalmology journal*, *6*, 65.

Hutton, J. T., Morris, J. L., Elias, J. W., & Poston, J. N. (1993). Contrast sensitivity dysfunction in Alzheimer's disease. *Neurology*, *43*(11), 2328-2328.

Ichhpujani, P., Thakur, S., & Spaeth, G. L. (2020). Contrast sensitivity and glaucoma. *Journal of glaucoma*, *29*(1), 71-75.

Jindra, L. F., & Zemon, V. (1989). Contrast sensitivity testing: a more complete assessment of vision. *Journal of Cataract & Refractive Surgery*, *15*(2), 141-148.

Joost, W., & Bach, M. (1990). Variability of the steady-state visually evoked potential: interindividual variance and intraindividual reproducibility of spatial frequency tuning. *Documenta ophthalmologica*, *75*(1), 59-66.

Kaplan, E. (2014). The M, P and K pathways of the primate visual system revisited. In J. S. Werner & L. M. Chalupa (Eds.), *The New Visual Neurosciences* (1 ed., pp. 215-226). MIT Press.

Kaplan, E., & Shapley, R. (1982). X and Y cells in the lateral geniculate nucleus of macaque monkeys. *The Journal of Physiology*, *330*(1), 125-143.

Kaplan, E., & Shapley, R. M. (1986). The primate retina contains two types of ganglion cells, with high and low contrast sensitivity. *Proceedings of the National Academy of Sciences of the United States of America*, *83*(8), 2755-2757.

Kelly, D. H. (1977). Visual contrast sensitivity. *Optica Acta: International Journal of Optics*, *24*(2), 107-129.

Kelly, D. H. (1979). Motion and vision. II. Stabilized spatio-temporal threshold surface. *Josa*, *69*(10), 1340-1349.

Krauzlis, R. J. (2004). Recasting the smooth pursuit eye movement system. *Journal of neurophysiology*, *91*(2), 591-603.

Kubová, Z., Kuba, M., Spekreijse, H., & Blakemore, C. (1995). Contrast dependence of motion-onset and pattern-reversal evoked potentials. *Vision research*, *35*(2), 197-205.

Kukkonen, H., Rovamo, J., Tiippana, K., & Näsänen, R. (1993). Michelson contrast, RMS contrast and energy of various spatial stimuli at threshold. *Vision research*, *33*(10), 1431-1436.

Kuo, H.-K., Kuo, M.-T., Tiong, S., Wu, P.-C., Chen, Y.-J., & Chen, C.-H. (2011). Visual acuity as measured with Landolt C chart and Early Treatment of Diabetic Retinopathy Study (ETDRS) chart. *Graefe's Archive for Clinical and Experimental Ophthalmology*, *249*(4), 601-605.

Kupersmith, M., Seiple, W. H., Nelson, J. I., & Carr, R. (1984). Contrast sensitivity loss in multiple sclerosis. Selectivity by eye, orientation, and spatial frequency measured with the evoked potential. *Investigative ophthalmology & visual science*, *25*(6), 632-639.

Kupersmith, M. J., Seiple, W. H., Nelson, J. I., & Carr, R. E. (1984). Contrast sensitivity loss in multiple sclerosis. Selectivity by eye, orientation, and spatial frequency measured with the evoked potential. *Investigative ophthalmology & visual science*, *25*(6), 632-639.

Lachapelle, J., Ouimet, C., Bach, M., Ptito, A., & McKerral, M. (2004). Texture segregation in traumatic brain injury—a VEP study. *Vision Research*, *44*(24), 2835-2842.

Laycock, R., Crewther, S. G., & Crewther, D. P. (2007). A role for the 'magnocellular advantage' in visual impairments in neurodevelopmental and psychiatric disorders. *Neuroscience & Biobehavioral Reviews*, *31*(3), 363-376.

Legge, G. E. (1978). Sustained and transient mechanisms in human vision: Temporal and spatial properties. *Vision research*, *18*(1), 69-81.

Legge, G. E., & Rubin, G. S. (1986). Contrast sensitivity function as a screening test: a critique. *American journal of optometry and physiological optics*, *63*(4), 265-270.

Lesmes, L. A., Lu, Z.-L., Baek, J., & Albright, T. D. (2010). Bayesian adaptive estimation of the contrast sensitivity function: The quick CSF method. *Journal of vision*, *10*(3), 17-17.

Lin, L., & Torbeck, L. D. (1998). Coefficient of accuracy and concordance correlation coefficient: new statistics for methods comparison. *PDA journal of pharmaceutical science and technology*, *52*(2), 55-59.

Liu, C. S., Bryan, R. N., Miki, A., Woo, J. H., Liu, G. T., & Elliott, M. A. (2006). Magnocellular and parvocellular visual pathways have different blood oxygen level–dependent signal time courses in human primary visual cortex. *American Journal of Neuroradiology*, *27*(8), 1628-1634.

Livingstone, M., & Hubel, D. (1988). Segregation of form, color, movement, and depth: anatomy, physiology, and perception. *Science (New York, N.Y.)*, *240*(4853), 740-749.

Lopes de Faria, J. M., Katsumi, O., Arai, M., & Hirose, T. (1998). Objective measurement of contrast sensitivity function using contrast sweep visual evoked responses. *The British journal of ophthalmology*, *82*(2), 168-173.

Ludbrook, J. (2010). Confidence in Altman–Bland plots: a critical review of the method of differences. *Clinical and Experimental Pharmacology and Physiology*, *37*(2), 143-149.

Maffei, L., & Fiorentini, A. (1973). The visual cortex as a spatial frequency analyser. *Vision research*, *13*(7), 1255-1267.

McBride, G. B. (2005). A proposal for strength-of-agreement criteria for Lin's concordance correlation coefficient. *NIWA Client Report: HAM2005-062*.

McCann, J. J., & Hall, J. A. (1980). Effects of average-luminance surrounds on the visibility of sine-wave gratings. *JOSA*, *70*(2), 212-219.

Merigan, W. H., Byrne, C. E., & Maunsell, J. H. (1991). Does primate motion perception depend on the magnocellular pathway? *Journal of Neuroscience*, *11*(11), 3422-3429.

Merigan, W. H., & Maunsell, J. H. R. (1993). How parallel are the primate visual pathways? *Annual Review of Neuroscience*, *16*(1), 369-402.

Mooney, S. W., Alam, N. M., Hill, N. J., & Prusky, G. T. (2020). Gradiate: a radial sweep approach to measuring detailed contrast sensitivity functions from eye movements. *Journal of Vision*, *20*(13), 17-17.

Mooney, S. W. J., Hill, N. J., Tuzun, M. S., Alam, N. M., Carmel, J. B., & Prusky, G. T. (2018). Curveball: A tool for rapid measurement of contrast sensitivity based on smooth eye movements. *Manuscript submitted for publication.*

Morand, S., Thut, G., de Peralta, R. G., Clarke, S., Khateb, A., Landis, T., & Michel, C. M. (2000). Electrophysiological evidence for fast visual processing through the human koniocellular pathway when stimuli move. *Cerebral cortex*, *10*(8), 817-825.

Morse, A. R. (2013). Vision function, functional vision, and depression. *JAMA ophthalmology*, *131*(5), 667-668.

Narayanan, D., Cheng, H., Tang, R. A., & Frishman, L. J. (2019). Multifocal visual evoked potentials and contrast sensitivity correlate with ganglion cell-inner plexiform layer thickness in multiple sclerosis. *Clinical Neurophysiology*, *130*(1), 180-188.

Nassi, J. J., & Callaway, E. M. (2009). Parallel processing strategies of the primate visual system. *Nature reviews neuroscience*, *10*(5), 360.

National Research, C. (1985). Emergent Techniques for Assessment of Visual Performance. In. The National Academies Press.

Nelson, J. I., & Seiple, W. H. (1992). Human VEP contrast modulation sensitivity: separation of magno-and parvocellular components. *Electroencephalography and Clinical Neurophysiology/Evoked Potentials Section*, *84*(1), 1-12.

Norcia, A., Tyler, C., Hamer, R., & Weseman, W. (1989). Measurement of spatial contrast sensitivity with the swept contrast VEP. *Vision Research*, *29*(5), 627-637.

Norcia, A. M., & Tyler, C. W. (1985). Spatial frequency sweep VEP: visual acuity during the first year of life. *Vision research*, *25*(10), 1399-1408.

Odom, J. V., Bach, M., Brigell, M., Holder, G. E., McCulloch, D. L., Mizota, A., . . . International Society for Clinical Electrophysiology of, V. (2016). ISCEV standard for clinical visual evoked potentials:(2016 update). *Documenta Ophthalmologica*, *133*(1), 1-9.

Ospina, L. H. (2009). Cortical visual impairment. *Pediatrics in review*, *30*(11), e81.

Owsley, C. (2003). Contrast sensitivity. *Ophthalmology Clinics of North America*, *16*(2), 171-177.

Owsley, C., Sekuler, R., & Siemsen, D. (1983). Contrast sensitivity throughout adulthood. *Vision research*, *23*(7), 689-699.

Padula, W. V., Argyris, S., & Ray, J. (1994). Visual evoked potentials (VEP) evaluating treatment for post-trauma vision syndrome (PTVS) in patients with traumatic brain injuries (TBI). *Brain Injury*, *8*(2), 125-133.

Pateras, E., & Karioti, M. (2020). Contrast Sensitivity Studies and Test-A Review. *Int J Ophthalmol Clin Res*, *7*, 116.

Peli, E. (1990). Contrast in complex images. *JOSA A*, *7*(10), 2032-2040.

Pelli, D., & Robson, J. (1988). The design of a new letter chart for measuring contrast sensitivity. Clinical Vision Sciences,

Pelli, D. G., & Bex, P. (2013). Measuring contrast sensitivity. *Vision research*, *90*, 10-14.

Pelli, D. G., & Farell, B. (1999). Why use noise? *JOSA A*, *16*(3), 647-653.

Pokorny, J., & Smith, V. C. (1997). Psychophysical signatures associated with magnocellular and parvocellular pathway contrast gain. *JOSA A*, *14*(9), 2477-2486.

Porciatti, V., Bonanni, P., Fiorentini, A., & Guerrini, R. (2000). Lack of cortical contrast gain control in human photosensitive epilepsy. *Nature neuroscience*, *3*(3), 259-263.

Ratliff, F., & Zemon, V. (1982). Some new methods for the analysis of lateral interactions that influence the visual evoked potential. *Annals of the New York Academy of Sciences*, *388*(1), 113-124.

Regan, D. (1966a). An effect of stimulus colour on average steady-state potentials evoked in man. *Nature*, *210*(5040), 1056-1057.

Regan, D. (1966b). Some characteristics of average steady-state and transient responses evoked by modulated light. *Electroencephalography and clinical neurophysiology*, *20*(3), 238-248.

Regan, D. (1989). Human brain electrophysiology. *Evoked potentials and evoked magnetic fields in science and medicine*.

Regan, D., Silver, R., & Murray, T. (1977). Visual acuity and contrast sensitivity in multiple sclerosis--hidden visual loss: an auxiliary diagnostic test. *Brain: a journal of neurology*, *100*(3), 563-579.

Rentschler, I. (1996). Objective measurement of contrast sensitivity and visual acuity with the steady-state visual evoked potential.

Richman, J., Lorenzana, L. L., Lankaranian, D., Dugar, J., Mayer, J., Wizov, S. S., & Spaeth, G. L. (2010). Importance of visual acuity and contrast sensitivity in patients with glaucoma. *Archives of Ophthalmology*, *128*(12), 1576-1582.

Richman, J., Spaeth, G. L., & Wirostko, B. (2013). Contrast sensitivity basics and a critique of currently available tests. *Journal of Cataract & Refractive Surgery*, *39*(7), 1100-1106.

Ridder, A., Müller, M., Kotagal, V., Frey, K. A., Albin, R. L., & Bohnen, N. I. (2017). Impaired contrast sensitivity is associated with more severe cognitive impairment in Parkinson disease. *Parkinsonism & related disorders*, *34*, 15-19.

Schade, O. H. (1956). Optical and photoelectric analog of the eye. *JoSA*, *46*(9), 721-739.

Schechter, I., Butler, P., Revheim, N., Saperstein, A., Silipo, G., Zemon, V., & Javitt, D. (2002). M-Pathway Deficits in Schizophrenia: VEPS, Contrast Sensitivity and Functional Outcome. *Investigative Ophthalmology & Visual Science*, *43*(13), 1810-1810.

Schiller, P. H. (1982). Central connections of the retinal ON and OFF pathways. *Nature*, *297*(5867), 580.

Schwartz, S. H. (2009). Visual perception: A clinical orientation.

Schütz, A. C., Braun, D. I., & Gegenfurtner, K. R. (2009). Improved visual sensitivity during smooth pursuit eye movements: Temporal and spatial characteristics. *Visual neuroscience*, *26*(3), 329-340.

Shandiz, J. H., Derakhshan, A., Daneshyar, A., Azimi, A., Moghaddam, H. O., Yekta, A. A., . . . Esmaily, H. (2011). Effect of cataract type and severity on visual acuity and contrast sensitivity. *Journal of ophthalmic & vision research*, *6*(1), 26.

Shapley, R. (1990). Visual sensitivity and parallel retinocortical channels. *Annual review of psychology*, *41*(1), 635-658.

Skottun, B. C. (2000). The magnocellular deficit theory of dyslexia: the evidence from contrast sensitivity. *Vision research*, *40*(1), 111-127.

Snellen, H. (1868). *Test-types for the determination of the acuteness of vision* (T. o. P. z. B. d. Sehschärfe. & Bound with the 2d ed. of the same title. Utrecht, Trans.; 4 ed.). Williams and Norgate.

Sokol, S., Moskowitz, A., Skarf, B., Evans, R., Molitch, M., & Senior, B. (1985). Contrast sensitivity in diabetics with and without background retinopathy. *Archives of ophthalmology*, *103*(1), 51-54.

Solomon, J. A. (2011). *Fechner's legacy in psychology: 150 years of elementary psychophysics*. Brill.

Souza, G. S., Gomes, B. D., Saito, C. A., da Silva Filho, M., & Silveira, L. C. L. (2007). Spatial luminance contrast sensitivity measured with transient VEP: comparison with psychophysics and evidence of multiple mechanisms. *Investigative ophthalmology & visual science*, *48*(7), 3396-3404.

Spering, M., Kerzel, D., Braun, D. I., Hawken, M. J., & Gegenfurtner, K. R. (2005). Effects of contrast on smooth pursuit eye movements. *Journal of Vision*, *5*(5), 6-6.

Storch, R. L., & Bodis-Wollner, I. (1990). Overview of contrast sensitivity and neuro-ophthalmic disease. In *Glare and contrast sensitivity for clinicians* (pp. 85-112). Springer.

Strasburger, H., Murray, I. J., & Remky, A. (1993). Sustained and transient mechanisms in the steady-state visual evoked potential. *Clinical vision sciences*, *8*(3), 211-234.

Strasburger, H., Remky, A., Murray, I., Hadjizenonos, C., & Rentschler, I. (1996). Objective measurement of contrast sensitivity and visual acuity with the steady-state visual evoked potential. *German journal of ophthalmology*, *5*(1), 42-52.

Tavassoli, A., & Ringach, D. L. (2009). Dynamics of smooth pursuit maintenance. *Journal of Neurophysiology*, *102*(1), 110-118.

Taylor, H. R. (1978). Applying new design principles to the construction of an illiterate E chart. *American Journal of Optometry and Physiological Optics*, *55*(5), 348-351.

Tobimatsu, S., Tomoda, H., & Kato, M. (1995). Parvocellular and magnocellular contributions to visual evoked potentials in humans: stimulation with chromatic and achromatic gratings and apparent motion. *Journal of the neurological sciences*, *134*(1-2), 73-82.

Tootell, R., Hamilton, S. L., & Switkes, E. (1988). Functional anatomy of macaque striate cortex. IV. Contrast and magno-parvo streams. *Journal of Neuroscience*, *8*(5), 1594-1609.

Tootell, R. B., & Nasr, S. (2017). Columnar segregation of magnocellular and parvocellular streams in human extrastriate cortex. *Journal of Neuroscience*, *37*(33), 8014-8032.

Tyler, C. W., Apkarian, P., Levi, D. M., & Nakayama, K. (1979). Rapid assessment of visual function: an electronic sweep technique for the pattern visual evoked potential. *Investigative ophthalmology & visual science*, *18*(7), 703-713.

Van Essen, D., Felleman, D., DeYoe, E., Olavarria, J., & Knierim, J. (1990). Modular and hierarchical organization of extrastriate visual cortex in the macaque monkey. Cold Spring Harbor symposia on quantitative biology,

Vanni, S., Warnking, J., Dojat, M., Delon-Martin, C., Bullier, J., & Segebarth, C. (2004). Sequence of pattern onset responses in the human visual areas: an fMRI constrained VEP source analysis. *Neuroimage*, *21*(3), 801-817.

Varinen, L., Laurinen, P., & Rovamo, J. (1983). Contrast sensitivity in evaluation of visual impairment due to macular degeneration and optic nerve lesions. *Acta Ophthalmologica*, *61*(2), 161-170.

Vassilev, A. (1973). Contrast sensitivity near borders: significance of test stimulus form, size and duration. *Vision Research*, *13*(4), 719-730.

Vaz, S., Falkmer, T., Passmore, A. E., Parsons, R., & Andreou, P. (2013). The case for using the repeatability coefficient when calculating test–retest reliability. *PloS one*, *8*(9), e73990.

Verrotti, A., Lobefalo, L., Petitti, M. T., Mastropasqua, L., Morgese, G., Chiarelli, F., & Gallenga, P. E. (1998). Relationship between contrast sensitivity and metabolic control in diabetics with and without retinopathy. *Annals of medicine*, *30*(4), 369-374.

Watson, P. F., & Petrie, A. (2010). Method agreement analysis: a review of correct methodology. *Theriogenology*, *73*(9), 1167-1179.

Westheimer, G. (1965). Visual acuity. *Annual Review of Psychology*, *16*(1), 359-380.

Wong, V. (1997). A neurophysiological study in children with Miller Fisher syndrome and Guillain-Barre syndrome. *Brain and Development*, *19*(3), 197-204.

Xiong, Y.-Z., Kwon, M., Bittner, A. K., Virgili, G., Giacomelli, G., & Legge, G. E. (2020). Relationship between acuity and contrast sensitivity: differences due to eye disease. *Investigative Ophthalmology & Visual Science*, *61*(6), 40-40.

Zemon, V., & Gordon, J. (2006). Luminance-contrast mechanisms in humans: visual evoked potentials and a nonlinear model. *Vision research*, *46*(24), 4163-4180.

Zemon, V., Gordon, J., & Welch, J. (1988). Asymmetries in ON and OFF visual pathways of humans revealed using contrast-evoked cortical potentials. *Visual neuroscience*, *1*(1), 145-150.

Zemon, V., Gutowski, W., & Horton, T. (1983). Orientational anisotropy in the human visual system: An evoked potential and psychophysical study. *International Journal of Neuroscience*, *19*(1-4), 259-286.

Zemon, V., Hartmann, E. E., Gordon, J., & Prunte-Glowazki, A. (1997). An electrophysiological technique for assessment of the development of spatial vision. *Optometry and vision science : official publication of the American Academy of Optometry*, *74*(9), 708-716.

Zemon, V., Herrera, S., Gordon, J., Revheim, N., Silipo, G., & Butler, P. D. (2021). Contrast sensitivity deficits in schizophrenia: A psychophysical investigation. *European Journal of Neuroscience*, *53*(4), 1155-1170.

Zemon, V., & Ratliff, F. (1982). Visual evoked potentials: evidence for lateral interactions. *Proceedings of the National Academy of Sciences of the United States of America*, *79*(18), 5723-5726.

Zemon, V., & Ratliff, F. (1984). Intermodulation components of the visual evoked potential: responses to lateral and superimposed stimuli. *Biological cybernetics*, *50*(6), 401-408.

Zemon, V., Victor, J. D., & Ratliff, F. (1986). Functional subsystems in the visual pathways of humans characterized using evoked potentials. In R. Q. Cracco & I. Bodis-Wollner (Eds.), *Fronteirs of clinical neuroscience* (3 ed., Vol. 3, pp. 203-210). Wiley-Liss.

Zemon, V. M., & Gordon, J. (2002). Luminance contrast mechanisms in human vision: visual evoked potentials (VEPs) and a nonlinear model. *Investigative ophthalmology & visual science*, *43*(13), 3933-3933.

Zihl, J., & Dutton, G. N. (2016). *Cerebral visual impairment in children*. Springer.

Zimmern, R., Campbell, F., & Wilkinson, I. (1979). Subtle disturbances of vision after optic neuritis elicited by studying contrast sensitivity. *Journal of Neurology, Neurosurgery & Psychiatry*, *42*(5), 407-412.

Table 1

Summary of Sample Demographic Characteristics

Variable	***M (SD)* or % (*n*)**
Female	66.67% (10)
Male	33.33% (5)
Age	37.13 (11.27)
Years of education	19.20 (2.46)
Ethnicity	
Asian	26.66% (4)
European	53.33% (8)
Hispanic	6.67% (1)
Other	6.67% (1)
African	6.67% (1)

Table 2

Descriptive Statistics for Contrast swp VEP log_{10} Contrast Sensitivity Estimates by Spatial Frequency

	Spatial Frequency (cpd)					
	0.8	**1.6**	**3.2**	**6.4**	**12.8**	**25.6**
	n = 15	*n* = 15	*n* = 15	*n* = 15	*n* = 15	*n* = 7
M (*SE*)	1.52 (0.07)	1.68 (0.61)	1.51 (0.09)	1.60 (0.05)	1.06 (0.10)	0.61 (0.11)
Mdn	1.57	1.78	1.62	1.69	1.08	0.58
SD	0.28	0.24	0.35	0.20	0.37	0.29
Minimum	0.98	1.01	0.45	1.22	0.46	0.20
Maximum	1.93	1.95	1.87	1.85	1.77	1.18

Table 3

Skewness and Kurtosis Statistics: Cswp log_{10} Contrast Sensitivity Estimates by Spatial Frequency

Spatial Frequency	Skewness (*SE*)	Kurtosis (*SE*)
0.8 cpd	-0.65 (0.58)	-0.36 (1.12)
1.6 cpd	-1.66 (0.58)*	3.73 (1.12)
3.2 cpd	-2.07 (0.58)*	5.42 (1.12)
6.4 cpd	-0.90 (0.58)	-0.30 (1.12)
12.8 cpd	0.11 ((0.58)	-0.38 (1.12)
25.6 cpd *(n* = 7)	1.10 (0.79)	3.43 (1.59)

Note. SE = standard error; cpd = cycles per degree

Table 4

Descriptive Statistics for Curveball log_{10} Contrast Sensitivity Estimates by Spatial Frequency

	Spatial Frequency (cpd)						
	0.24	**0.5**	**1.0**	**2.0**	**4.0**	**8.0**	**10.0**
	n = 15	*n* = 15	*n* = 15	*n* = 15	*n* = 15	*n* = 15	*n* = 15
M(*SE*)	2.24 (0.06)	2.51 (0.02)	2.55 (0.04)	2.53 (0.05)	2.00 (0.06)	1.13 (0.06)	0.81 (0.06)
Mdn	2.23	2.56	2.56	2.50	1.92	1.08	0.76
SD	0.22	0.10	0.16	0.20	0.23	0.22	0.25
Minimum	1.96	2.34	2.33	2.22	1.50	0.84	0.56
Maximum	2.66	2.64	2.90	2.94	2.34	1.55	1.33

Note. SE = standard error; cpd = cycles per degree

Table 5

Descriptive Statistics of Peak log_{10} CS by Measure

	Curveball	**Gradiate - Single**	**Gradiate - Full**	**C-swp VEP**
	n = 15	*n* = 15	*n* = 15	*n* = 15
M (*SE*)	2.67 (0.03)	2.38 (0.05)	2.46(0.03)	1.80(0.02)
Mdn	2.66	2.31	2.48	1.80
SD	0.13	0.19	0.11	0.10
Minimum	2.48	2.14	2.22	1.62
Maximum	2.94	2.66	2.66	1.99

Note. SE = standard error

Table 6

Descriptive Statistics of Areas Under the CSF Curve by Measure

	Curveball	**Gradiate - Single**	**Gradiate - Full**	**C-swp VEP**
	n = 15	*n* = 15	*n* = 15	*n* = 13
M (SE)	3.49 (0.42)	2.76 (0.07)	2.85 (0.05)	1.95 (0.07)
Mdn	3.50	2.70	2.86	1.87
SD	0.16	0.25	0.19	0.28
Minimum	3.20	2.31	2.48	1.43
Maximum	3.73	3.13	3.11	2.47

Note. SE = standard error

Table 7

Descriptive Statistics of Acuity Estimates in cpd by Measure

	Gradiate - Single	**Gradiate - Full**	**SF-swp VEP**	**C-swp VEP**
	n = 15	*n* = 15	*n* = 15	*n* = 13
M (SE)	11.69 (0.51)	12.48(0.47)	23.85 (0.99)	21.73 (2.15)
Mdn	11.55	11.55	25.19	18.87
SD	1.96	1.82	3.85	7.74
Minimum	8.66	10.00	15.56	13.39
Maximum	15.40	15.40	28.55	34.09

Note. SE = standard error; cpd = cycles per degree